Removing iron under anoxic conditions

Removing iron by operating rapid sand filters in intermittent regeneration mode

Frank Schoonenberg Kegel

TU Delft Delft University of Technology

Challenge the future

Removing iron under anoxic conditions

Removing iron by operating rapid sand filters in intermittent regeneration mode

Frank Schoonenberg Kegel

for the degree of:

Master of Science in Civil Engineering

Date of submission: 15th of September 2015
Date of defense: 24th of September 2015

Committee:

Prof. dr.ir. W.G.J van der Meer	Delft University of Technology Sanitary Engineering Section
Prof.dr.ir T.N. Olsthoorn	Delft University of Technology Water Resources Section
Dr.ir. D. van Halem	Delft University of Technology Sanitary Engineering Section
Dr. ir. P.S. Hofs	KWR Watercycle Research Institute
Ing. J.A.M. van Paassen	Vitens NV

Sanitary Engineering Section, Department of Water Management
Faculty of Civil Engineering and Geosciences
Delft University of Technology, Delft

Frontcover:
Heureka is a large kinetic sculpture made of iron bars, steel wheels, metal pipes and various electric motors. It was created by Jean Tinguely for (1925-1991) the Swiss National Exhibition in Lausanne and has been located at Zürichhorn in Zurich since 1967. Tinguely's idle machines are recognized worldwide as an allegory about the consumer and industrial society. Jean Tinguely was a Swiss artist and follower of the French Nouveau Réalisme art movement.
(Myswitzerland, 2015; Wikimedia, 2015)

Abstract

Aeration and rapid sand filtration are common practice for the treatment of iron, manganese and ammonium containing ground water for more than a century. Nevertheless, this process has not become obsolete. On the contrary, this thesis assumes that enhanced rapid sand filters remain standard treatment technology in the 21st-century.

Iron can be removed by homogeneous, heterogeneous and biological oxidation. The potential advantages of heterogeneous iron oxidation over homogeneous iron removal are high filtration rates, excellent iron removal and reduced losses of backwash water as demonstrated by the excellent performance of the pre-filters of water treatment plant Grobbendonk. Heterogeneous iron oxidation dominates at Grobbendonk because the supernatant is slightly anoxic and the pH is low. Thus adsorption and oxidation occur simultaneously.
The target feed water in this thesis is deep anoxic ground water, characterized by high iron and methane concentrations. The typical high methane values demand intensive aeration to prevent excessive formation of mucus or slime by methanotrophic bacteria. This research focuses therefore on heterogeneous iron oxidation that can be applied by running an adsorptive filter under anoxic conditions and regenerate it intermittently under oxic conditions. In other words, adsorption and oxidation are separated in time.

This work consists of three main parts: characterization of filter medium, batch experiments and pilot plant experiments.

Sequential extraction provided useful information about the accumulation on filter medium grains. The accumulation on sand/anthracite grains of the two investigated production sites contained predominantly iron(hydr)oxides e.g. ferrihydrite, which was in agreement with literature.

A method was developed to determine Freundlich isotherms constants that describe the adsorption of iron or manganese on filter medium of water treatment plants Holten and Spannenburg. These Freundlich isotherms allowed a rough estimation of the maximum operating time of a rapid sand filter in intermittent regeneration mode, which amounted to 189 bed volumes.

Pilot plant research was initiated following up on these positive results. The pilot plant consisted of two columns. The first column was filled with iron-coated sand of Holten as an adsorbent. The aim of the experiments was to determine the optimal regeneration time and the influence of the Empty-Bed Contact Time (EBCT). An increase of the EBCT, e.g. a reduction of flow rate, resulted in an increase of the iron removal.
Nevertheless, the performance was lower than estimated from the batch experiments. The explanations are: 1) there was no sharp-edged adsorption front, 2) calcium adsorption competed with iron adsorption. The absence of a sharp-edged adsorption indicates that kinetic limitations play an important role. Furthermore, a salt spiking experiment showed that the filter column did not show ideal plug flow reactor behavior.

The anoxic process requires a considerable amount of oxic water for its regeneration. Oxic water beyond that to oxidize adsorbed iron(II) was necessary to expel methane.
The slow start-up with virgin sand is an additional drawback, because it results in high water losses. However, a start-up with iron-coated sand is, of course, an option to be further investigated.

The second filter column was filled with virgin sand and then used to determine the time that the process requires to get going, i.e. the startup time. It took more than 123 cycles, which implies a water loss of 3295 bed volumes, before iron became significantly removed.

The research proved that a conventional oxic filter with aerators performs better than an anoxic filter in intermittent mode. With equal iron removal efficiencies, the number of bed volumes that can be treated and the accumulated iron load of a conventional filter are much higher. It is plausible that the anoxic pilot plant performs better at an even lower EBCT. However, this comes at the expense of one of the potential advantages of heterogeneous iron oxidation, a high filtration rate. Therefore, the outcome of this thesis does not yet warrant a change of the process configuration.

When we furthermore compare the outcome of the pilot plant experiments with the performance of the pre-filters of Grobbendonk, we have to conclude that heterogeneous iron removal performs better when adsorption and oxidation occur simultaneously, instead of separated in time.

Preface

The desire to expand my skills, to challenge myself and to explore my limits was the main driving force to enrol for a part-time MSc degree course in Water Management. Emeritus professor Hans van Dijk initiated this mid-career course. When I started as a mature student, I was fully aware of the challenge to balance academic study with my professional career and family commitments. Although it has been a long road, it will be worth it in the long run.

It was an obvious choice to focus on iron removal in rapid sand filters. In spite of the fact that rapid filters are standard practice in groundwater treatment, a fundamental understanding of the process is limited when compared to other treatment processes, causing design and troubleshooting to be often based on historical data and rules-of-thumb.

In 2012, Patrick Teunissen, André Hilhorst and myself conducted an interesting experiment: We switched off the aeration of a full-scale rapid sand filter in order to feed it with anoxic water. It was striking to see that the iron-removal was virtually complete. The experiment was stopped after 60 minutes to avoid disturbing the ammonia removal, but also prevented obtaining an iron breakthrough curve. This experiment raised the question whether we could apply anoxic iron removal on full-scale.

At the risk of forgetting someone, I would like to thank those who have contributed to this thesis.

First of all I am grateful to the graduation committee: Walter van der Meer, Doris van Halem, Theo Olsthoorn, Bas Hofs and Jacques van Paassen. Without their guidance and support, this thesis would not have been completed in this form.

I would like to express my special appreciation and thanks to my employer Vitens NV. In particular, Idsart Dijkstra who encouraged me to start this course and Johan Driessen who supported me over the last years.

The characterization of filter medium was supported by Thilo Behrends of Utrecht University and Ruud Hendrikx of the Department of Materials Science and Engineering, Delft University of Technology. Annoesjka Cabo of the Department of Applied Mathematics, Delft University of Technology, supported me with the statistical elaboration of the results.
The batch experiments would not have been possible without the hospitality and support of Wolter Siegers, Hendrik Beverloo, Danny Harmsen and Harry van Wegen of KWR Watercycle Research Institute, who also made my using of the glovebox possible.
I would like to thank Dik Brummel, Janneke Duiven and Betty van Benthem-van Loo of Vitens for supporting the pilot plant experiments at the Vitens Innovation Centre in Noardburgum.
My gratitude also goes to Martin de Jonge and Gerrit Jan Zweere of Vitens and Saroj Kumar Sharma of IHE for their useful advices and discussions. The people of Vitens Laboratory were also very helpful. I would also like to thank Koen Joris of Pidpa for the very useful performance data of water treatment plant Grobbendonk.

Two of my fellow students, Bas Rietman and Ron Jong were also colleagues. Their motivation and assistance was invaluable.

Last but not least I want to thank my wife Hilde and four children Kristel, Timo, Lieke and Jesse. I am deeply thankful for their love, support, and sacrifices. Without them, this thesis would never have been written.

Content

1 Introduction

1.1 Introduction to groundwater treatment

Groundwater accounts for 60% of the Dutch drinking water production. It has the advantage that it can be abstracted in the close vicinity of communities, which limits transport distance. It is hygienically reliable and has also a constant composition. The Dutch drinking water supply also distinguishes itself through the excellent state of the distribution system. As a result, chlorination or more advanced disinfection systems are not needed. Impact of the lowering of the ground water level associated with groundwater recovery can be a drawback that sometimes limits its availability. Abstracted groundwater often contains iron, manganese and ammonia. These constituents are generally removed by oxidation followed by sand filtration. In the Netherlands, aeration is used to introduce oxygen as the obvious and strong oxidizing agent. Aeration is cost effective and addition of chemicals like chlorine or potassium permanganate can be avoided.

The first known illustrated publication on sand filters stems from 1685 (*Figure 1*). However, there is evidence that people have used filtration on a small scale for many centuries (Baker, 1949). In 1804, the first filter to supply water to a whole town was completed at Paisly, Scotland. The first iron-removal plant was built in 1874, in Charlottenburg, Germany. However, Baker also referred to the Netherlands: "Among the earliest plants for the removal of iron, were the filters constructed at Amsterdam and The Hague, Holland". Baker probably referred to the slow sand filters, commissioned in 1851 by the water supply of Amsterdam that removed small traces of iron and manganese (Lerk, 1965). Since that time, the Dutch drinking water industry expanded rapidly, mainly by means of small groundwater abstractions (De Moel, 2006). The rapid growth of groundwater abstractions implicated a rapid introduction of groundwater treatments in the Netherlands. These days, aeration and rapid sand filtration are common practice for the removal of iron, manganese and ammonium from ground water. This thesis raises the question whether a different concept has benefits, namely the iron removal by operating rapid sand filters in intermittent anoxic mode.

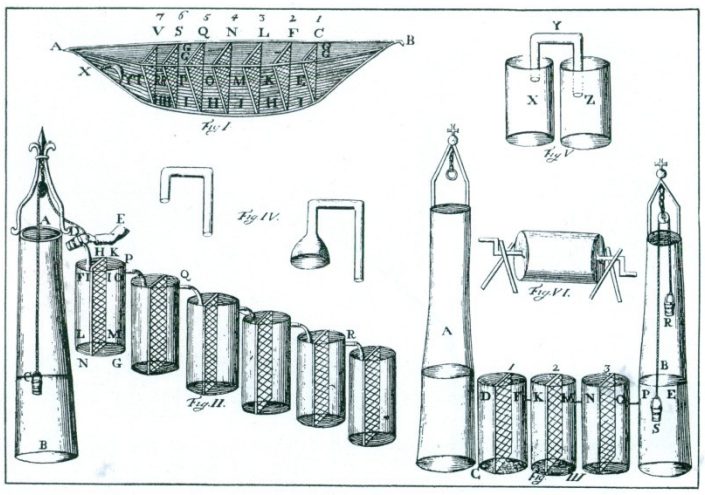

FIG. 3. PORZIO'S MULTIPLE FILTER
Three types of filters are shown: one floating; two on land, for well water
(From *Militis in Castro Sanitate Tuenda*, 1685. Translated into English as *The Soldier's Vade Mecum*, 1747)

Figure 1: First known illustrated description of sand filters

1.2 Classification of well fields

Public supply well fields in the Netherlands show a variety in raw water quality, caused by different hydrological and geochemical settings of the subsurface. From a civil engineering perspective, the level of oxygen is important. De Moel (2006) distinguishes between aerobic groundwater, slightly anaerobic groundwater and deep anaerobic groundwater. Berner (1981) distinguishes between oxic and anoxic environments. Oxic groundwater contains measurable amounts of oxygen. The anoxic environments are subdivided in *post-oxic*, *sulfidic* and *methanic*. The *post-oxic* zone is dominated by the reduction of nitrate, manganese oxides and iron oxides. Sulfate reduction occurs in the *sulfidic* zone. Methane formation occurs in the *methanic* zone. This thesis focuses on *methanic* or *deep anoxic* ground water. Deep anoxic groundwater is characterized by absence of oxygen, nitrate and sulfate, whereas methane is present, and the iron content is relatively high.

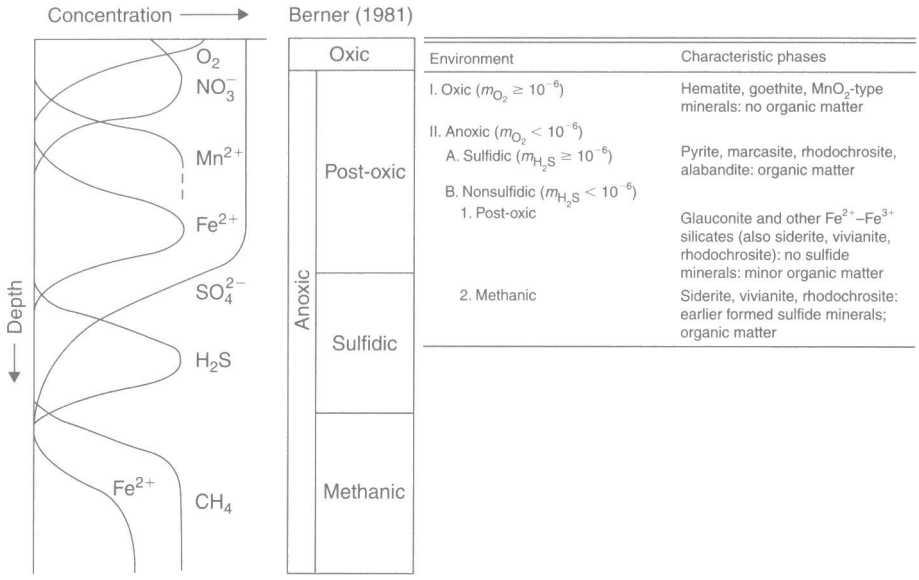

Figure 2: Left: The sequence of reduction processes as displayed in groundwater chemistry. Right: Berner's (1981) classification of redox environments together with solids expected to form in each zone (Appelo, 2006)

1.3 Iron removal by different pathways

Three different pathways can be involved in the removal of iron using rapid sand filters. The two physical-chemical pathways are homogeneous iron oxidation and heterogeneous iron removal. The third pathway are iron-oxidizing bacteria contributing to iron removal in rapid sand filters (Van Beek *et al.*, 2012).

In homogeneous iron oxidation or flocculent iron removal, soluble iron(II) that is present in anoxic groundwater is oxidized (1). The next step is the formation of insoluble iron(III) hydroxide flocs by hydrolysis (2). The iron(III) hydroxide flocs should be removed by filtration. Expressed in chemical equations:

Oxidation:	$Fe^{2+} + ¼O_2 + H^+ \rightarrow Fe^{3+} + ½H_2O$	(1)
Hydrolysis:	$Fe^{3+} + 3H_2O \rightarrow Fe(OH)_3\downarrow + 3H^+$	(2)
Sum:	$Fe^{2+} + ¼O_2 + 2½H_2O \rightarrow Fe(OH)_3\downarrow + 2H^+$	(3)

The rate equation can be written as (Stumm and Morgan, 1996; Davison and Seed, 1982):

$$-\frac{d[Fe(II)]}{dt} = k_{\text{hom}} * \frac{[Fe(II)]*[O_2(aq)]}{[H^+]^2} \qquad (4)$$

Where:

K_{hom}	= rate constant homogeneous iron oxidation (M/s)
[Fe(II)]	= iron(II) concentration (M)
$[O_2(aq)]$	= dissolved oxygen concentration (M)
$[H^+]$	= hydrogen ion concentration (M)

In heterogeneous iron oxidation or adsorptive iron removal, iron(II) adsorbs onto the surface of the filter media (sand grains) as expressed in equation 5. After adsorption the iron (II) is oxidized (equation 6) and hydrolyzed (equation 7). In a typical rapid sand filter, adsorption and oxidation will occur simultaneously. However, adsorption and oxidation are separated in time when subsurface iron removal is applied.

Adsorption:	$S\text{-}OH^0 + Fe^{2+} \rightarrow S\text{-}OFe(II)^+ + H^+$	(5)
Oxidation:	$S\text{-}OFe(II)^+ + ¼O_2 + H^+ \rightarrow S\text{-}OFe(III)^{2+} + ½H_2O$	(6)
Hydrolysis:	$S\text{-}OFe(III)^{2+} + 2H_2O \rightarrow S\text{-}OFe(III)(OH)_2^0 + 2H^+$	(7)
Overall:	$S\text{-}OH^0 + Fe^{2+} + ¼O_2 + \frac{3}{2} H_2O \rightarrow S\text{-}OFe(III)(OH)_2^0 + 2H^+$	(8)

The rate equation can be written as (Tamura *et. al.*,1978):

$$-\frac{d[Fe(II)]}{dt} = k_{het} * \frac{[S-OH^0]*[Fe(II)]*[O_2(aq)]}{[H^+]} \qquad (9)$$

Where:

K_{het}	= rate constant heterogeneous iron oxidation (M^{-1} s^{-1})
$[S\text{-}OH^0]$	= concentration iron(hydr)oxides (M)

Iron-oxidizing bacteria can contribute to iron removal in rapid sand filters. In Northern Germany, *Gallionella spp.,* amongst other bacteria, is reported in drinking water filters. *Gallionella spp.* is generally regarded strictly lithotrophic, which means it uses inorganic substrate for biosynthesis, i.e. the inorganic substrate iron.

To investigate where the three iron removal pathways occur, we should distinguish the supernatant and the filter medium (Figure 3). Homogeneous iron oxidation may occur in the supernatant whereby flocs are formed. Heterogeneous iron oxidation on these flocs might also occur. Biological iron oxidation will not occur in the supernatant, due to lack of medium for bacteria to attach to.
All three pathways are expected to occur in the filter medium. However, process understanding allows controlling which pathway will dominate, whereby the raw water composition is a key factor.
Nevertheless, the process conditions during aeration and in the supernatant are also significant for the overall filtration result. When we create more favorable conditions for homogeneous iron oxidation in the aeration and supernatant, a reduced amount of iron(II) will be available for heterogeneous oxidation or biological iron oxidation in the filter medium.
As can be seen in equation 4, oxidation of iron (II) accelerates at a high pH and high oxygen concentration. Both the pH and the oxygen concentration can be increased by intensive aeration. The residence time in the supernatant can be increased by increasing the supernatant volume or by reducing the flow rate.
Heterogeneous iron oxidation (equation 9) and biological iron oxidation will dominate when the supernatant is slightly anoxic and the pH is low. Both the oxygen concentration and pH can be achieved by a less intensive aeration.

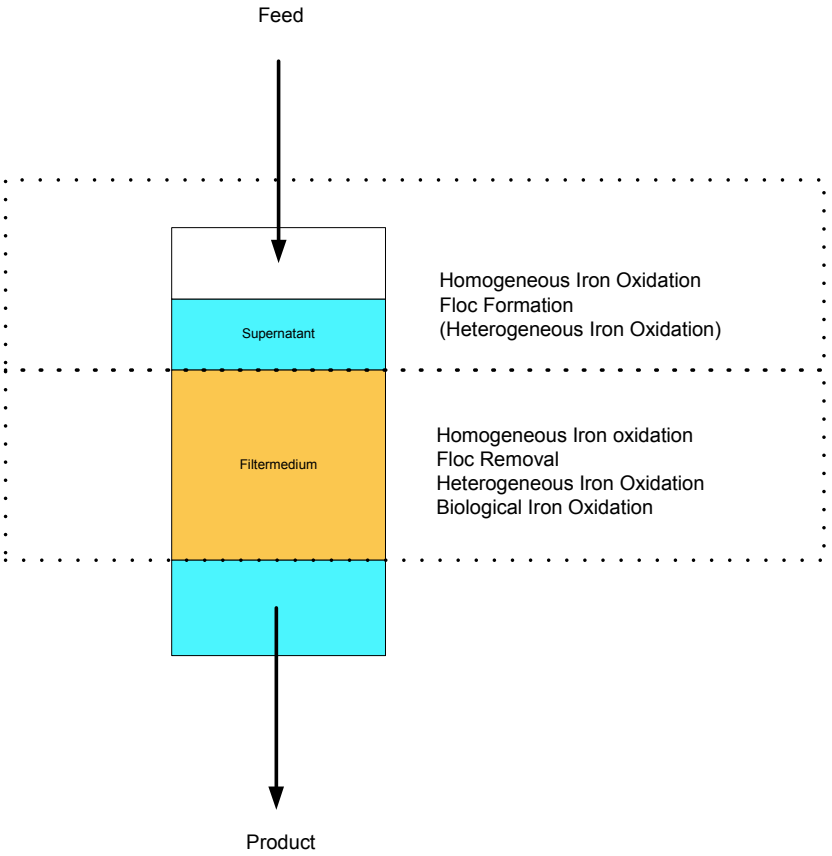

Figure 3: Location three iron removal pathways in a down flow rapid sand filtration

1.4 Focus on heterogeneous iron oxidation

This research focuses on heterogeneous iron oxidation because this pathway provides potential advantages such as high filtration rates, excellent iron-removal efficiency and low backwash losses. Furthermore, fouling of aerators can be reduced with iron oxidation as the first treatment step.

1.5 Research on heterogeneous iron oxidation

Early research on heterogeneous iron oxidation related to the geochemistry. Van Beek and Vaessen (1979) were the first to propose heterogeneous iron oxidation as the mechanism of subsurface iron removal (SIR). SIR is applied to reduce the iron concentration in groundwater (Van Beek, 1985; Olsthoorn, 2000). A promising new application is the removal of arsenic (Van Halem, 2011).
One cycle of SIR starts with the injection of oxygenated water in the aquifer (Figure 4A), partially displacing the native iron(II) containing groundwater. The introduced oxygen oxidizes iron(II) in the aquifer around the well where it precipitates as iron hydroxides. The oxygen front lags, therefore, behind the injection-water front. The next step involves the withdrawal of injectied water and groundwater (Figure 4B). In the process, Iron(II) adsorbs on the recently formed iron hydroxides. Thus, the iron concentration of the abstracted ground water is lower than that in the native ground water. The volume of water that can be abstracted (volume V) is generally several times larger than the injected volume (Vi). The efficiency of the system is determined by the volumetric ratio (V/Vi).

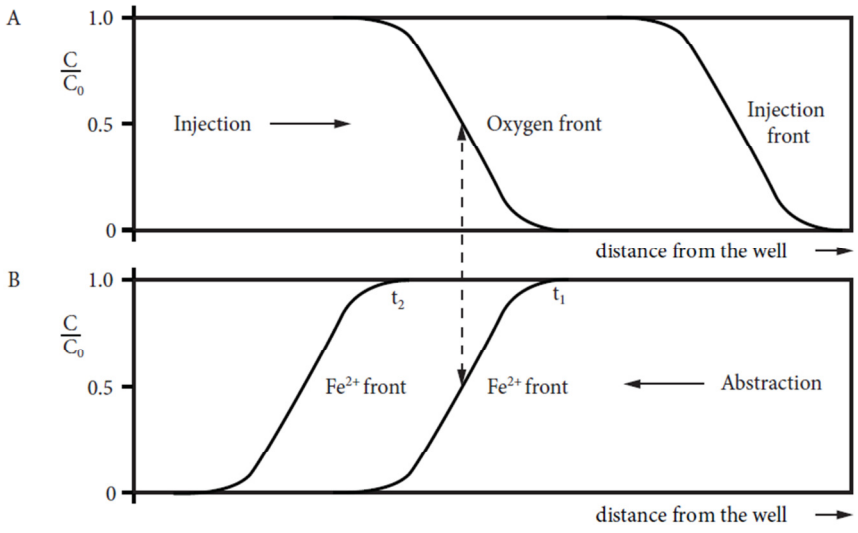

Figure 4: The two cycles of subsurface iron removal (SIR) Oxygen and iron front at a distance from the well (obtained from van Beek, 1983)l

Vitens water supply company has been operating SIR plants for decades. Currently 7 SIR plants are working. Experience from Vitens shows that no recognizable clogging occurred after over 27 years of use. The volumetric ratio (V/Vi) varies between 1:3 and 1:20 when the injection water is saturated with oxygen under atmospheric conditions. The injected water volume (Vi) varies between 1000 and 3000 m^3 (Hinkamp *et. al.*, 2004).

Appelo *et. al.* (1999) successfully used Phreeqc, a hydrochemical transport model, to model SIR. He calibrated his model with the data of column experiments of Olthoff (1986). Appelo's research supports the theory that heterogeneous iron oxidation is the key mechanism of SIR.

Sharma (2001) did comprehensive research on heterogeneous iron oxidation in rapid sand filters that involved batch experiments, pilot plant experiments and modelling. Sharma mentions several potential advantages of heterogeneous iron oxidation over homogeneous iron removal:

- Lower head loss development leading to reduced water losses involved with backwashing of rapid sand filters
- Shorter ripening time after backwashing
- Better average quality of the filtrate

1.6 Experience with full-scale heterogenic iron oxidation

Heterogenic and biological iron oxidation are the dominant removal mechanisms in the full scale rapid sand filters of water treatment plant Grobbendonk (Hofs, 2011; Joris, 2015). The Belgian drinking water company Pidpa operates these rapid sand filters. Table 1 illustrates the groundwater compositions of Grobbendonk. The pre-treatment consists of a three stage cascade aeration and rapid sand filtration. The uptake of oxygen is limited by split stream aeration, i.e. some of the raw water is bypassed and blended with the stream leaving the cascade. Paragraph 1.4 concluded that heterogeneous iron oxidation and biological iron oxidation will dominate when the supernatant is slightly anoxic and the pH is low. The iron concentration is lowered from 36 to 0.1 mg/L. Next, a seven stage cascade aerator and lime dosage raise the oxygen concentration and pH. Finally, a second rapid sand filter removes ammonium and manganese. It can be concluded that the rapid sand filters of Grobbendonk demonstrate an impressive iron removal efficiency.

Table 1: Composition anoxic ground water and product of the pre-filter of water treatment plant Grobbendonk (Joris, 2015).

		Ground water	Product pre-filter
pH	pH	6.7	6.0
Iron	mg/L	35.7	0.05
Manganese	mg/L	0.22	0.22
Ammonium	mg NH_4 / L	0.25	0.15
Calcium	mg/L	54.1	54.1
Magnesium	mg/L	5.1	5.1
Total Hardness	mmol/L	1.56	1.56
Bicarbonate	mg/L	120	55
Nitrate	mg NO_3 / L	<1	<1
Sulfate	mg SO_4 / L	96.2	96.2
Methane	µg/L	15	<5
Temperature	°C	11.9	11.9

1.7 The challenge of anoxic iron removal

This thesis focuses on deep anoxic ground water, which is always abstracted below confining layers. Table 2 illustrates typical deep anoxic groundwater compositions of public supply well fields in the northern part of the Netherlands. The Dutch drinking water company Vitens operates these well fields. As expected for deep anoxic ground water, the nitrate and sulfate concentrations are low. High levels of iron, manganese, ammonium and methane are present and high total hardness and color of the ground water are typical for this type of groundwater. An important distinction between the groundwater composition of Grobbendonk and the deep anoxic well fields in Table 2 is the low methane concentration and the extremely high iron content in Grobbendonk. Grobbendonk can therefore be characterized as anoxic iron rich groundwater. The methane concentration is an important factor that influences the design of a water treatment as discussed in the remainder of this paragraph.

Table 2: Typical composition deep anoxic ground water compositions, from well fields of ground water production sites, average over 2013 and 2014

		Noardburgum	Oldeholtpade	Sint Jansklooster	Spannenburg
pH	pH	7.2	7.0	7.0	6.8
Iron	mg/L	8.9	12.0	7.5	12.1
Manganese	mg/L	0.32	0.29	0.33	0.56
Ammonium	mg NH_4 / L	0.9	1.8	2.2	2.4
Calcium	mg/L	123	75	88	118
Magnesium	mg/L	12.4	5.3	6.2	9.7
Total Hardness	mmol/L	3.6	2.1	2.4	3.3
Bicarbonate	mg/L	334	272	281	416
Nitrate	mg NO_3 / L	<1	<1	<1	<1
Sulfate	mg SO_4 / L	10	6.8	16	<2
Methane	µg/L	6700	4000	6400	37900
Temperature	°C	12	11	11	11

The drinking water treatment at these four well fields is similar (Figure 5, process configuration 1). The pre-treatment consists of intensive aeration and rapid sand filtration. The typical high methane values demand intensive aeration. The mucus or slime in rapid sand filters that is produced by methanotrophic bacteria is not completely removed by backwashing. High methane concentrations in the inflow also link with the growth of other bacteria like *Aeromonas*, especially in the distribution system. The methane concentration should be reduced to below 100 µg/l to prevent these problems (Reijnen, 1994). Plate aeration is excellent for methane removal, but a disadvantage of the plates is their sensitivity for fouling caused by iron(hydr)oxides and calcium carbonate deposits that can clog the small holes in the bottom plates. Periodic cleaning of the bottom plates is therefore inevitable. Rapid sand filters aim to remove remaining methane, iron, manganese and ammonium. Next oxygen is added and carbon dioxide is removed by intensive aeration. The water is finally softened by a pellet reactor and the color is reduced by ion exchange.

This thesis focuses on the pre-treatment. A plate aerator removes considerable amounts of CO_2, thereby raising the pH significantly. Homogeneous iron oxidation is, therefore, expected to be more dominant within the rapid sand filter.
Based on the advantages of heterogeneous iron removal, it may be interesting to convert the pre-treatment from homogeneous to heterogeneous iron removal.

1.8 Rapid sand filter in intermittent regeneration mode

There are two paths to favor heterogeneous iron oxidation in a sand filter. As mentioned in paragraph 1.3, a less intensive aeration reduces the oxygen content and the pH in the water feeding a sand filter. A more intensive aeration will be required with high a methane concentration in the raw water. However, intensive aeration minimizes heterogeneous iron removal. The subsurface iron removal, where the adsorption of iron(II) and heterogeneous iron oxidation do not occur simultaneously, inspired the approach of this thesis, which can be applied by running an adsorptive filter under anoxic conditions and by regenerating it intermittently under oxic conditions. Figure 5 depicts the optional process configurations 2 and 3. In configuration 2, a second filtration step removes manganese and ammonia. Alternatively, a pellet reactor in configuration 3 softens aerated water. Configuration 1 conventionally uses aeration by plate aeration and rapid sand filters to treat deep anoxic groundwater.

1.9 Aim of this thesis

This thesis aims to determine the feasibility of heterogeneous iron oxidation by a rapid sand filter in intermittent regeneration mode. Its target feed water is deep anoxic groundwater, that is characterized by high iron and methane concentrations. Expected advantages of this concept include reduced backwash water losses and to a lesser extent less required cleaning of the plate aerators.

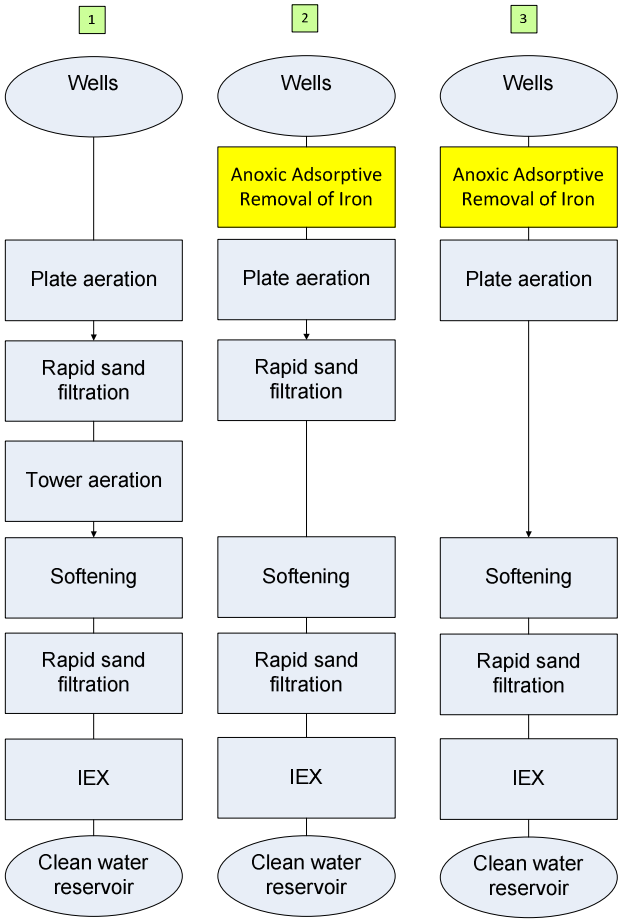

Figure 5: Schematic diagram optional process configurations for implementation intermittent iron removal

1.10 Empty Bed Contact Time

The Empty Bed Contact Time (EBCT) is the initial contact time when the filter bed is still clean and empty, i.e. the pore volume of the clean filter bed divided by the flow rate [$m^3/(m^3/h)=h$]. The EBCT is the sole parameter to characterize the time behavior of the iron removal and is used throughout this MSc thesis. An increase of the EBCT, e.g. a reduction of flow rate or increase of the thickness of the filter, may influence the iron removal.

1.11 Objectives

This research focuses on heterogeneous iron oxidation that can be applied by running an adsorptive filter under anoxic conditions that can be regenerated intermittently under oxic conditions. The target feed water is deep anoxic ground water, characterized by high iron and methane levels. The presumed advantages of this concept are high filtration rates, excellent iron removal, reduced backwash water losses and to a lesser extent reduced cleaning of the plate aerators.

1.12 Outline

Description outline:
Chapter 2: Sampling and characterization of filter medium
Chapter 3: Batch experiments
Chapter 4: Pilot plant experiments
Chapter 5: Discussion
Chapter 6: Conclusions and recommendations

2 Sampling and Characterization of the filter medium

2.1 Introduction

Adsorption of iron on iron(hydr)oxides is the first step in heterogeneous iron oxidation. It seems plausible that the physico-chemical properties of iron(hydr)oxides will affect the adsorption of ferrous iron. The batch experiments described in chapter 3 were carried out with filter medium collected from rapid sand filters of water treatment plants Holten and Spannenburg. Although both sampled rapid sand filters were pre-filters, the quality of the feed water was different. Due to lower pH of the feed water of Holten compared to Spannenburg, the dominant iron removal mechanism would be heterogeneous iron oxidation. Another difference between these pre-filters was their filter medium. The filter medium of the pre-filters of Holten consisted of sand grains (1.5-2.5 mm); those in Spannenburg were dual media filters, equipped with an upper layer of anthracite grains (1.4-2.5 mm) and a lower layer of sand grains (0.8-1.25 mm). However, it is seems that the two layers were actually mixed due to operational problems.

Table 3: Composition inflow and outflow pre-filters Holten (VF3) and Spannenburg(VF11).

	Holten VF3		Spannenburg VF11	
	inflow	outflow	inflow	outflow
pH	6.0	6.0	7.6	7.4
Fe	6.4	0.01	12.4	0.03
Mn	0.8	0.8	0.5	0.4
NH_4	0.14	<0.03	3.3	1.8

Schwertmann *et. al.* (2000) reviewed various methods used to identify and characterize iron oxides, amongst others spectroscopy, diffractometry, thermal analysis and microscopy. Previously, filter medium of water treatment plant Holk was examined with the help of SEM (scanning electron microscope) and Raman spectroscopy (Schoonenberg Kegel, 2013). The Raman spectra indicated the presence of ferrihydrite and haematite. The presence of the latter was unexpected because the formation of this mineral is a slow process at the low temperatures prevailing in groundwater. SEM_EDS showed that mainly iron, oxygen and carbon were present. The presence of iron and oxygen was in line with the assumption that iron(III) (hydr)oxides were deposed on the filter medium. The presence of carbon was explained by the formation of biomass in the rapid sand filter.

This thesis focuses on:

- Examination of the particle-size distribution of filter-medium grains by laser diffraction
- Chemical analysis of the inorganic composition of the accumulation on filter-medium grains
- XRD analysis of filter-medium grains to provide information about the structure of an iron-oxide compound.
- Examination of iron partitioning by sequential extraction.

Samples of the filter medium were collected with a peat sampler. A peat sampler is in fact a kind of gouge auger that enables to take undisturbed samples of filter medium at predetermined depths. Table 4 presents an overview of the collected samples.

Table 4: Overview of the collected samples

WTP	Filter	Sampling date	Sampling depth	Purpose[1]
Spannenburg	VF11	5 November 2013	0-50 cm	Chapter 2 and 3
Holten	VF1	28 October 2013	0-50 cm	Chapter 2 and 3
Holten	VF1	28 October 2013	50-100 cm	Chapter 2
Holten	VF3	4 March 2014	0-50 cm	Chapter 4

1) Purpose:
   - Chapter 2 Sampling and characterization of filter medium
   - Chapter 3 Batch experiments
   - Chapter 4 Pilot plant experiments

2.2 Characterization of the filter medium

2.2.1 Particle-size distribution

Vitens' laboratory measured the dry-matter content and the particle-size distribution. Table 5 shows a significant lower dry-matter content of the filter medium of Spannenburg. An explanation is the sampling procedure. The filter in Holten was drained before sampling, while the filter in Spannenburg was still submerged. Moreover, the different process conditions may have influenced the oxidation and hydrolysis of iron, and as a result the dry-matter content. Laser diffraction was used to determine the particle-size distribution. The low D10 value of the medium for the filter in Spannenburg is in line with the presumption that anthracite and sand layers were mixed due to operational problems. The mixing of the two media of the originally dual media filter also explains the markedly inferior (i.e. high) uniformity coefficient.

Table 5: The particle size distribution of filter medium based on a single measurement. The sampling depth was 0-50 cm. The uniformity coefficient (UC) is defined as: D60/D10

	Dry matter	D10	D50	D60	D90	UC
	%	µm	µm	µm	µm	N/A
Holten VF1	92	1200	1900	2000	2500	1.6
Spannenburg VF11	71	650	1300	1500	2200	2.3

2.2.2 Composition of the accumulation on the filter medium

The laboratory of Vitens analyzed the composition of the accumulation on filter medium. The protocol boils down to dissolving the accumulation, by shaking a grain sample with a 4 M Hydrochloric Acid and 2 g/L Oxalic Acid solution for 16 h. The filter medium itself, sand or anthracite will not dissolve. The dissolved metals were analyzed by ICP-MS. Virgin sand was tested as a blank. The relatively low mass percentage of the accumulation in Holten as presented in Table 6 can be explained by the short operating time. The filter medium was replaced 3 months before the sample was collected. In contrast, the filter medium in Spannenburg was put into operation 6 years earlier. Furthermore a significantly higher calcium and magnesium content can be seen at the treatment plant in Spannenburg, which is in line with the higher total hardness of the feed water. The iron and magnesium contents are more or less similar.

Table 6: The composition of the accumulation based on single measurement. The sampling depth was 0-50 cm.

	Accumulation	Composition of the accumulation			
		Ca	Mg	Fe	Mn
	mass accumulation/ mass filter medium	mg/g	mg/g	mg/g	mg/g
Virgin Sand 0.8 - 1.25 mm	1.5%	6.2	13	100	1.8
Holten VF1	16.4%	1.7	2.7	310	0.28
Spannenburg VF11	99.6%	24	0.27	240	0.85

2.2.3 XRD analysis

X-ray diffraction is a non-destructive technique that can be used to determine the crystal structure and crystalline compounds in a sample. Department of Materials Science and Engineering of the Delft University of Technology carried out the XRD analysis of the filter medium grains. Both samples were dried at 30 °C and grinded. The samples showed the brownish color of iron oxide that covered the grain surface, but iron oxide could not be detected in the XRD patterns. The higher background in the patterns between 20 and 40º 2θ shows the presence of an amorphous phase (Hendrikx, 2013).
This conclusion may seem disappointing at first sight, but the absence of crystalline compounds is interesting and important in its own right.

2.2.4 Sequential extraction

Sequential extraction is an interesting method to examine the accumulation on filter medium grains (Behrends, 2014). Sequential extractions, involving the addition of a series of reagents to a single soil sample, could differentiate between amorphous and crystalline iron oxides. Geochemists use this method to determine the partitioning of a chosen element in soil and sediment materials. Utrecht University Faculty of Geosciences, Department of Earth Sciences, carried out the sequential extraction experiments employed in this thesis. The procedure was developed by Claff *et. al.* (2010) and involves five steps. Table 7 summarizes for each step, the extraction conditions and target.

Table 7: Sequential extraction procedure

Step	Extractant	Conditions	Target
1	1 M Magnesium chloride ($MgCl_2$)	1 hour at RT	Exchangeable fraction of adsorbed Fe and readily soluble Fe-salts.
2	1 M Sodium acetate, pH 4.5	48 hours at 50 °C	Carbonates
3	1 M Hydrochloric acid (HCl)	4 hours at RT	Fe (hydr)oxides with high reactivity towards acids (amorphous Fe(hydr)oxides, ferrihydrite)
4	Sodium citrate/dithionite solution buffered to a pH of 7.5 with $NaHCO_3$ (CDB)	15 minutes at 75 °C	Crystalline iron oxides
5	Concentrated nitric acid (HNO_3)	2 hours at RT	Pyrite and some clay minerals

Note: RT= Room Temperature

The samples were dried for around 20 minutes in a stove at 60-70 °C. A centrifuge separated the suspension between each successive extraction step. Next, the supernatant was filtered through a 0.2 µm syringe filter. The *medium:extractant* ratio was *1:40*.

Figure 6 and Figure 7 show the iron and manganese extracted from the filter medium. The results were discussed with Behrends (2015).
The majority of iron was extracted in step 3. This indicates the presence of amorphous iron(hydr)oxides e.g. ferrihydrite. The iron extracted in step 2 may indicate the presence of iron carbonate. However, decantation of the extracted solutions was a problem and some iron particles were not retained. This was particularly a problem in the first two extraction steps, and may have lead to an overestimation of iron concentrations in step 2.
In many cases manganese correlates with iron. Here the majority of the manganese was extracted in step 2, although the manganese concentration was low across all steps. Comparing the results of Figure 6 with Table 6 reveals that the total extracted amount of iron measured with sequential extractions is significantly lower than measured by the laboratory of Vitens. Figure 6 shows that the total amount of iron recovered from filter medium from Spannenburg was relatively high compared to that of Holten. This observation is in contrast with Table 6 that shows that the iron content in the accumulation is comparable in both production sites.

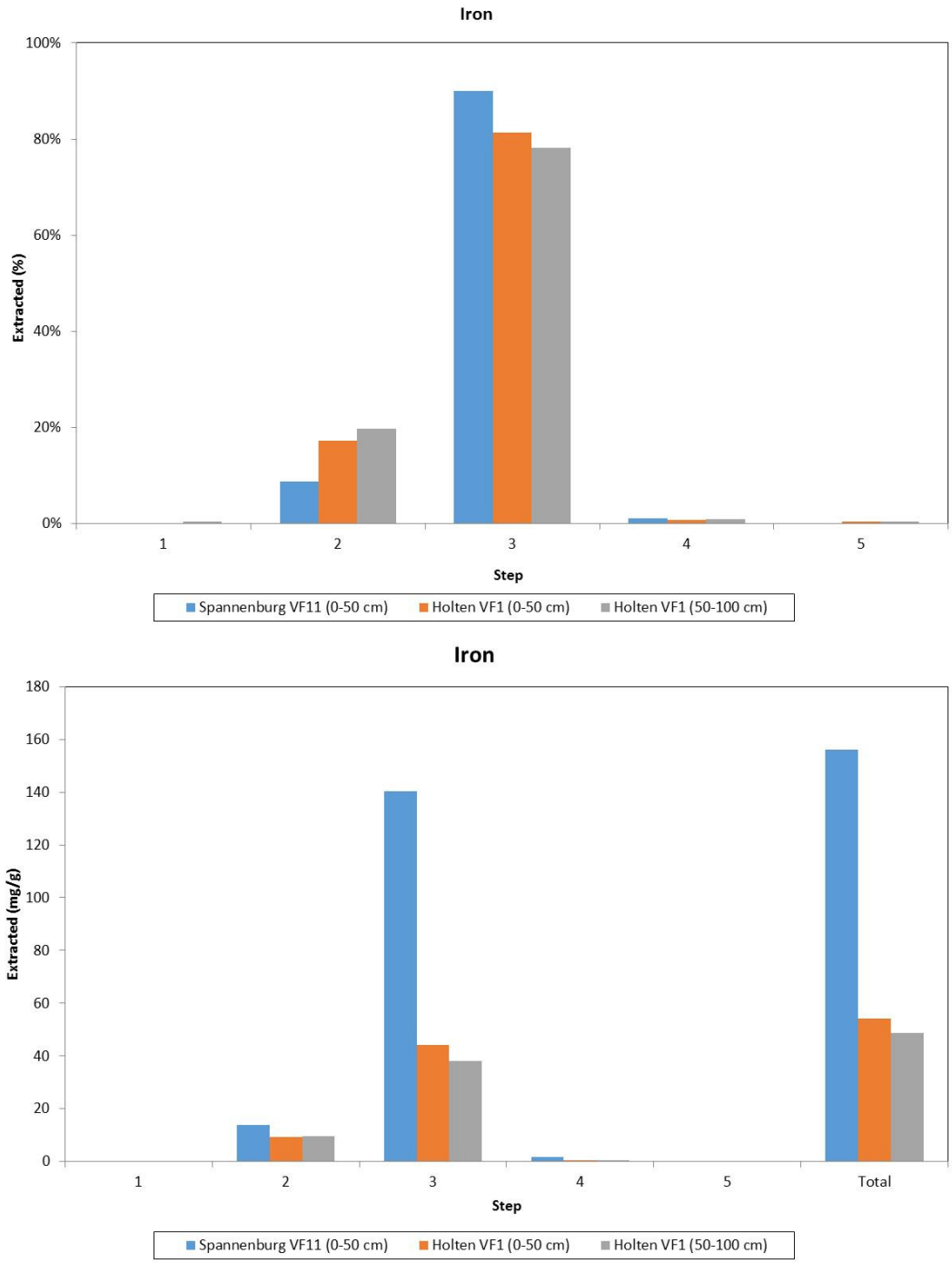

Figure 6: Iron removed from filter medium in each step of a 5 step sequential extraction experiment. The top graph shows percentages while the bottom graph shows extractability expressed in mg/g. All values represent the means of in duplo analysis.

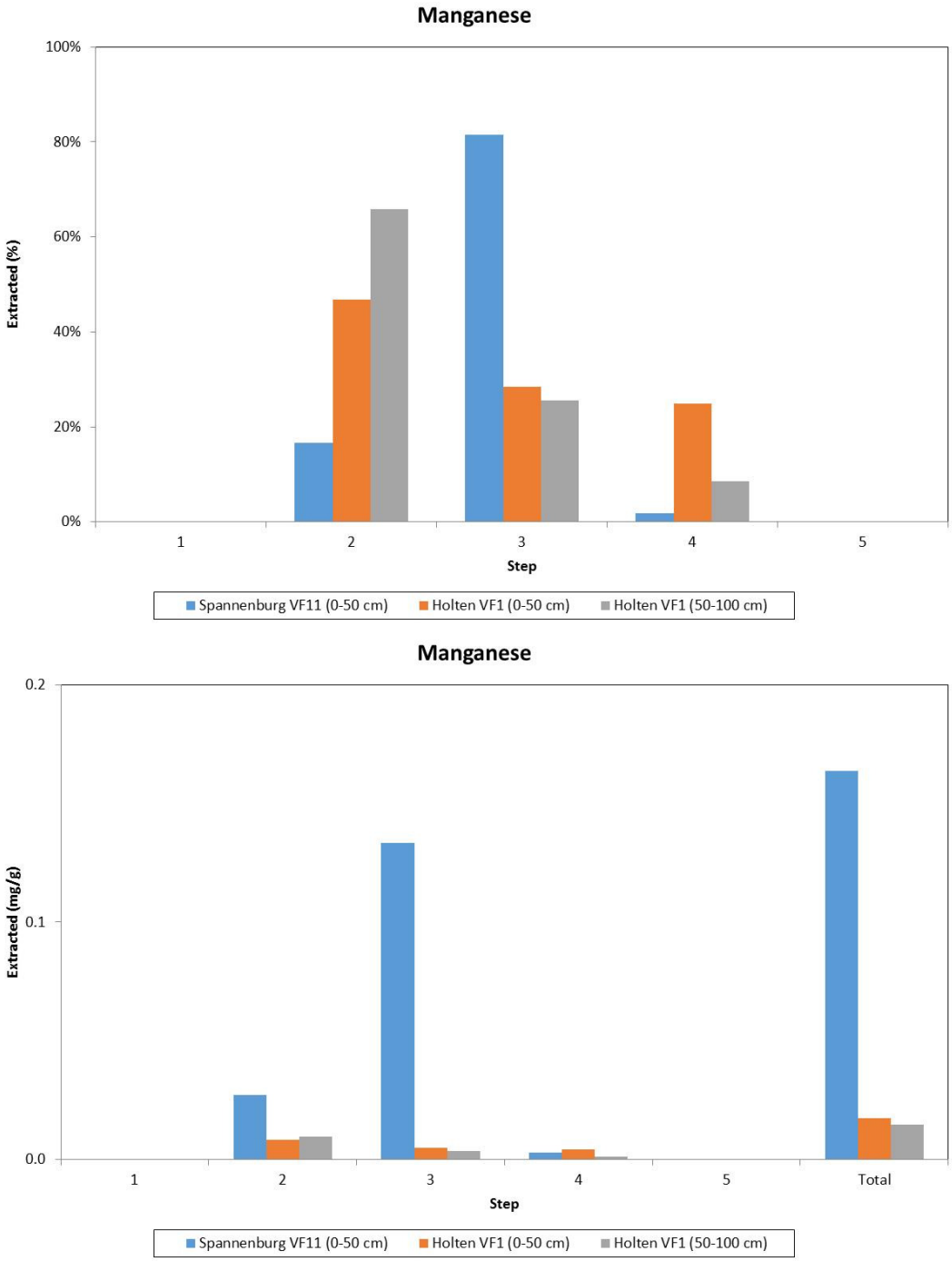

Figure 7: Manganese removed from filter medium in each step of a 5 step sequential extraction experiment. The top graph shows percentages while the bottom graph shows extractability expressed in mg/g. All values represent the means of in duplo analysis.

2.3 Conclusions

The particle-size distribution measurement showed that the uniformity coefficient of filter medium of water treatment plant Spannenburg was markedly inferior compared to that of Holten. The measured values were 2.3 and 1.6. The high value was explained by unintended mixing of the dual media filter due to operational problems. The accumulation was larger on the filter medium of Spannenburg compared to that of Holten.

The mass percentages of the accumulation on filter medium in Spannenburg and Holten were 16.4% and 99.6%. The relatively low mass percentage of the accumulation on filter medium in Holten can be explained by the short time the filter medium has operated before the samples were taken.

Sequential extraction provided useful information about the accumulation on filter-medium grains. The accumulation on the sand grains of both production sites contained predominantly iron(hydr)oxides e.g. ferrihydrite. This is in agreement with the observation of Carlson and Schwertmann (1987) that iron(III)hydroxides that precipitated during iron removal from groundwater consist of poorly ordered HFO.

The presence of HFO may be beneficial for the adsorption of iron(II) due to the large specific surface area (Drijver *et. al.*, 1997). Moreover, the value for k_{het} in equation (9) ranges by a factor of 10 between the most amorphous and the most crystalline phase (Tamura *et. al.*, 1980). Therefore the availability of amorphous iron(hydr)oxides on the filter medium favors heterogeneous iron oxidation.

3 Batch experiments

3.1 Freundlich isotherms

Adsorption can be described in terms of isotherms that represent the relationship between equilibrium concentration of the solute and the amount of solute adsorbed at constant temperature. Various isotherm equations can describe the equilibrium characteristics of adsorption. The Freundlich isotherm (Freundlich, 1906) is frequently applied to describe non-linear sorption. Dzombak and Morel (1990) reported that cation sorption onto hydrous oxides can usually be approximated by the Freundlich isotherm (Sharma, 2001).
The Freundlich isotherm assumes an exponential relation between the concentration of the solute and the amount of solute adsorbed (equation 10)

$$q=kC_e^n \quad (10)$$

Where:
q = the amount of solute adsorbed [g/g]
C_e = equilibrium concentration of the solute [g/L]
K = Freundich isotherm constant $(L/g)^{1/n}$
n = Freundlich isotherm constant (-)

The constants in the Freundlich isotherm expression can be derived by linearization (equation 11) and plotting on a double log scale:

$$\log q=\log k+n \log C_e \quad (11)$$

3.2 Procedure for the batch adsorption experiments

A special procedure for the batch adsorption experiments was developed.
Iron is readily oxidized when oxygen is present; therefore the most challenging part of the batch adsorption experiments was to maintain anoxic conditions. A glovebox was used to meet this requirement (Figure 8).

A comprehensive procedure of the batch adsorption experiments can be found in annex 1. The protocol was divided in 5 steps (Figure 9). In advance, two series of eight 100 mL serum bottles, were filled with an increasing amount of adsorbent. Furthermore two serum bottles were used as blanks and were not filled with filter medium. After closing the glovebox, each experiment started with the preparation of a 10 mg/L Fe(II) or 5 mg/L Mn(II) by solving iron(II)sulfate ($FeSO_4.7H_2O$) or manganese(II)chloride ($MnCl_2.4H_2O$) in milliQ water under anoxic conditions (Figure 10). Sodium bicarbonate ($NaHCO_3$, 6 mmol/L) was used as a buffering agent. The pK_a, the negative logarithm of the equilibrium constant K_a for the dissociation of carbonic acid is 6.46 at 10 °C (Stumm and Morgan, 1996). Thus the experiments were carried out within the useful range of the pH buffer. An Orbisphere Laboratories oxygen indicator model 26060 equipped with sensor 2110 checked the dissolved oxygen level. The pH was adjusted to the required value by adding 1 M hydrochloric acid or 1 M sodium hydroxide. Next the iron(II) or manganese(II) solution was poured into all the serum bottles.
The serum bottles were thoroughly sealed by a crimper. The closed serum bottles were transferred from the glovebox to the incubator, where the suspension was stirred at a constant temperature.
When the required adsorption time has passed, the serum bottles were transferred back to the glovebox. A sample was collected after the water was filtered with a 0.45-micron filter under anoxic conditions (Figure 11). The samples were analyzed on iron and manganese by ICP-MS.

The mass of the adsorbed iron or manganese per mass adsorbent was calculated with equation 12.

$$q = \frac{mass\ adsorbed\ solute}{mass\ adsorbent} = \frac{\frac{(m3-m2-m4)}{\rho w} * (\mathrm{Cb}-\mathrm{Ce})}{dm*(m2-m1)} \quad (12)$$

Where:

q = mass adsorbed iron or manganese per mass adsorbent (g/g)
m1 = mass serum bottle + stir bar (g)
m2 = mass serum bottle + stir bar + adsorbent (g)
m3 = mass serum bottle + stir bar + adsorbent + synthetic water + seal + stopper (g)
m4 = average mass seal + stopper (g)
Ce = equilibrium concentration iron or manganese (g/L)
Cb = average iron or manganese concentration in filtered blank (g/L)
dm = dry matter percentage adsorbent (%)
ρw = density water (g/L)

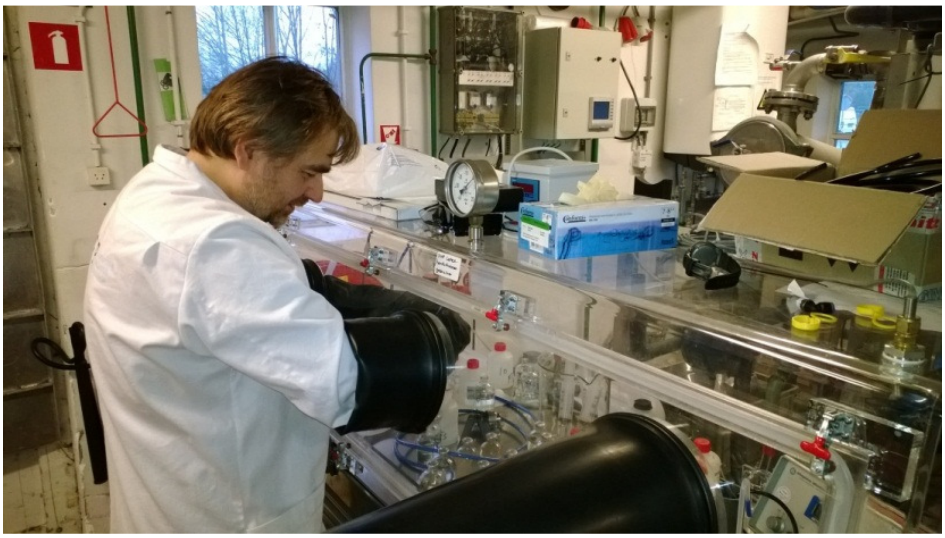

Figure 8: Experiments under anoxic conditions in a glovebox

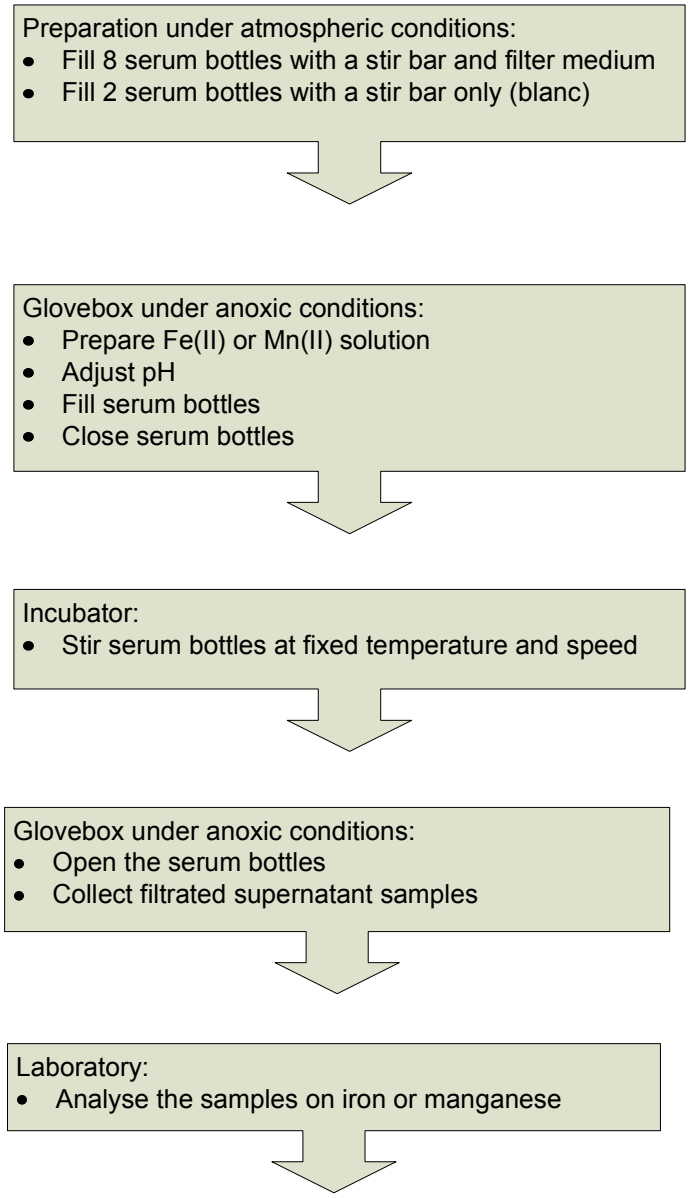

Figure 9: Experimental set-up

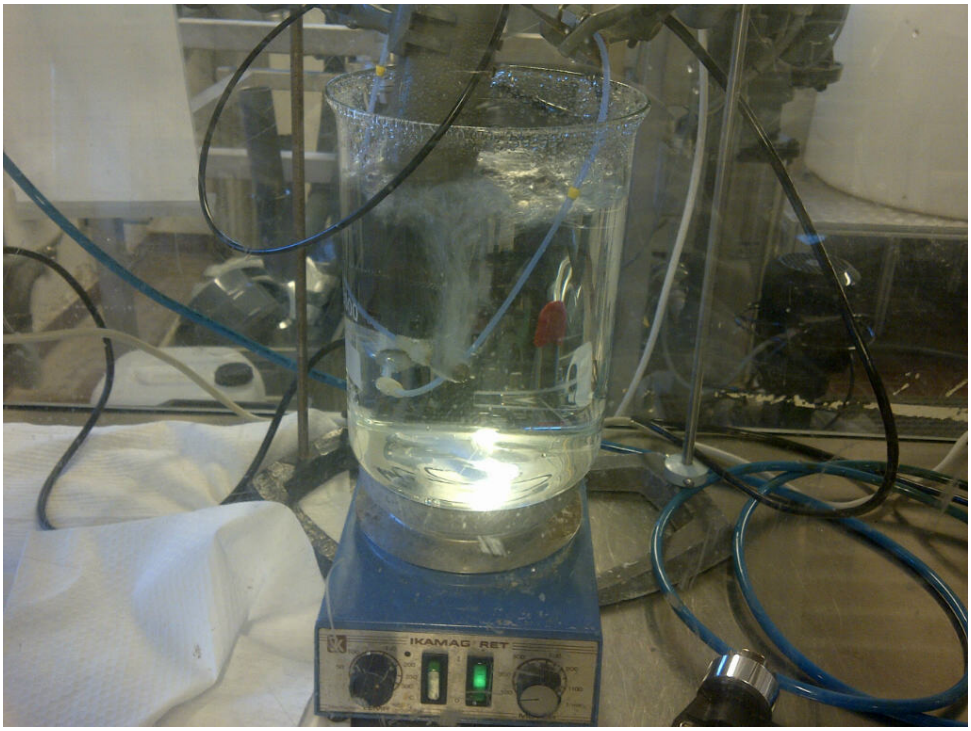

Figure 10: Purging of a beaker filled with milliQ with nitrogen gas in the glovebox

Figure 11: Collecting samples of the liquid phase the glovebox

3.3 Preliminary experiments

3.3.1 Selection purge gas, determination purge time

The glovebox was purged with nitrogen gas. The nitrogen gas was supplied by the inlet of the glovebox and 2 spargers which were submerged in the beaker that was used for the preparation of the anoxic iron(II) or manganese(II) solution. The spargers were commonly used for sparging solvents with helium in high-performance liquid chromatography (HPLC). This raises the question if helium was a more effective purge gas. Two tests were conducted: a beaker with milliQ water was purged with nitrogen, or with helium gas. The glovebox itself was purged with nitrogen gas in both cases. Figure 12 proves that the efficiency of helium and nitrogen gas is comparable. The required purge time is 150 minutes. Furthermore, in Figure 12 can be seen that immediately after the supply of purge gas to the spargers was ended, the dissolved oxygen concentration increased. An explanation is the diffusion of oxygen into the beaker, originating from small traces of oxygen still present in the glovebox atmosphere.

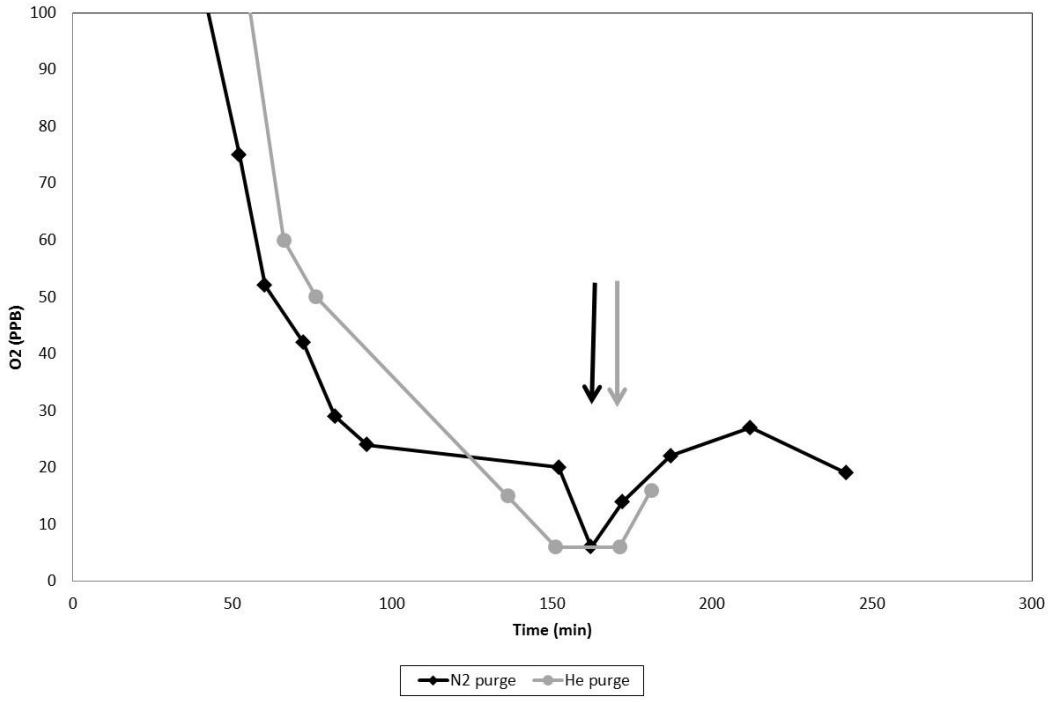

Figure 12: Comparison oxygen removal by purging with nitrogen or helium gas. The oxygen concentration (PPB) is plotted versus the purge time (min.).

3.3.2 Determination of the optimal adsorption time

Preliminary experiments were conducted to determine the optimal adsorption time and to check the air tightness of the serum bottles. Virgin sand with a grain size of 0.8-1.25 mm, and GEH® 102 were used as adsorbent because filter medium was not yet available. GEH® 102 is a high performance adsorbent based on the chemistry of ferric hydroxide produced by GEH Wasserchemie GmbH & Co. The adsorption conditions were: pH 7.5 and T=10 ºC. Samples were collected when an adsorption time of 17, 41 and 65 hours had passed.

Figure 13 and Figure 14 show that an adsorption time between 17 and 41 hours is optimal. An adsorption time of 17 hours was selected for the main experiments because of limited availability of equipment.

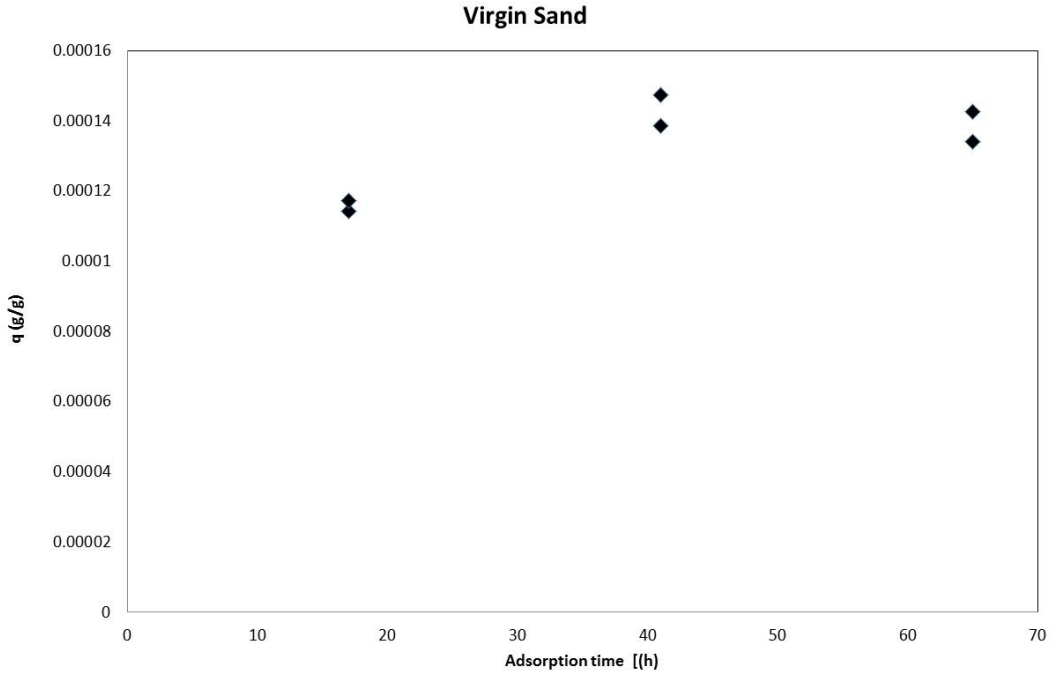

Figure 13: Iron adsorbed on new sand (g/g) versus the adsorption time (h). The 100 mL serum bottles were filled with approx. 5 g virgin sand and approx. 95 mL iron(II) solution under anaerobic conditions.

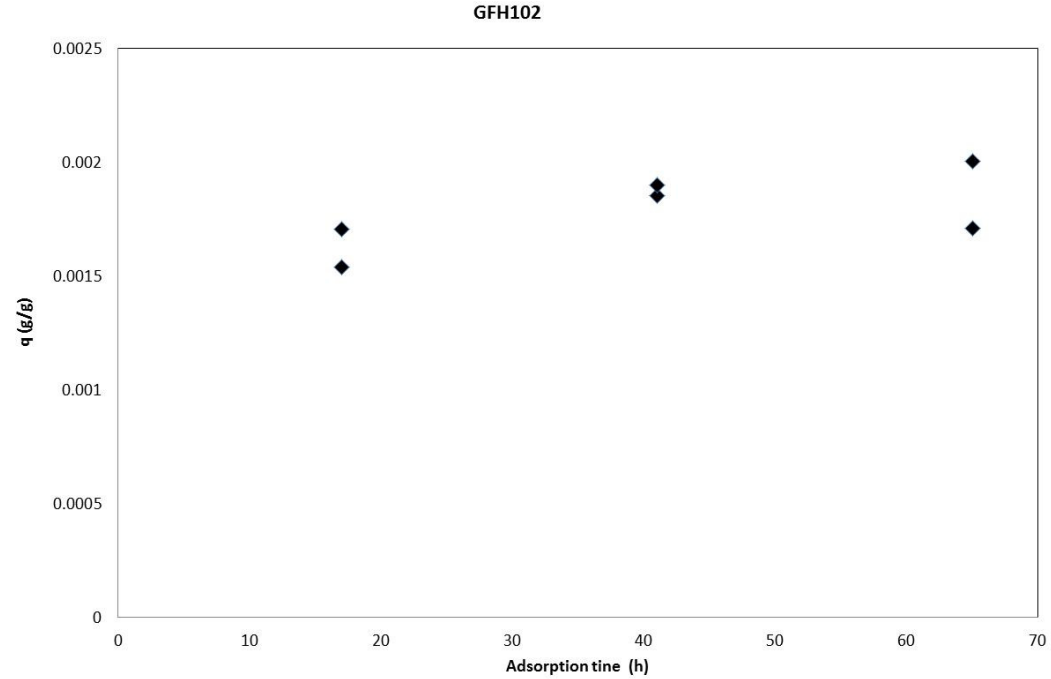

Figure 14: Iron adsorbed on granular GEH102 (g/g) versus the adsorption time (h). The 100 mL serum bottles were filled with approx. 0.55 g GEH102 and approx. 95 mL iron(II) solution under anaerobic conditions.

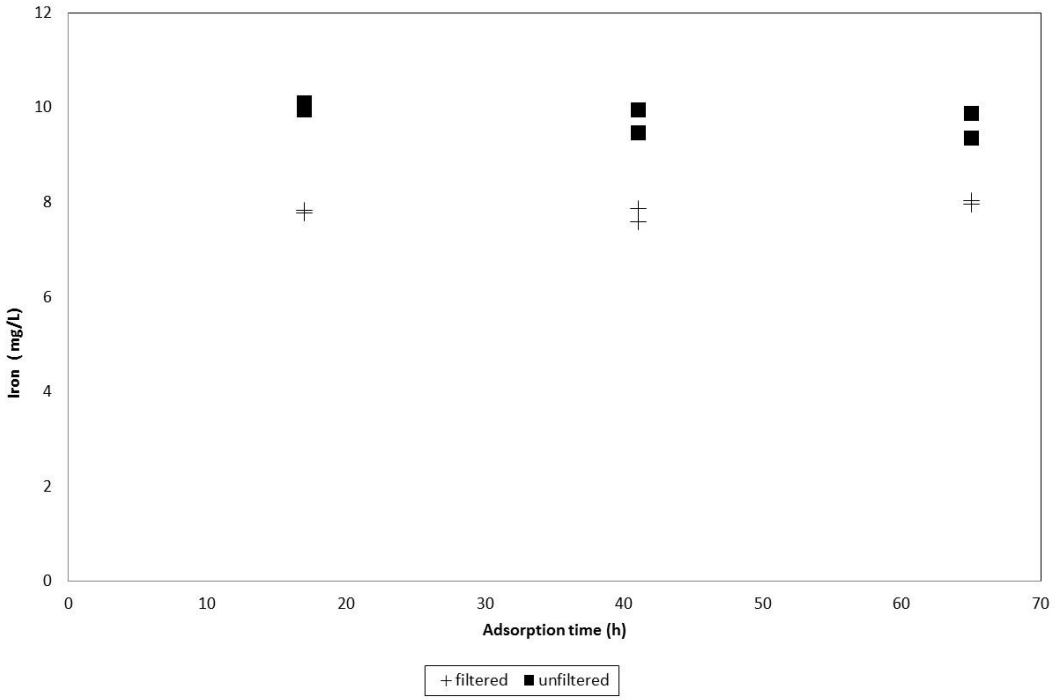

Figure 15: Iron content in filtered and unfiltered blank (mg/L)versus the adsorption time (h)

Figure 15 presents the iron content in a filtered and unfiltered blank sample versus the adsorption time. As mentioned before, a blank is a serum bottle without adsorbent. Although there is significant difference between the filtered and unfiltered blank. The difference between the filtered and unfiltered blank requires an explanation. Adsorption on the 0.45 µm membrane filter was ruled out by additional experiments.

Obviously, the first hypothesis is oxidation. Since no correlation with the adsorption time was observed, the air tightness of the serum bottles was proven.
However, the dissolved oxygen concentration in the beaker at the point of iron(II) addition was below 10 PPB. Such a low dissolved oxygen concentration does not match with the observed difference between iron content in the filtered and unfiltered blank. On the other hand, Figure 12 indicated diffusion of oxygen into the beaker, originating from small traces of oxygen still present in the glovebox atmosphere.

A second hypothesis is the formation of iron(III) carbonate particles which can be removed by a 0.45 µm filter. Carbonate was introduced by the addition of sodium bicarbonate. Table 8 displays the ion product of iron carbonate. At pH=7.5, the ion product significantly exceeds the solubility product of $FeCO_3 = 10^{-10.7}$ mol^2/L^2 (Stumm and Morgan, 1996).

Both hypotheses are plausible. The problem of the difference between the filtered and unfiltered blank is solved in equation 12 by using the filtered blank. In addition, it is recommended to conduct experiments with various sodium bicarbonate concentrations in future research.

Table 8: Ion product $FeCO_3$, the solubility product of $FeCO_3 = 10^{-10.7}$ mol^2/L^2 (Stumm and Morgan, 1996), iron(II)= 5 mg/L, $NaHCO_3$= 6 mmol/L

pH	-	7.5	7.0	6.5
CO_3^{2-}	mol/L	$6.7\ 10^{-06}$	$1.8\ 10^{-06}$	$3.3\ 10^{-07}$
Fe^{2+}	mol/L	$1.8\ 10^{-04}$	$1.8\ 10^{-04}$	$1.8\ 10^{-04}$
Ion product	mol^2/L^2	$1.2\ 10^{-09}$	$3.3\ 10^{-10}$	$6.0\ 10^{-11}$

3.4 Determination of the adsorption isotherms

The aim of the batch experiments was to determine the constants of the Freundlich isotherms for iron(II) or manganese(II). The filter media of the treatment plant Holten (VF1) and Spannenburg (VF11) were used as adsorbent. The experiments were conducted at various temperatures and pH, using the procedure described in § 3.2. The constants of the Freundlich isotherm were determined by plotting *loq(q)* versus *log(Ce)* and fitting with the method of least squares. An example is depicted in Figure 16.

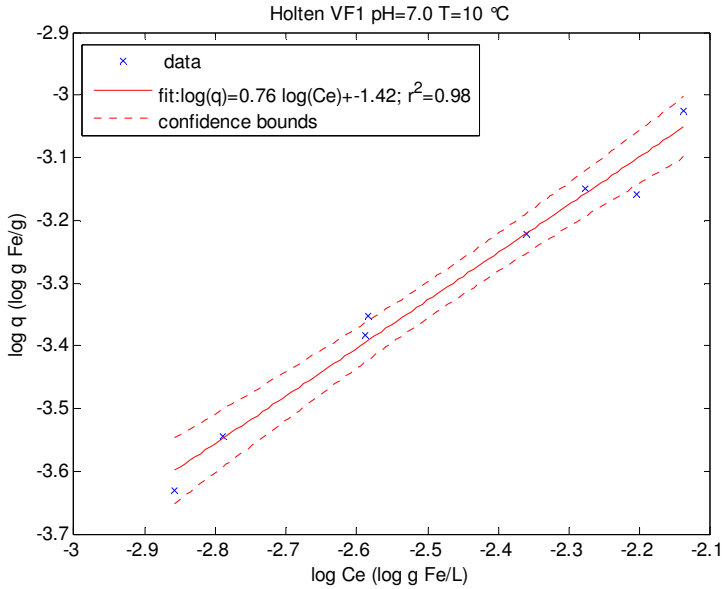

Figure 16: The constants of the Freundlich isotherm were determined with the method of least squares depicted with a solid line. The 95% confidence bounds are depicted with a dotted line

Table 9 and Table 10 show a good correlation for the filter medium collected at the Holten plant (VF1). This was in contrast with the poor correlation obtained in the experiments with the medium collected at the Spannenburg plant (VF11). This was probably due to the relative poor uniformity of the Spannenburg filter medium.
Therefore, the datasets were analyzed on *outliers*. The so-called *hat-value hi* is a common measure of leverage (Cabo, 2014; Fox, 2008). A rough cutoff for noteworthy hat-values is:

$$hi > \frac{2(k+1)}{n} \qquad (13)$$

where:
i = the hat-value, in fact the diagonal entry *hi* of the hat matrix
k = the numbers of regressors in the model, excluding the constant. In this case k=1.
n = the sample size. In this case n=8.

A second test calls attention to studentized residuals (Ei*) that are relatively large. Under ideal conditions about 5% of the studentized residuals are outside the range |Ei*|≤2 (Fox, 2008). The *hat-values* and the *studentized residuals* were calculated and plotted with the statistics toolbox of MATLAB® (Annex 9). While the calculated *hat-values* did not nominate points than can be discarded, the calculated *studentized residuals* did in 8 out of 10 cases (Annex 5 and 6). It was required to discard one outlier in 7 of these cases to achieve a value for the square of the correlation coefficient (R^2) which is larger than 0.8. In the remaining case it was required to discard two outliers. The results of the above described data analysis is presented in Table 11 and Table 12.

During the batch experiments, two series of eight serum bottles were filled with an increasing amount of adsorbent. Figure 17 shows that most outliers can be related to a low weight of adsorbent in the serum bottles. This supports the explanation that a less uniform particle size distribution is related to poor correlation.

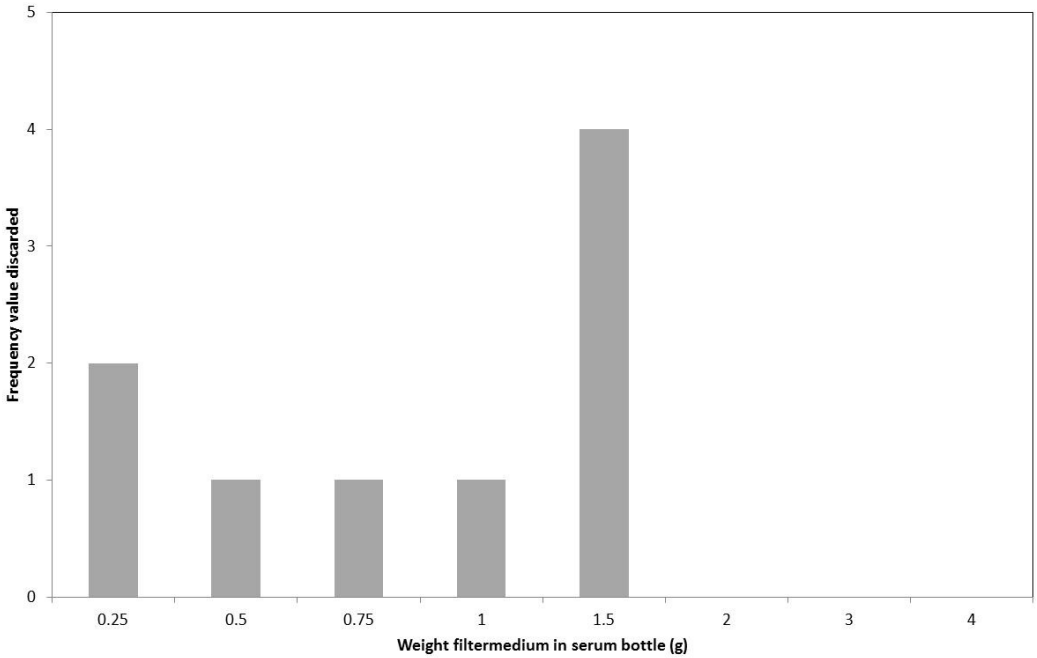

Figure 17: Frequency value of discarded outliers versus weight of the filter medium in a serum bottle

Table 9: Results iron adsorption on Holten filter medium, derived Freundlich isotherm constants, no outlier discarded (annex 4)

pH	T	log k	K	n	R^2
6.5	10	-0.97	$1.07\ 10^{-01}$	1.23	0.91
7	4	-1.73	$1.86\ 10^{-02}$	0.64	0.96
7	10	-1.42	$3.80\ 10^{-02}$	0.76	0.98
7	20	-0.14	$7.24\ 10^{-01}$	1.37	0.95
7.5	10	-1.29	$5.13\ 10^{-02}$	0.78	0.95

Table 10: Results manganese adsorption on Holten filter medium, derived Freundlich isotherm constants, no outlier discarded (annex 6)

pH	T	log k	K	n	R^2
6.5	10	0.28	$1.91\ 10^{+00}$	1.81	0.81
7	4	-1.46	$3.47\ 10^{-02}$	0.87	0.96
7	10	-1.09	$8.13\ 10^{-02}$	0.95	0.99
7	20	0.65	$4.47\ 10^{+00}$	1.59	0.98
7.5	10	-1.52	$3.02\ 10^{-02}$	0.72	0.94
7.5	10	-0.53	$2.92\ 10^{-01}$	1.13	0.92

Table 11: Results iron adsorption on Spannenburg filter medium, derived Freundlich isotherm constants, outliers discarded (annex 5)

pH	T	log k	K	n	R^2
6.5	10	-2.45	$3.55\ 10^{-03}$	0.34	0.97
7	4	-1.24	$5.75\ 10^{-02}$	0.81	0.81
7	10	-1.28	$5.25\ 10^{-02}$	0.74	0.91
7	20	-1.07	$8.51\ 10^{-02}$	0.76	0.93
7.5	10	-1.03	$9.33\ 10^{-02}$	0.79	0.96

Table 12: Results manganese adsorption on Spannenburg filter medium, derived Freundlich isotherm constants, outliers discarded (annex 7)

pH	T	log k	K	n	R^2
6.5	10	-1.21	$6.17\ 10^{-02}$	0.85	0.88
7	4	1.77	$5.89\ 10^{+01}$	1.93	0.90
7	10	-1.44	$3.63\ 10^{-02}$	0.76	0.88
7	20	-0.13	$7.41\ 10^{-01}$	1.19	0.98
7.5	10	-0.69	$2.04\ 10^{-01}$	1.03	0.86

3.5 Estimation operation time fixed bed column

3.5.1 Approach

Freundlich isotherms can be used to obtain a rough estimation of the maximum operating time of a rapid sand filter in intermittent regeneration mode. Input data for the calculations are presented in Table 13. An example of the calculation is listed in Table 14. The underlying assumptions in the calculation are a sharp edged adsorption front and no competition with other ions.

Table 13: Input data which are used to estimate the maximum operating time of a rapid sand filter in intermittent regeneration mode.
The iron removal is 99.3%. The manganese removal is 99.7%.

	Symbol	Unit	Iron	Manganese
Inflow concentration	C_{in}	mg/L	7	0.3
Outflow concentration	C_{out}	mg/L	0.05	0.01
Bulk density filter medium	P	g/L	1500	

Table 14: Example calculation, estimation of the maximum operating time of a rapid sand filter in intermittent regeneration mode

Input data:
Freundlich isotherm constants:
$K = 3.8*10^{-2}$
$n = 0.76$

Calculation of the mass adsorbed iron per mass adsorbent using equation 10:

$q=kC_e^n$ => $q = 3.8*10^{-2}*(7*10^{-3})^{0.76} = 8.76*10^{-4}$ (g/g)

Calculation of the estimated volume of water that can be treated per unit volume of adsorbent.

$Y=[q/(C_{in}-C_{out})]* \rho$

$Y = [8.76*10^{-4}/(7*10^{-3} - 5*10^{-5})]*1500 = 189$ L/g **/** g/L =189 BV

An increase of the pH improves the operating time as can be seen in Figure 18 and Figure 19. This observation is in line with equation 5.

Figure 20 and Figure 21 show that the relation between operating time and temperature is unclear. Few studies have looked at the effect of temperature on adsorption of iron (II) onto iron(hydr)oxides. These studies have concerned the temperature dependence of the adsorption of one or more of cadmium(II), copper(II), lead(II) and zinc(II) onto goethite (Johnson, 1990; Rodda *et. al.* 1993). Both studies found that adsorption increases when temperature increases. Furthermore, Rodda *et. al.* (1993) suggests that adsorption reactions for many divalent cations are endothermic. An important difference with this thesis is the temperature range, which was between 10 and 70 °C. The unclear dependence between adsorption and temperature in this thesis, can be explained by the different temperature range, or physico-chemical properties of the solute or adsorbent.

The filter medium of Spannenburg performs better in almost all experiments, which matches with the observations in chapter 2. Although the iron content in the accumulation was comparable, the mass percentage of the accumulation was much higher (paragraph 2.2.2). Furthermore, during the sequential extraction the total amount of iron recovered from filter medium of Spannenburg was relatively high compared to Holten (paragraph 2.2.4).
The only measurement which was conducted twice showed a large difference in the calculated operating time. It is obvious that more measurements are required to prove the reproducibility of this test.
Typical deep anoxic groundwater (Table 2) has a temperature of 10 °C and a pH between 6.8 and 7.2. Based on Figure 18 and Figure 19, a maximum operating time of 189 h is achievable with filter medium of Holten.

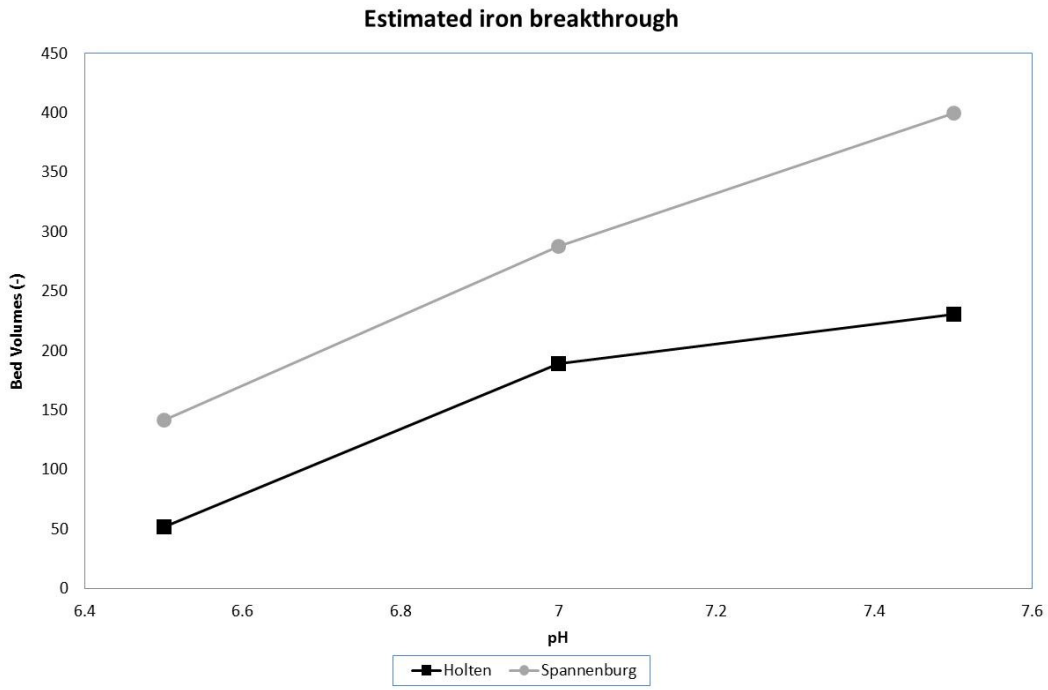

Figure 18: The influence of the pH on the estimated iron breakthrough. The estimated bed volumes are plotted versus the pH. The temperature was 10 °C.

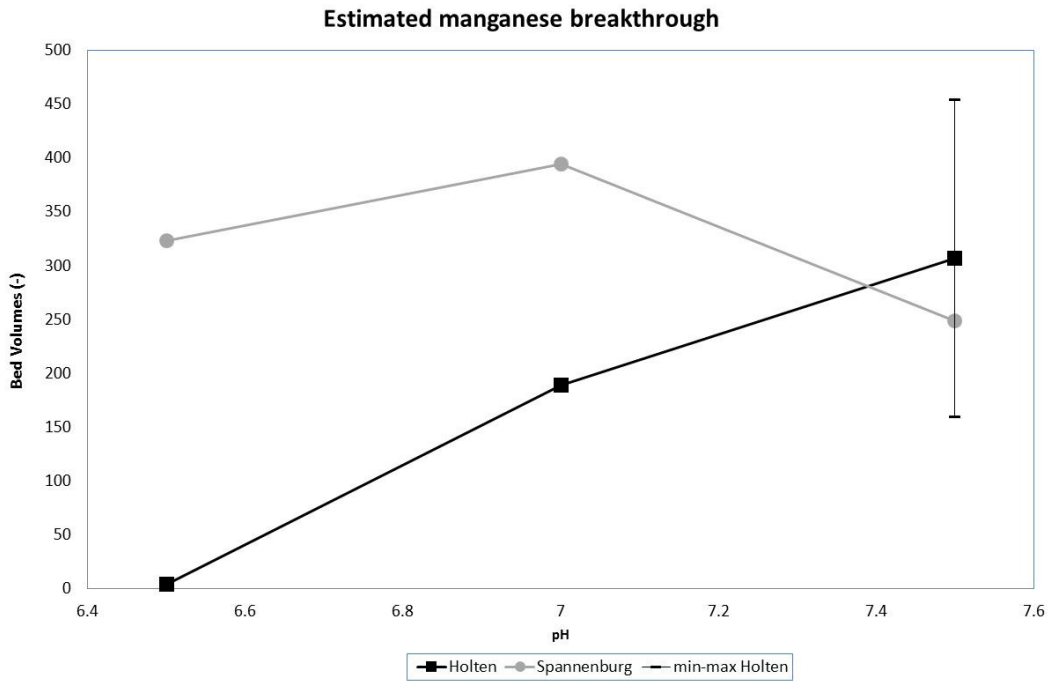

Figure 19: The influence of the pH on the estimated manganese breakthrough. The estimated bed volumes are plotted versus the pH. The temperature was 10 °C.

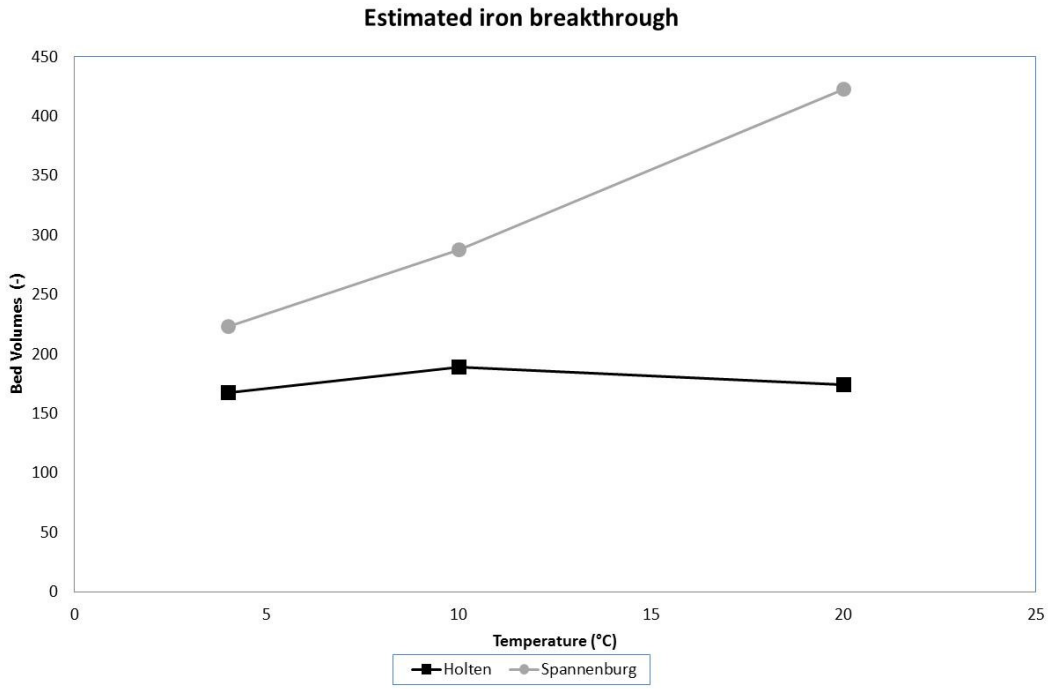

Figure 20: The influence of the temperature on the estimated iron breakthrough. The estimated bed volumes are plotted versus the temperature (°C). The pH was 7.0.

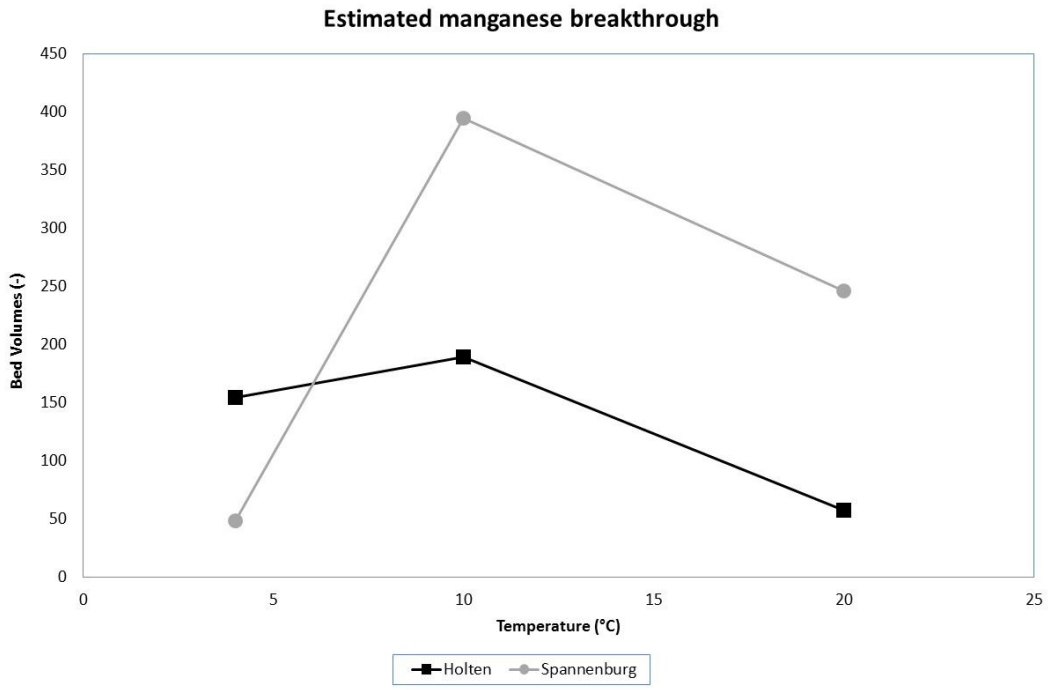

Figure 21: The influence of the temperature on the estimated manganese breakthrough. The estimated bed volumes are plotted versus the temperature (°C). The pH was 7.0.

3.6 Conclusions batch experiments

A method was developed to determine the constants for the Freundlich isotherms that describe the adsorption of iron or manganese on the filter medium of the treatment plants Holten (VF1) and Spannenburg (VF11). It is recommended to assess the reproducibility of this method, paying attention to the fast oxidation of iron by small traces of oxygen and the possible formation of iron(III)carbonate particles.
The Freundlich isotherms were used to obtain a rough estimation of the operating time of a rapid sand filter in intermittent regeneration mode. An increase of the pH improved the operating time, which was in agreement with equation 5. The estimated operating time was increased from 52 to 231 bed volumes when the pH was increased from 6.5 to 7.5 with filter medium of the plant in Holten. A clear relation between operating time and temperature was not observed.
The filter medium of the Spannenburg plant performed somewhat better in almost all experiments. This matches with the observation that the grains of this plant were coated with more iron(hydr)oxides. Typical deep anoxic groundwater (Table 2) has a temperature of 10 °C and a pH between 6.8 and 7.2. Based on a rough estimation at pH=7.0 and a temperature of 10 °C, a maximum operating time of 189 and 288 bed volumes are achievable with filter media of Holten and Spannenburg. The underlying assumptions in the calculation are a sharp edged adsorption front and no competition with other ions. An additional assumption is an ideal regeneration, i.e. the oxidation of all adsorbed iron(II).

4 Pilot plant experiments

4.1 Experimental set-up

The aim of the pilot-plant experiments was to determine optimal regeneration and contact time of a rapid sand filter in intermittent regeneration mode. The first column was filled with the filter medium of treatment plant Holten. It was used to determine the influence of the regeneration time and the hydraulic load. Filter medium of Holten was preferred over that of treatment plant Spannenburg because of its better uniformity coefficient. A second column that was filled with virgin sand, was used to determine the startup time.

4.2 Pilot plant

Two Perspex pilot-scale columns of 150 mm diameter were designed and fabricated. Figure 22 depicts a simplified process flow-diagram. The columns (Figure 23) were equipped with six sample points as specified in Table 15.
Each column was fed with anoxic water from the well field Ritskebos of treatment plant Noardburgum (Table 2) and operated in up-flow mode to rule out the uptake of oxygen. Regeneration and backwashing was facilitated by feeding the column with clean water of the Noardburgum plant that was saturated with oxygen. Rota meters measured the flow.

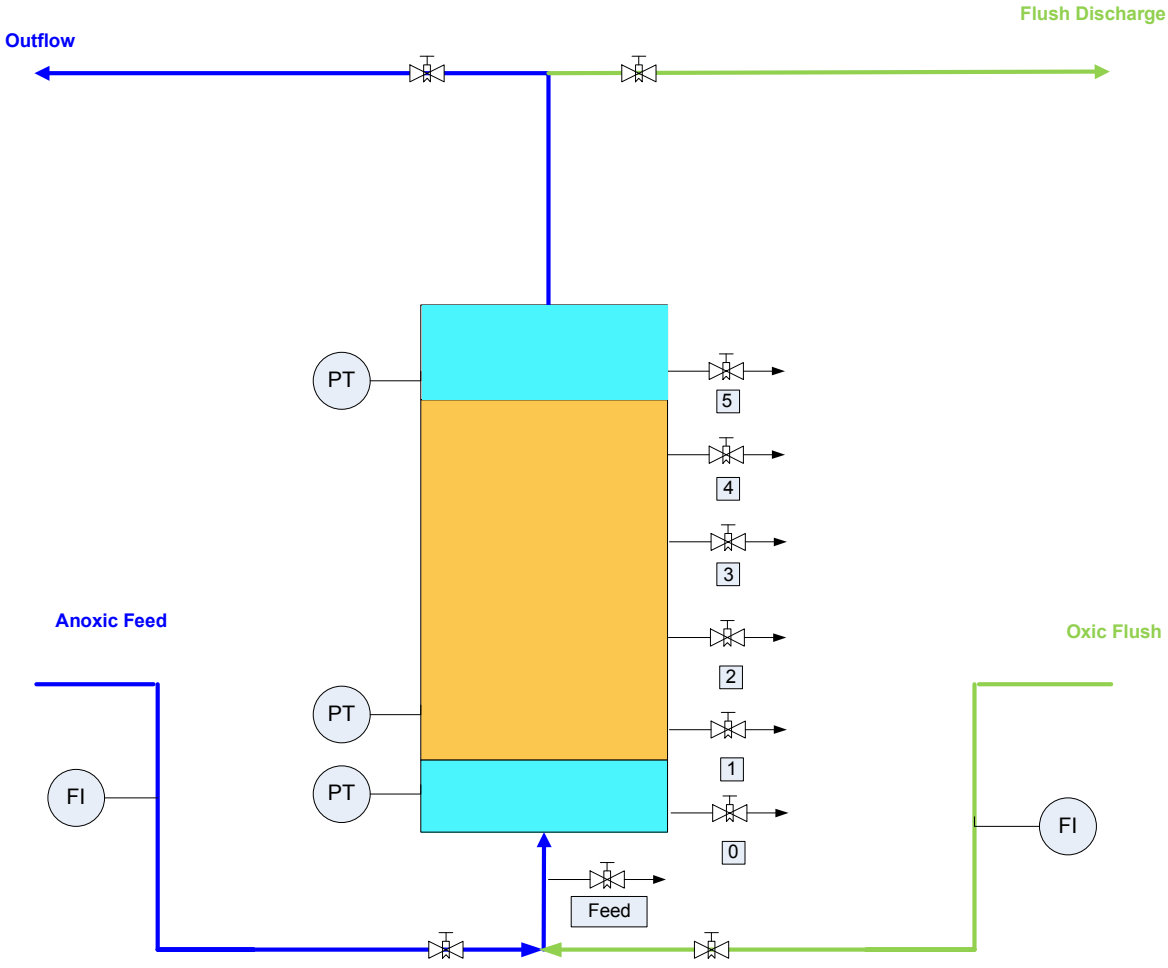

Figure 22: Process flow diagram one column of the pilot plant

Table 15: Dimensions pilot plant

Diameter	m	0.15
Height sample points	m m	0.19 m below the nozzle plate 0.47, 0.84, 1.16, 1.48 and 2.10 above the nozzle plate
Height filter medium	m	2.00
Grain size	mm	1.5-2.5

Figure 23: Photographs pilot plant, front and rear side

4.3 Overview of the experiments

In total, 26 pilot plant experiments were conducted. The goal of the first 8 experiments was to determine the optimal regeneration time while maintaining a fixed empty-bed contact time (EBCT). In the second part of the experiments, the influence of the EBCT was investigated.

Table 16 and Table 17 present an overview of important process conditions maintained during both experiments. The content of both tables is explained below:

- Column 1: Experiment number
- Column 2: Notification of a backwash. A backwash was initiated when an excess of air bubbles was observed within the filter medium.
- Column 3: Flow of oxic water during regeneration
- Column 4: EBCT during regeneration
- Column 5: Regeneration time
- Column 6: Dissolved oxygen concentration measured after the regeneration ended, at sample point 4
- Column 7: Flow of anoxic water during production
- Column 8: EBCT during production

Table 16: Overview experiment 1-8, determination optimal regeneration time

Run	Backwash		Regeneration			Production	
		Flow	EBCT	Time	O2 end	Flow	EBCT
		L/h	min	h	mg/L	L/h	min
1	1 min 1200 L/h	85	25	18.42	8.60	244	9
2	15 min 350 L/h	85	25	63.42	NM	244	9
3		85	25	329.58	9.30	244	9
4		85	25	1.00	6.20	244	9
5		85	25	16.67	9.40	244	9
6		85	25	0.50	NM	244	9
7		85	25	0.25	8.40	244	9
8		85	25	0.25	8.30	244	9

NM = Not Measured

Table 17: Overview experiment 9-26, determination effect EBCT, the row color reflects to the EBCT

Run	Backwash		Regeneration			Production	
		Flow	EBCT	Time	O2 end	Flow	EBCT
		L/h	min	h	mg/L	L/h	min
9		85	25	0.25	4.10	314	7
10	1 min 300 L/h	85	25	0.25	8.40	150	14
11		85	25	0.25	8.00	150	14
12		85	25	0.25	7.00	103	21
13		85	25	0.25	7.70	150	14
14	1 min200 L/h	85	25	0.25	0.70	103	21
15		85	25	0.25	NM	103	21
16	15 min 1000L/h, 20 min200 L/h	85	25	0.58	NM	103	21
17		85	25	3.00	0.90	244	9
18	20 min 1000L/h, 20 min200 L/h	175	12	0.33	NM	244	9
19		85	25	0.25	<0.5	314	7
20		85	25	0.25	1.30	103	21
21		85	25	0.25	<0.5	244	9
22		85	25	41.08	8.00	244	9
23		85	25	113.83	9.20	244	9
24		85	25	187.17	8.40	314	7
25		85	25	452.08	8.50	150	14
26		85	25	837.00	9.40	103	21

NM = Not Measured

4.4 Influence of the regeneration time

Figure 24 and Figure 25 show the outcome of the first eight experiments. They show that a regeneration time of more than 15 minutes did not improve the iron removal or the iron load. When we consider that this equals around one pore volume of the filter medium, it appears that the regeneration procedure is rather efficient. Based on these preliminary results, a regeneration time of 15 minutes was applied during the subsequent experiments.
The second part of the experiments revealed, however, that a longer regeneration time was required, as oxic conditions were not achieved at a regeneration time of 15 minutes from experiment 13 onward. Oxic conditions during regeneration were restored at the start of experiment 22 by a regeneration lasting 41 h. An incomplete regeneration deteriorates markedly the iron removal as can be seen in Figure 26 and Table 18. It seems that the oxygen demand during the regeneration increased from one regeneration to the next. An explanation for this phenomenon is discussed in paragraph 4.5. As a consequence, the optimum regeneration time was not found; this should be a task of future research.

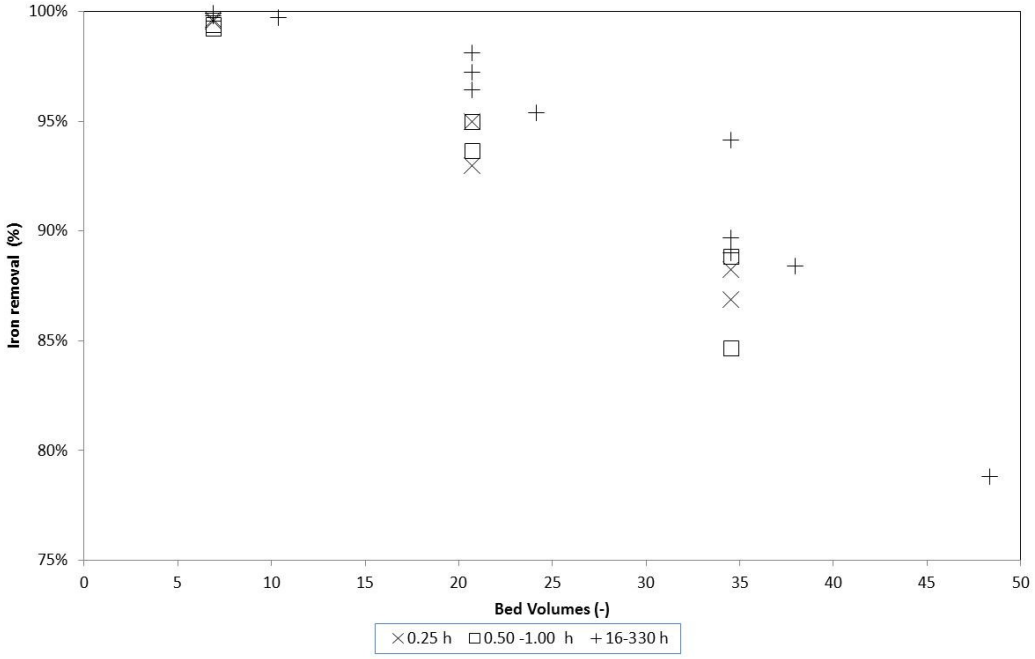

Figure 24: Influence regeneration time on iron removal. The iron removal is plotted versus the produced bed volumes.

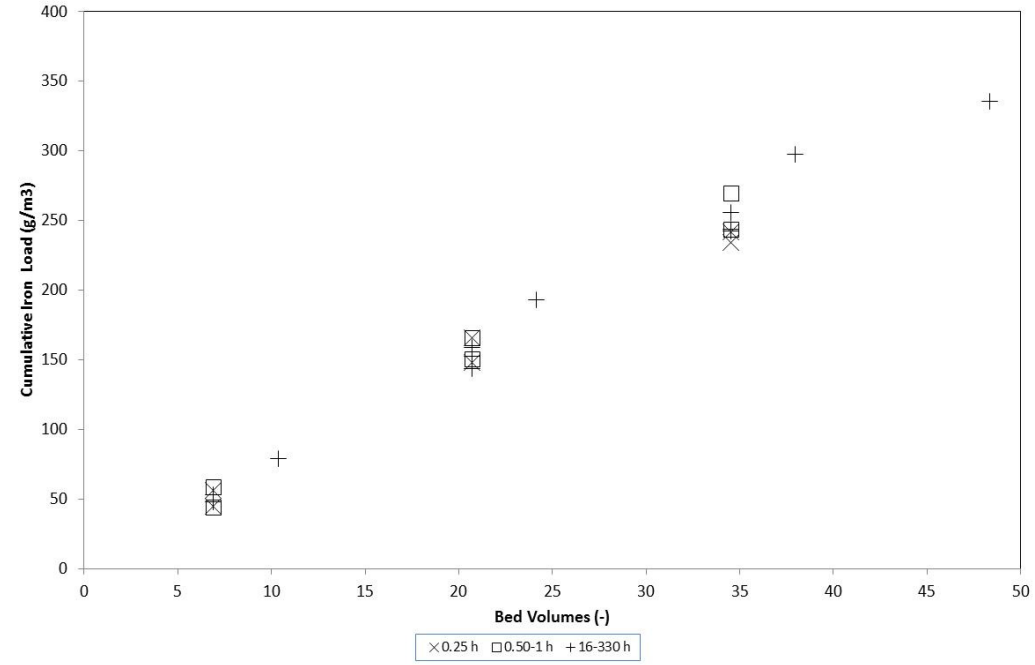

Figure 25: Influence regeneration time on cumulative iron load. The cumulative iron load (g/m^3) is plotted versus the produced bed volumes.

Table 18: Overview runs EBCT=9 min.

Run	Backwash		Regeneration			Production	
		Flow	EBCT	Time	O2 end	Flow	EBCT
		L/h	min	h	mg/L	L/h	min
3		85	25	329.58	9.30	244	9
5		85	25	16.67	9.40	244	9
7		85	25	0.25	8.40	244	9
8		85	25	0.25	8.30	244	9
21		85	25	0.25	<0.5	244	9
22		85	25	41.08	8.00	244	9
23		85	25	113.83	9.20	244	9

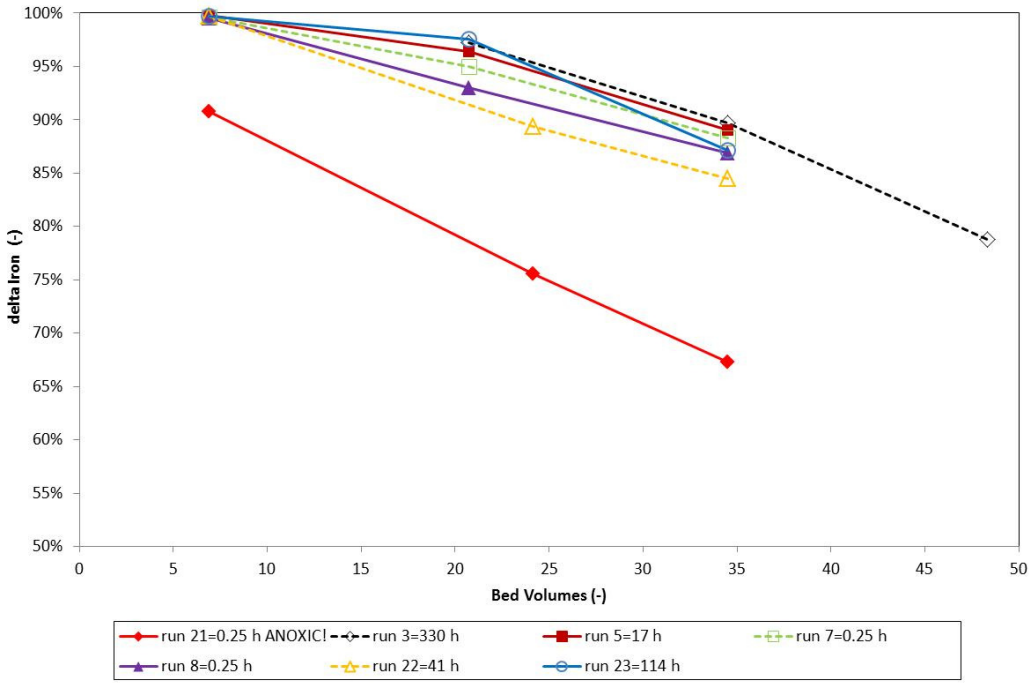

Figure 26: Poor iron removal due to incomplete regeneration during run 21. The iron removal is plotted versus the produced bed volumes

4.5 Hypotheses of the increased oxygen demand for filter medium regeneration

Paragraph 4.4 concludes that the oxygen demand during the regeneration increased from one regeneration to the next. There are three hypotheses for the increased oxygen demand during regeneration: 1) an increased iron load, 2) biological ammonium oxidation and 3) biological methane oxidation. Figure 27 rules out a difference in iron load. In addition, nitrification occurred from the first experiment onward as depicted in Figure 28. Furthermore, the average ammonium concentration in the anoxic well water of 0.9 mg/L was not in line with the almost complete oxygen consumption observed in e.g. experiment 21. The most likely hypothesis is, therefore, biological methane oxidation. During the regeneration, an anoxic water volume is displaced by an oxic water volume. A mixed, slightly oxic transition zone is therefore thinkable. This transition zone will contain methane. Assuming that short-term anoxic conditions does not deactivate methane oxidizing bacteria, biological oxidation of methane will take place. The average methane concentration was 6.7 mg/L, which equals an oxygen demand of 26.8 mg/L; the observation that the oxygen demand increased over time can be explained by this hypothesis. The filter medium was from the Holten plant where methane was absent in the raw water. It is plausible that methane-oxidizing bacteria adapted on the filter medium causing methane removal to increase exponentially.
Unfortunately methane measurements were not conducted. Instead, the hypothesis was tested by salt-spiking experiments, which should provide useful information about the transition zone. In other words, we seek the change in the concentrations of oxygen, iron, ammonium and methane in the transition zone.

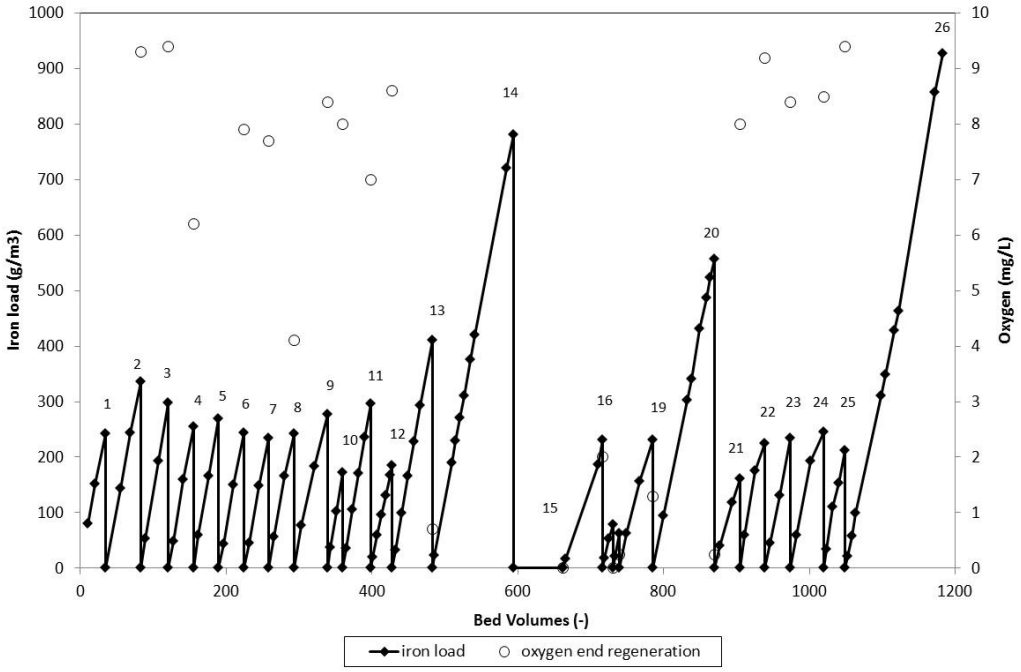

Figure 27: Iron load (g/m^3), and oxygen concentration (mg/L) at the end of the regeneration procedure versus cumulative bed volumes. The numbers refer to the run number

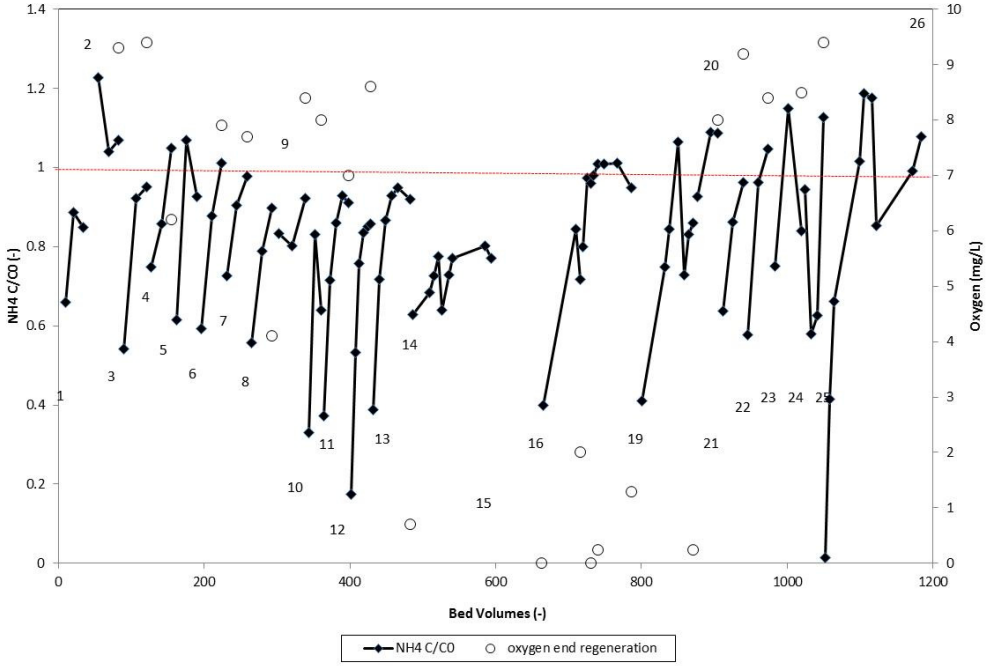

Figure 28: Ratio inflow/outflow ammonia concentration, and oxygen concentration (mg/L) at the end of the regeneration procedures plotted versus the cumulative bed volumes. The numbers refer to the run number

The salt-spiking experiments were carried out on 28 January 2015. The inflow of the test column was spiked with saturated sodium chloride solution at a water flow of 100 L/h. At the moment that the electrical conductivity of the inflow was equal to the outflow, the experiment was started. The spiking was stopped and the course of the sodium chloride concentration in sample points 0, 4 and 5 (Figure 22) was monitored by the measurement of the electrical conductivity. Thus the displacement of an anoxic volume by an oxic water volume was simulated. Based on the course of the electrical conductivity (Figure 29) the concentrations of oxygen, iron, ammonium and methane were calculated (Figure 30). Next, the delay of the oxygen front in the transition zone was calculated. Figure 31 shows that biological methane oxidation can explain the observed increase of the oxygen demand during the regeneration procedure, because after 2.3 bed volumes, the calculated delay by methane oxidation reaches 80% of the end value. Figure 29 demonstrates also that the filter column does not show ideal plug flow reactor behavior.

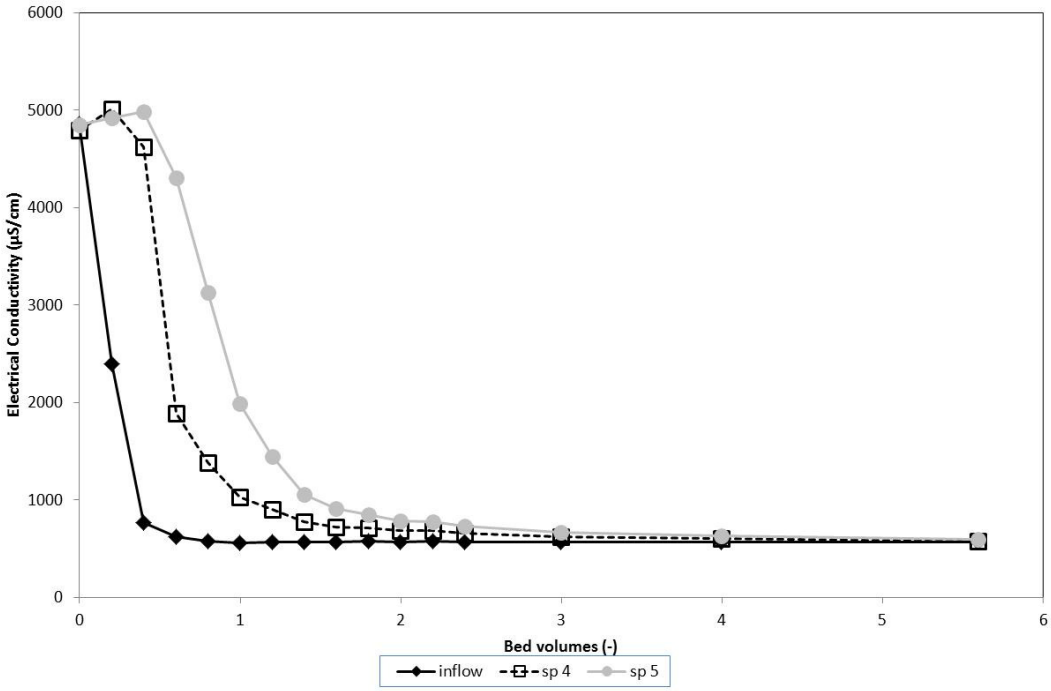

Figure 29: Course of the electrical conductivity (µS/cm) versus bed volumes

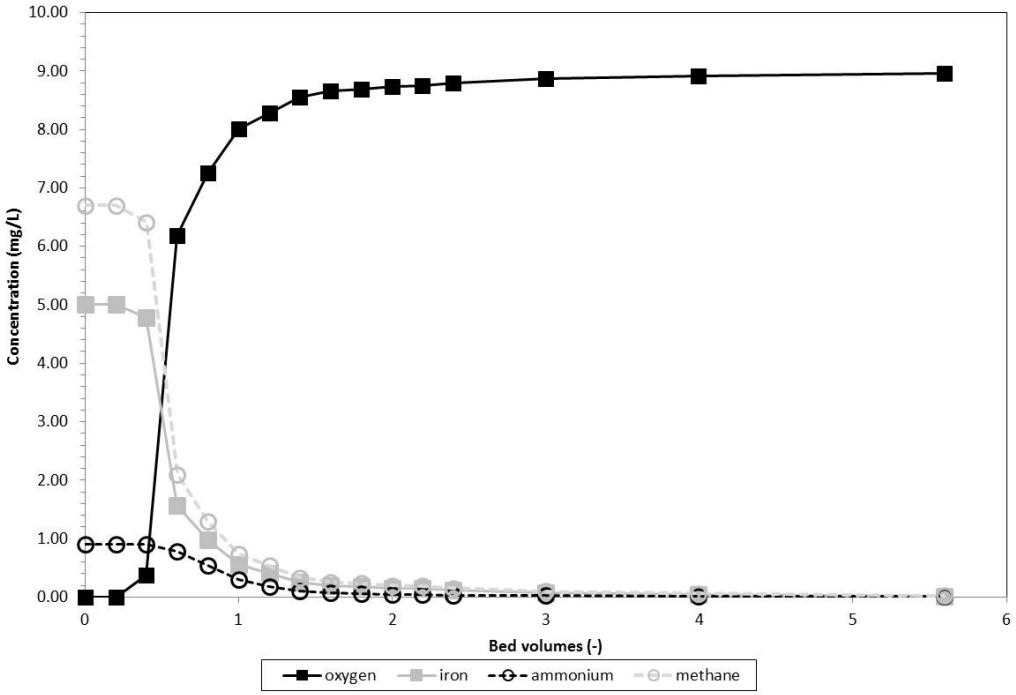

Figure 30: Calculated course of the concentrations of iron, ammonium and methane in the transition zone. No oxidation is assumed. Initial concentration: iron 5 mg/L, ammonium 0.9 mg/L, methane 6.7 mg/L. Oxic water contains 9 mg/L oxygen.

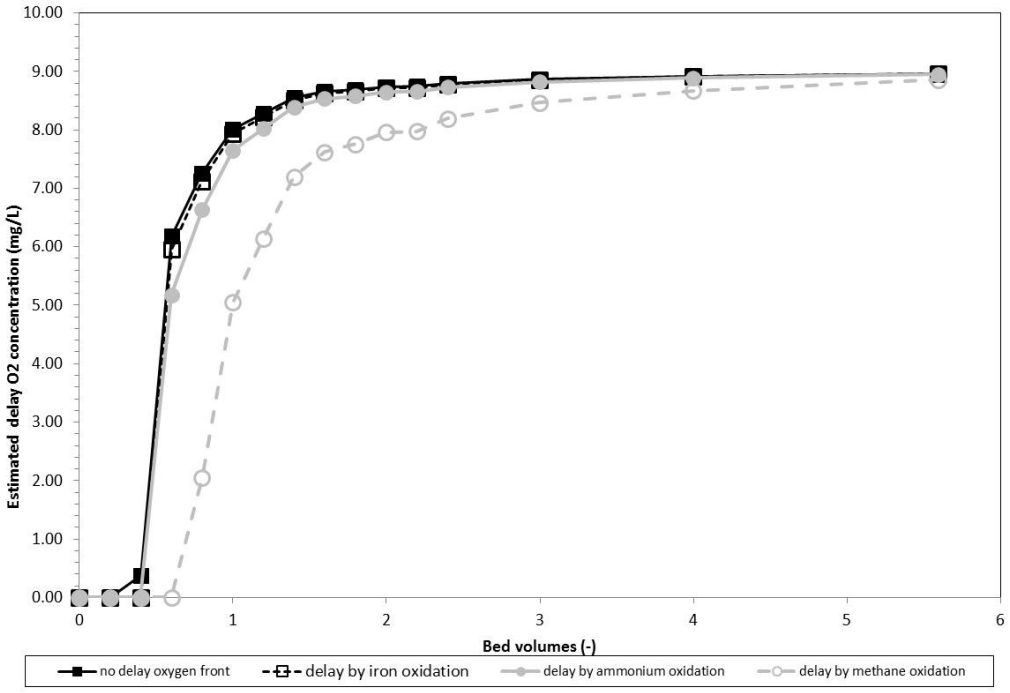

Figure 31: Computed delay of the oxygen front during regeneration due to the oxidation of iron, ammonium or methane. Assumed oxygen demand: iron 0.14 mg/mg O_2, ammonium 3.6 mg/mg O_2, methane 4 mg/mg O_2

4.6 Influence of empty bed contact time, the EBCT

Figure 32 shows how the iron removal markedly decreased when the Empty Bed Contact Time, (EBCT), is decreased. An additional advantage of a larger EBCT is an increased cumulative iron load (Figure 33). This implies that kinetic limitations play an important role. The plots of the concentrations of iron, manganese and calcium versus the height of the filter medium also indicate kinetic limitations at work (Figure 34).
At an EBCT of 21 minutes, the iron removal dropped below 99% after 17 bed volumes and below 98% after 73 bed volumes. An operating time of 189 bed volumes was estimated based on the batch experiments that were described in chapter 3. Although we assumed a sharp edged concentration front and no competition with other ions, the salt spiking experiments lead to the conclusion that there exists no such sharp-edged adsorption front (Figure 29).
The cumulative load of iron, manganese and calcium is depicted in Figure 35 at various EBCT. It appeared that iron-coated sand acted like a cation exchanger. It is striking to see that the cumulative calcium load is larger than the cumulative iron load. This means that calcium competition will affect the adsorption of iron under anoxic conditions. Adsorption of manganese is, however, negligible.The low cumulative manganese load can be explained by the low influent concentration. The cumulative iron load is rather high compared to the cumulative calcium load when we take the inflow concentration into account. Iron(hydr)oxides have probably more affinity for the more similar iron(II) than for other divalent cations like calcium or magnesium. In contrast to iron and manganese, calcium is usually not removed by full-scale rapid sand filters which are operated under oxic conditions. This difference between oxic and anoxic filtration requires an explanation. Heterogeneous oxidation will attach iron and manganese irreversibly to the filter medium. On the other hand, heterogeneous oxidation of calcium is not possible so that calcium can still be desorped and replaced by iron and manganese under oxic conditions. Moreover, iron can be removed by homogeneous and biological oxidation.

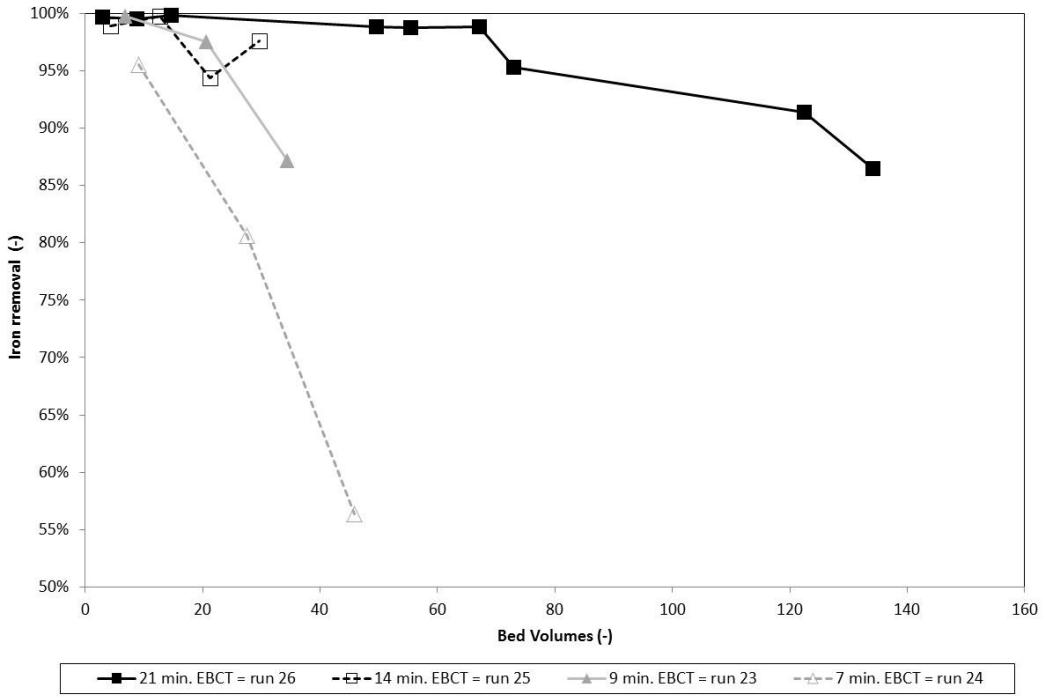

Figure 32: Iron removal vs produced bed volumes at various EBCT

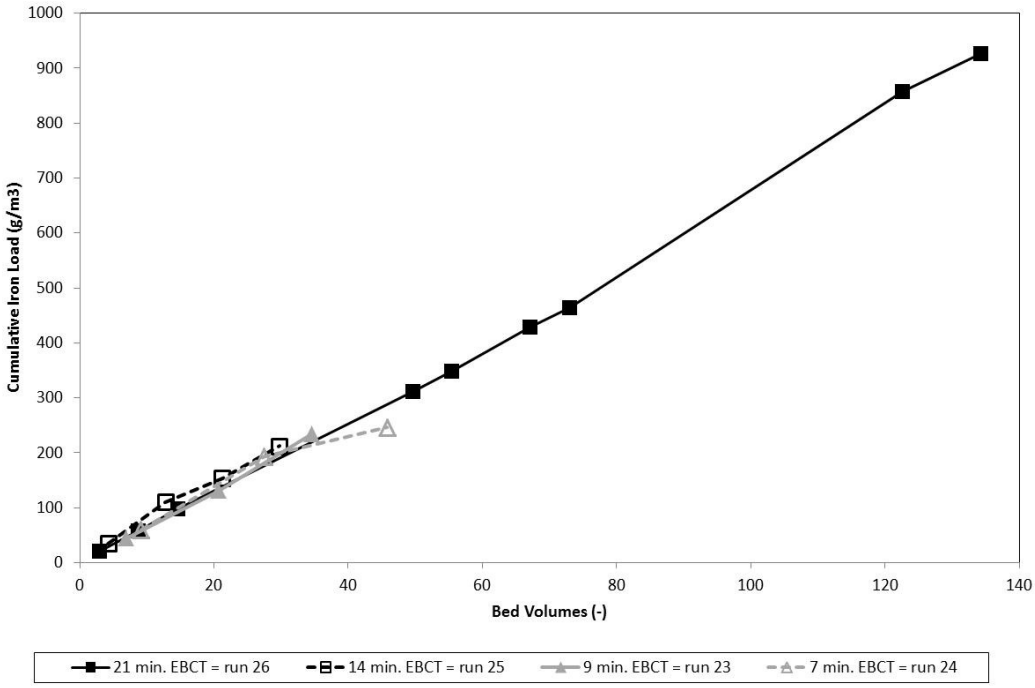

Figure 33: Cumulative iron load (g/m^3) vs produced bed volumes at various EBCT

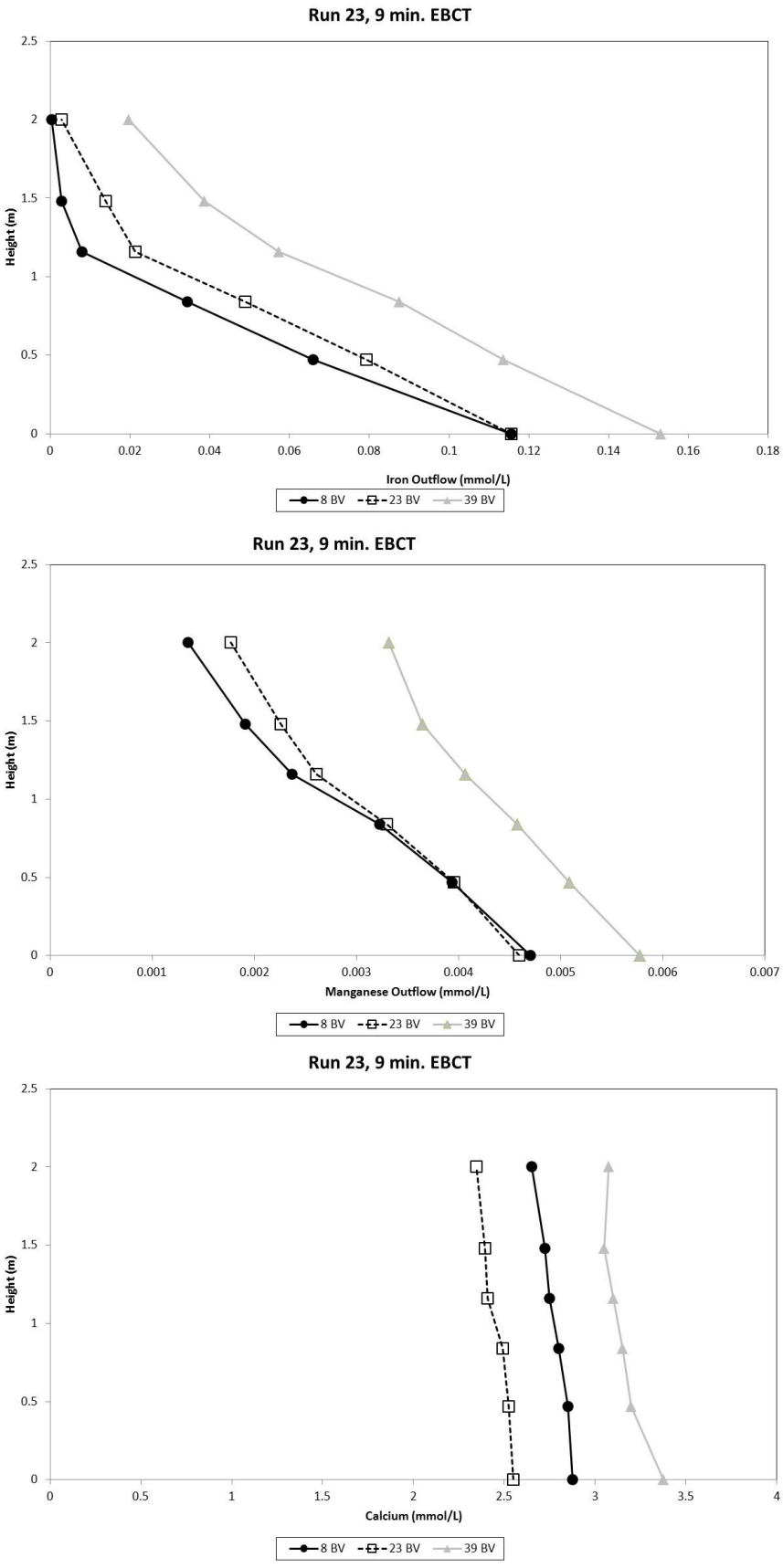

Figure 34: The concentration (mmol/L) of Iron (top), manganese (middle) and calcium (bottom) versus the height of the filter medium (m), at various bed volumes. Mind the different scale of the x-axis.

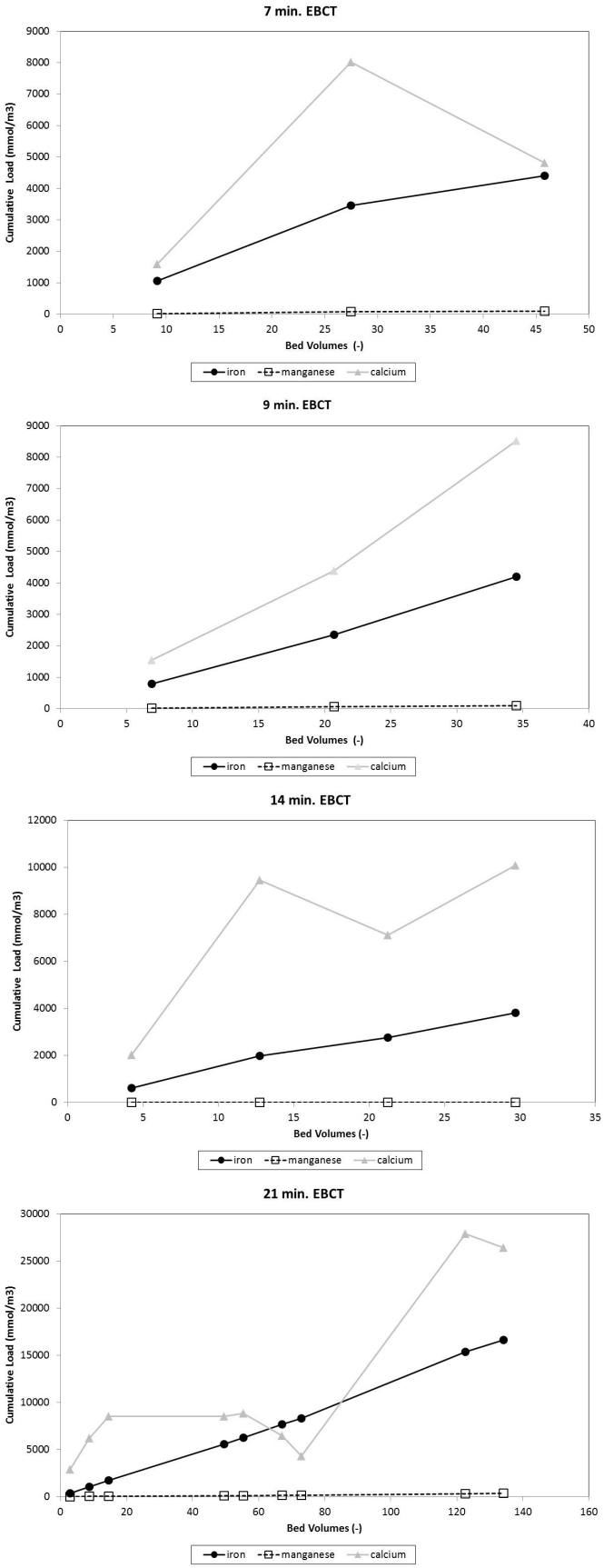

Figure 35: Cumulative load of iron, manganese and calcium at various EBCT. Mind the different scale of the y-axis.

4.7 Start-up time for virgin sand

The remaining question was the startup time of rapid sand filters in intermittent regeneration mode. Therefore, a second column was filled with virgin sand (1.5-2.5 mm). Switching between the oxic regeneration and anoxic production was enabled by a set of control valves and a PLC. Phase 1 started with a regeneration time of 1 hour and 4 cycles per day. The regeneration time was extended to 3 hours, after 103 cycles in phase 2 to accelerate the start-up (Table 19). Figure 36 and Figure 37 show the course of the iron removal and cumulative iron load. More than 123 cycles were required to get the iron-removal process going, which implies a water loss of 3295 bed volumes. Sharma (2001) achieved almost complete iron removal in less than 75 cycles. The slightly faster start of the iron removal observed by Sharma was probably caused by the use of finer sand, a lower iron concentration and a higher calcium and methane concentration. Iron oxidizing bacteria may also play a role.

Table 19: Process conditions start-up virgin sand

		Phase 1	Phase 2
Cylces	cycles /day	4	3
Regeneration			
Time	h	1	3
Flow	L/h	150	150
EBCT	min.	14	14
Bed Volumes	BV	4	13
Production			
Time	h	5	5
Flow	L/h	150	150
EBCT	min.	14	14
Bed Volumes	BV	21	21

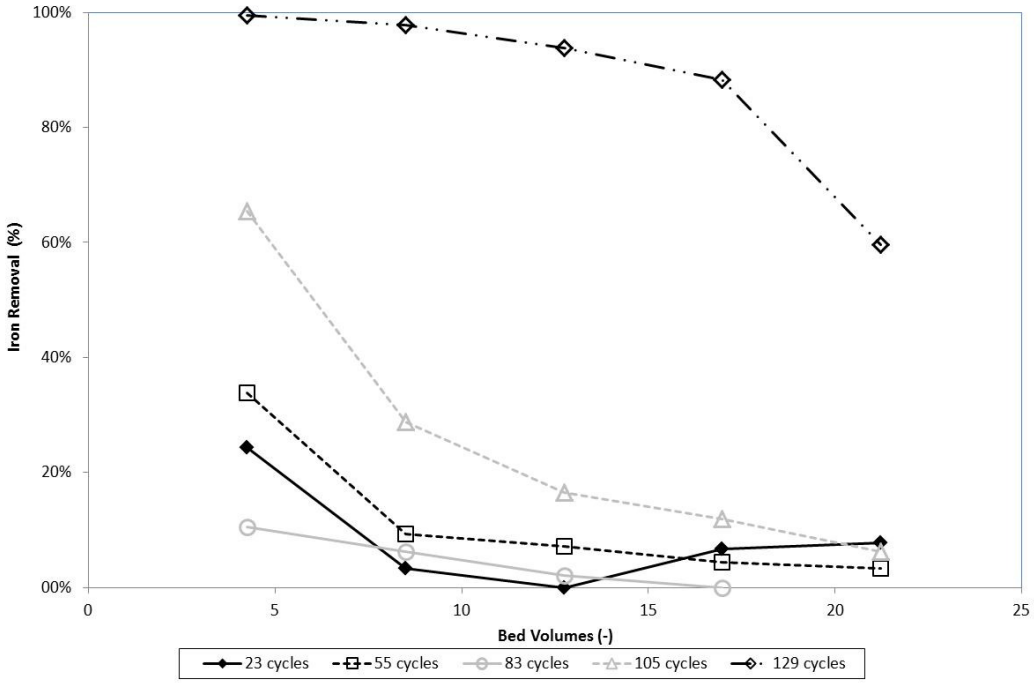

Figure 36: Iron removal start-up with virgin sand

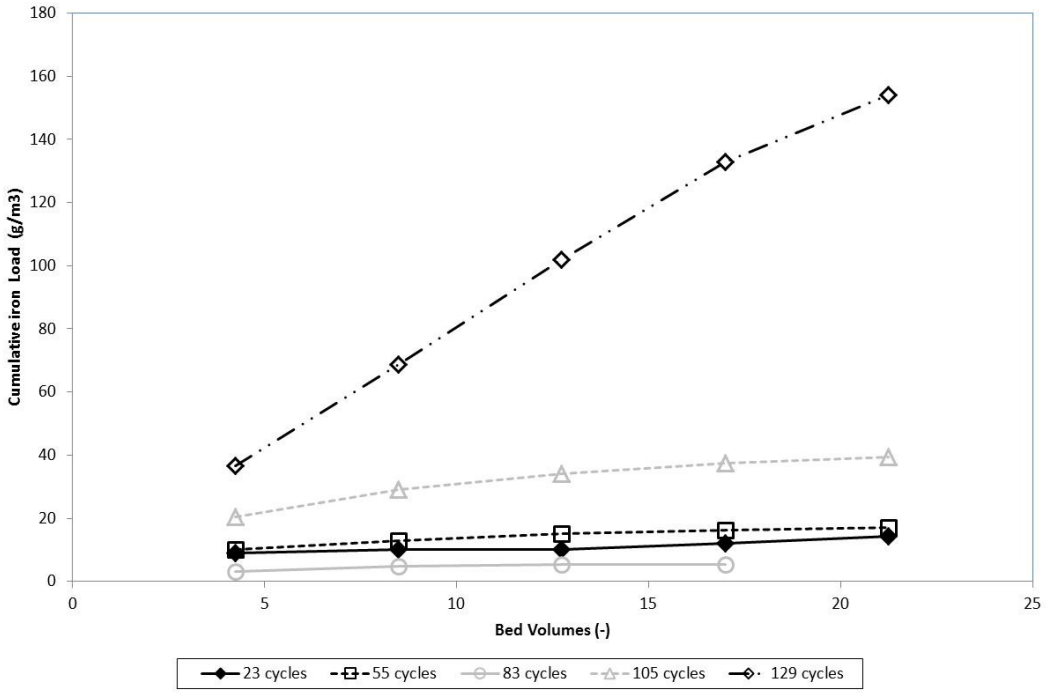

Figure 37: Cumulative iron load versus produced bed volumes during start-up with virgin sand

4.8 Conclusions with respect to the pilot plant

Two pilot-scale columns were used to study the performance of rapid sand filters to remove iron in intermittent regeneration mode. A column that was filled with filter medium was used to determine the influence of the regeneration time and the hydraulic load. High methane concentrations impeded the determination of the optimal regeneration time. Salt-spiking experiments showed that 2.3 bed volumes were required to expel 80% of the methane during the regeneration procedure. It is obvious that the oxidation of adsorbed iron requires oxygen. However, the results of the experiments did not provide information about the oxygen demand of the adsorbed iron. An alternative approach is to compute it with equation 6.
The iron removal markedly increased when the EBCT was increased, indicating that Kinetic limitations played an important role. At an EBCT of 21 minutes, 49 bed volumes could be treated before the iron removal dropped below 98.8%, a performance below what was estimated on the basis of the batch experiments. The difference may be explained by the absence of a sharp adsorption front as was proven by the salt-spike experiments. Moreover, calcium adsorption was shown to compete with iron adsorption.
A second column that was filled with virgin sand was used to determine the startup time. More than 123 cycles were required to get the iron removal going, which equals a water loss of 3295 bed volumes.

5 Discussion

5.1 Comparison with full-scale filters

The aim of this thesis was to determine the feasibility of heterogeneous iron oxidation by a rapid sand filter in intermittent mode. Therefore, the results of this research were compared with full-scale filters of water treatment plant: 1) Sint Jansklooster and Spannenburg, where homogeneous iron oxidation is expected to be more dominant, 2) Grobbendonk, where heterogeneous and biological iron oxidation is expected to be more dominant.
An important distinction between the groundwater composition of Grobbendonk, and Sint Jansklooster and Spannenburg, is the very low methane concentration and the extremely high iron content in Grobbendonk (Table 2).
The conventional oxic pre-treatment of Sint Jansklooster and Spannenburg consists of rapid sand filters preceded by plate aeration. The aeration of Grobbendonk is less intensive, it consists of a split stream cascade aerator. Table 20 shows that Grobbendonk perform better than Sint Jansklooster and Spannenburg. The number of bed volumes treated water and the cumulative iron load at Grobbendonk is much higher. As a consequence, the water volume required for backwashing is lower. These observations confirm the potential advantages of heterogeneous iron oxidation over homogeneous iron removal. By contrast, the anoxic pilot pilot plant performed less than the oxic full-scale filters of Sint Jansklooster and Spannenburg. For example, if we compare equal iron-removal efficiencies, the number of bed volumes and the cumulative iron load of a conventional filter is much higher. At an EBCT of 21 minutes, 49 bed volumes could be treated before the iron removal dropped below 98.8%. The oxic pre-filters of Sint Jansklooster demonstrated an iron removal of 99.3 % and could treat 100 bed volumes.
It is plausible that the pilot plant performs better at a lower EBCT, that is more similar to the EBCT in the oxic full-scale filters. However, this comes at the expense of one of the potential advantages of heterogeneous iron oxidation, a high filtration rate.
It is more complicated to compare the regeneration phase with the backwash phase. In the first place, the results of the experiments did not provide information about the oxygen demand of adsorbed iron. Although we have learned that at least 2.3 bed volumes are required to expel 80% of the methane during the regeneration procedure. Therefore, 2.3 bed volumes are a minimal value in the most right column of Table 20. The maximum oxygen demand of adsorbed iron was, however, calculated with equation 6 with underlying assumptions that all the adsorbed iron(II) is oxidized and a regeneration stream contains 9 mg/L oxygen. Thus after the treatment of 72 bed volumes anoxic water, 7.4 bed volumes oxic water were required to regenerate the filter, thus, yielding the maximum computed value is 9.7 bed volumes.
The experiments did not answer the question if water that was used for regeneration should be considered a loss; it is plausible that a sizable quantity of it can be reused in the treatment. However, reuse of the regeneration water will increase the required capacity of the filters. When a filter is regenerated, it is obviously not available for production. The required filter volume will, therefore, increase.

Table 20: Performance oxic full-scale rapid sand filters compared with performance pilot plant. At Sint Jansklooster and Spannenburg is homogeneous iron oxidation expected to be more dominant. At Grobbendonk is heterogeneous and biological iron oxidation expected to be more more dominant. The four data points of the pilot plant are measured values from run 26.

		st. Jansklooster	Spannenburg	Grobbendonk	Results pilot plant run 26			
Production phase								
Iron inflow	mg/L	7	12	36	6.91	6.14	6.96	6.26
Iron outflow	mg/L	0.05	0.02	0.1	0.01	0.07	0.08	0.29
Operating Time	h	59	40	50	5	17	23	25
Flow	m3/h	85	175	170	0.1	0.1	0.1	0.1
Area	m2	25	40	30	0.018	0.018	0.018	0.018
Medium height	m	2	2.5	2.5	2	2	2	2
EBCT	min	35	34	26	21	21	21	21
BV	BV	100	70	113	15	49	67	72
Iron removal	%	99.3%	99.8%	99.7%	99.8%	98.8%	98.8%	95.3%
Cumulatvie Iron Load	g/m3	697	839	4069	98	311	429	463
Backwash phase								
Water volume	m3	163	310	102	0.08-0.14	0.08-0.26	0.08-0.32	0.08-0.34
Water volume	BV	3.3	3.1	1.4	2.3-3.9	2.3-7.2	2.3-9.1	2.3-9.7
Efficiency								
Backwash:Production	BV/BV	1:33	1:22	1:83				
Regeneration:Production	BV/BV				1:7-1:1.4	1:26-1:8	1:29-1:7	1:31-1:7

5.2 Comparison with subsurface iron removal

As stated in chapter 1, subsurface iron removal (SIR) and heterogeneous iron oxidation in rapid sand filters are analogue. The volumetric ratio (V/Vi) in subsurface treatment varies between 1:3 and 1:20 when the injection water is saturated with oxygen under atmospheric conditions. This ratio is of the same order of magnitude as the *ratio of the number of produced bed volumes over the number of bed volumes required for regeneration* in Table 20, thus demonstrating the analogy.

5.3 Opportunities change process configuration

Two process configurations that allow heterogeneous iron oxidation by a rapid sand filter in intermittent mode were discussed in paragraph 1.8. They are shown below as configurations 2 and 3 in Figure 38. Configuration 1 shows typical treatment of deep anoxic, methane-rich groundwater using plate aeration followed by rapid sand filtration. In configuration 2, a prefixed extra filtration step removes manganese and ammonia. Alternatively, in configuration 3, aerated water is softened by a pellet reactor.
The presumed advantages of this concept were high filtration rates, excellent iron removal, reduced backwash water losses and reduced cleaning of the plate aerators.
A high filtration rate is equivalent to a short EBCT. The EBCT during the experiments was short compared to that of a conventional filter. Reuse of regeneration water may limit water losses, but it does not solve the problem that a filter is unavailable for production during regeneration. Table 20 indicates that an excellent iron removal is at least achievable for a short time; from approximately 15 bed volumes onward, the iron removal efficiency decreased gradually.

Configurations 2 and 3 offer both the opportunity to reduce the cleaning frequency of the plate aerators, but the relatively low cost of cleaning the plate aerators of € 72000 for the Spannenburg plant in 2014 (Westra-Marsman, 2015) does not warrant a change of the process configuration.
An additional problem is the observed slow start-up with virgin sand, which would result in high water losses. A startup with iron-coated sand is still an option.

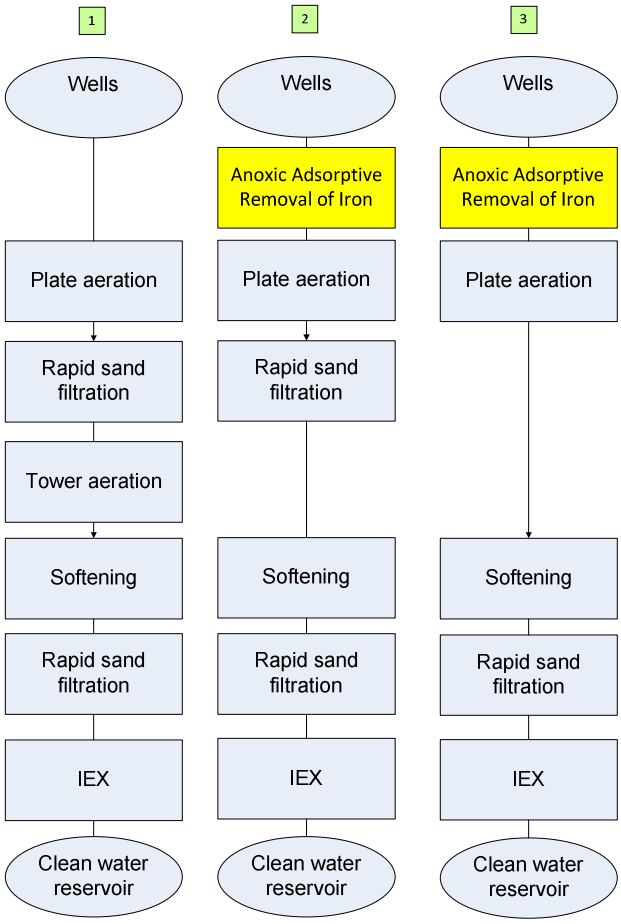

Figure 38: Schematic diagram optional process configurations for implementation intermittent iron removal

6 Conclusions

The potential advantages of heterogeneous iron oxidation over homogeneous iron removal are high filtration rates, excellent iron removal and reduced losses of backwash water as demonstrated by the excellent performance of the pre-filters of water treatment plant Grobbendonk. Heterogeneous iron oxidation dominates at Grobbendonk because the supernatant is slightly anoxic and the pH is low. Thus adsorption and oxidation occur simultaneously.
The target feed water in this thesis is deep anoxic ground water, characterized by high iron and methane concentrations. The typical high methane values demand intensive aeration to prevent excessive formation of mucus or slime by methanotrophic bacteria.
This research focuses therefore on heterogeneous iron oxidation that can be applied by running an adsorptive filter under anoxic conditions and regenerate it intermittently under oxic conditions. In other words, adsorption and oxidation are separated in time.

A method was developed to determine the constants for Freundlich isotherms that describe the adsorption of iron and manganese on the filter medium. The adsorption experiments were conducted using the filter medium of Holten and Spannenburg as an adsorbent. The coating of the medium in the filters that remove iron was predominantly amorphous iron(hydr)oxides e.g. ferrihydrite. An increase of pH improves adsorption of iron or manganese. A clear relation between temperature and adsorption of iron or manganese was not found. The Freundlich isotherms allowed a rough estimation of the maximum operating time of a rapid sand filter in intermittent regeneration mode, which amounted to 189 bed volumes.

Pilot plant research was initiated following up on these positive results. The pilot plant consisted of two columns. The first column was filled with iron-coated sand of Holten as an adsorbent. The aim of the experiments with this filter medium was to determine the optimal regeneration time and the influence of the Empty Bed Contact Time (EBCT). The experiments demonstrated a positive relation between iron removal and the EBCT. Unfortunately, the EBCT was lower than estimated from the batch experiments. The explanations are: 1) there was no sharp-edged adsorption front, 2) calcium adsorption competed with iron adsorption. The absence of a sharp-edged adsorption indicates that kinetic limitations plays an important role. Furthermore, a salt spiking experiment showed that the filter column did not show ideal plug flow reactor behavior.

We don't fully understand the required number of bed volumes to regenerate the filter. Oxic water beyond that to oxidize adsorbed iron(II) was necessary to expel methane. The explanation is that a slightly oxic, methane rich, transition zone occurs during the regeneration procedure. Biological oxidation of methane will take place in this transition zone. It is therefore complicated to compare the regeneration phase of the pilot plant with the backwash phase of full-scale filters. A sizable portion of the backwash water could probably be reused in the treatment. Reuse of the regeneration water will, however, increase the required capacity of the filters. The regeneration water was almost completely saturated with oxygen. Stronger oxidizing agents such as hydrogen peroxide may improve the regeneration process.

The slow start-up of the second column, filled with virgin sand is an additional drawback. More than 123 cycles were required to get the iron-removal process going, which implies a water loss of 3295 bed volumes. A start-up with iron-coated sand is, of course, an option to be further investigated.

The research proved that a conventional oxic filter with aerators performs better than an anoxic filter in intermittent mode. With equal iron removal efficiencies, the number of bed volumes than can be treated and the accumulated iron load of a conventional filter are much higher. It is plausible that the anoxic pilot plant performs better at an even lower EBCT. However, this comes at the expense of one of the potential advantages of heterogeneous iron oxidation, a high filtration rate. Therefore, the outcome of this thesis does not yet warrant a change of the process configuration.

When we furthermore compare the outcome of the pilot plant experiments with the performance of the pre-filters of Grobbendonk, we have to conclude that heterogeneous iron removal performs better when adsorption and oxidation occur simultaneously, instead of separated in time.

7 Recommendations

A range of recommendations can be made, most notably:

- The conclusions about the influence of the Empty Bed Contact Time (EBCT) on the iron removal were based on four experiments. Additional experiments could prove the reproducibility.
- The required number of bed volumes to regenerate an anoxic filter is not fully understood. It is recommended to perform additional experiments, whereby mass balances are taken for iron and oxygen.
- Improve the start-up of a filter filled with virgin sand. Investigate whether the addition of iron oxidizing bacteria can accelerate this process.
- Investigate the underlying mechanism of heterogeneous iron oxidation.
- Investigate the competition of calcium adsorption with iron adsorption with simulation software, such as Phreeqc. These simulation could also include the completion of other cations and phosphate.

When we look at this work from a wider perspective, it could be interesting to combine the classification of public supply well fields in the Netherlands, as presented in paragraph 1.2, with the existing process configuration of water treatments. Would we make the same choices again?

List of references

Appelo, C.A.J., Drijver, B, Hekkenberg, R, and Jonge, M. de: (1999) *Modeling in situ removal from groundwater.* Groundwater, Vol.37, No.6.

Appelo, C.A.J., Postma, D. (2006) *Geochemistry, Groundwater and Pollution, 2nd edition*. Balkema, Rotterdam.

Baker, M.N.: (1949) *The Quest For Pure Water,* American Water Works Association, New York, USA

Beek C.G.E.M. van (1983) *Ondergrondse ontijzering, een evaluatie van uitgevoerd onderzoek* (in Dutch). KIWA mededeling 78.

Beek, C.G.E.M. van, Hiemstra, T. Hofs, B. Nederlof, M. M., Paassen, J. A. M. van and Reijnen, G. K.: (2012) *Homogeneous, heterogeneous and biological oxidation of iron(II) in rapid sand filtration.* Journal of Water Supply: Research and Technology—AQUA

Behrends, T (2014), *Discussion on 15 May 2014*, Utrecht University Faculty of Geosciences, Department of Earth Sciences.

Behrends, T (2015), *Discussion on 9 February 2015*, Utrecht University Faculty of Geosciences, Department of Earth Sciences.

Berner, R.A. (1981) *A new geochemical classification of sedimentary environment.* Journal of Sedimentary Research June 1, 1981 51:359-365

Cabo, A.J. (2014) *Discussion on 28 January 2014 and 30 April 2014,* Department of Applied Mathematics of the Delft University of Technology

Carlson, L., Schwertmann, U. (1987)· Iron and manganese oxides in Finnish ground water treatment plants. Water Res. 21, 165–170.

Claff, S.R., Sullivan, L.A., Burton, E.D., Bush, R.T. (2010) *A sequential extraction procedure for acid sulfate soils: Partitioning of iron,* Geoderma 155, 224–230.

Davison, W., Seed, G. (1983). *The kinetics of the oxidation of ferrous iron in synthetic and natural waters*, Geochimica et Cosmochimica Acta, Volume 47, Issue 1Pages 67–79

DHV Water BV: (2009) *CoP Kostencalculatie, Niveau beleidsplan en systeemkeuze, Drinkwater* dossier A6745-02-001 versie 6 (in Dutch)

Drijver, B.C., Hekkenberg, R., (1997). *Modellering van ondergrondse ontijzering, toepassing van een PHREEQC model op de waterwinning La Cabine* (in Dutch). Vrije Universiteit, Amsterdam

Dzombak, D.A. and Morel, F.M.M. (1990) *Surface Complexation Modelling - Hydrous Ferric Oxides.* John Wiley & Sons Inc., USA.

Fox, J.: (2008) *Applied Regression Analysis and Generalized Linear Models*, 2nd edition, Sage Publications, Los Angeles, USA

Freundlich, H.M.F. (1906) *Über die adsorption in lösungen*, Z. Phys. Chem. 57385–470.

Hendrikx, R, (2013) *e-mail 13 December 2013*, Department of Materials Science and Engineering of the Delft University of Technology

Hinkamp, J., Bergevoet, H., Schoonenberg, F. Könning, G. (2004) *Ondergondse ontijzering met behulp van technisch zuiver zuurstof (concept)* (in Dutch). Vitens

Hofs, P.S. (2011) *Kennisinventarisatie ontijzering* (in Dutch). BTO 2011.018 , KWR, Nieuwegein

Johnson, B.B., (1990) *Effect of pH, temperature, and concentration on the adsorption of cadmium on goethite*, Environ. Sci. Technol., 24 (1), pp 112–118

Joris, K. (2015) *e-mail 7, 8 and 10 September 2015.* Pidpa.

Moel, P.J. de Verberk, J.Q.J.C., and Dijk, J.C. van. (2006): *Drinking Water: Principles and Practice.* World Scientific Publishing, New Yersey, USA

Myswitzerland (2015) Heureka by Jean Tinguely, Retrieved from www.myswitzerland.com on 11 September 2015

Olsthoorn T.N. (2000) Background of subsurface iron and manganese removal, Amsterdam Water Supply Research and Development, Hydrology Department.

Olthoff, R. (1986) *Removal of iron and manganese in the aquifer.* Dissertation. Veröffentl. Inst. Siedlungswasserwirtschaft Abfalltechn. 63, Univ. Hannover (in German).

Reijnen, G.K. (1994) *Behandeling van methaanhoudend grondwater: effecten van het vóórkomen en de verwijdering van methaan op de fysisch-chemische en biologische kwaliteit van het drinkwater* (in Dutch). KIWA mededeling 78.

Rodda, D.P., Johnson, B.B., and Wells, J.D. (1993) *Modeling the Effect of Temperature on Adsorption of Lead(II) and Zinc(II) onto Goethite at Constant pH*, Journal of Colloid and Interface Science, Volume 161, Issue 1, Pages 57–62

Schoonenberg Kegel, F. (2013) *Optimization of iron removal in rapid sand filters, Increasing heterogenic iron removal by reducing the supernatant level*, Additional Thesis, TU Delft, Delft

Schwertmann, U., Cornell, R.M., (2000) *Iron Oxides in the Laboratory, Preparation and Characterization,* Wiley, New York, USA

Sharma, S.K.: (2001) *Adsorptive Iron Removal from Groundwater* Thesis, IHE, Delft, The Netherlands

Sharma, S.K.: (2014) *Discussion on 14 March 2014*, Environmental Engineering and Water Technology Department of UNESCO-IHE Institute for Water Education

Stumm, W., Morgan, J.J.: (1996) *Aquatic Chemistry, Chemical Equilibria and Rates in Naturals Waters,* page 152 and 390, 3rd edition, Wiley, New York, USA

Westra-Marsman, A. (2015) *e-mail 9 September 2015.* Vitens.

Wikimedia (2015) *Zürich-Seefeld: Heureka sculpture by Jean Tinguely at Zürichhorn*, Picture of Robert ZH, Retrieved from www.wikimedia.org on 11 September 2015

Annex 1: Protocol glovebox experiments

Safety

- Safety glasses
- Disposable gloves
- Portable oxygen gas detector, Buveco Ecotox

Equipment

- Peat sampler set, Eijkelkamp Agrisearch Equipment, art. No. 04.09
- Balances:
  - Sartorius type 1419 MP8-1
  - Kern DE36K10N
- Dissolved oxygen measurement:
  - Orbisphere model 26060 equipped with sensor 2110
  - The sensor was cleaned and checked by Hach Lange on 17 October 2013
  - The sensor was not brand new, according to Hach Lange the accuracy is still:
    - 1 ppb in the range: 0-100 ppb
    - 1% of the measured value, in the range: 100-20,000 ppb
- Filtration samples:
  - syringe with Luer-Lock connector: BD Plastipak 50mL Ref 300865
  - 0.45 um regenerated cellulose filter unit: Whatman Spartan 30/0.45 RC
- Glassware:
  - 1 beaker 3L
  - 2 beakers125 mL
  - 18 Serum bottles 100 mL
  - 18 stir bars 2 cm
  - 1 stir bar 8 cm
  - 2 medicine cups 30 mL
- Glovebox: Plexmaster Pro Quick, Ganuk GMBH
- 1 single point magnetic stirrer: Ikamag type RET
- 3 ultra-flat magnetic stirrer with 6 stirring positions, Variomag multipoint 6
- 2 Support stands and clamps
- Hypodermic needle: Henke Sass Wolf Fine-Ject Ref 4710006030
- Incubator: Hettich HettCube 400R
- pH measurement: Hach HQ 40d equipped with a PHC20101 sensor
- Reagens
  - 99,9% pure nitrogen gas: Linde gas
  - Milli-Q ultrapure water
  - Iron(II) sulfate heptahydrate,:Boom, product number 20698, zeer zuivere kwaliteit
  - Manganese(II) chloride tetrahydrate: Merck, product number 105927, grade acs
  - Sodium Hydrogen carbonate: JT Baker, product number 0263, grade acs
  - 1 L Hydrochloric Acid, 1 molar solution
  - 1 L Sodium hydroxide, 1 molar solution
- Sealing serum bottles
  - butyl rubber stopper
  - crimp seal 20 mm
  - hand crimper 20 mm
  - hand decapper 20 mm
- 2 spargers, commonly used for sparging solvents with helium in high performance liquid chromatography (HPLC)
- Disposable transfer pipettes

Procedure

Sample filter medium

- Collect a sample of the filter medium with a peat collector;
- Conserve the sample in a freeze at a temperature of -22 °C to rule out aging;
- Defrost the sample at room temperature the day before the glovebox experiment.

Preparation glovebox

- Adjust the temperature of the incubator
- The glassware was cleaned with amongst others hydrochloric acid and nitric acid to rule out disturbance by metals which are adsorbed on glassware
- Connect to the nitrogen inlet of the glovebox:
    - two spargers
    - air tubing to purge remaining oxygen out of glassware (e.g. 8 x 1.25 mm)
- Place in the glovebox:
    - 2 Support stands and clamps
    - Single point magnetic stirrer
    - crimp seals and butyl rubber stoppers;
    - hand crimper and hand decapper
    - 125 mL beaker filled with 1 M hydrochloric acid
    - 125 mL beaker filled with 1 M sodium hydroxide
    - 2 transfer pipettes
    - calibrated pH measurement
    - calibrated oxygen measurement
- Weigh accurately approximately 2.4 kg milli-Q into a 3 L beaker. Transfer the beaker to the glovebox. Place the beaker with a stir bar on the magnetic stirrer. Immerse the oxygen sensor and the spargers in the liquid. Stir the liquid at 100 rpm.
- Weigh accurately approximately 123 mg $FeSO_4.7H_20$ or 44 mg $MnCl_2.4H_20$ into a medicine cup and transfer it to the glovebox
- Weigh accurately approximately 1200 mg $NaHCO_3$ in a medicine cup and transfer it to the glovebox
- Number 18 serum bottles with a waterproof marker
- Measure the weight of the 18 serum bottles filled with a stir bar
- Fill 16 serum bottles with an increasing amount of filter medium and measure the weight again. In this experiment: 0.25, 0.5, 0.75, 1.0, 1.5, 2.0, 3.0 and 4.0 g.
- Two serum bottles are used as blanks and are not filled with filter medium;
- Transfer the serum bottles to the glovebox

Glovebox experiments day 1

- Close the glovebox;
- Open the nitrogen gas valve and set the flow to 1200 L/h. Divide the nitrogen over the spargers and the glovebox inlet by manipulating the valves. Keep the gauge pressure below 30 mbar.
- After 1 hour:
    - Reduce the nitrogen gas flow to 400 L/h;
- After 2 hours:
    - Purge the remaining oxygen out of the glassware and serum bottles;
- After 2 hours and 30 minutes:
    - Add $NaHCO_3$ to the milli-Q water.
    - Check the pH;
    - Set the pH to the desired value by adding HCl or NaOH with a transfer pipette;
- After 2 hours and 50 minutes;
    - Ad $FeSO_4.7H_2O$ or $MnCl_2.4H_2O$ to the milliQ water.
    - Flush the medicine cup with milli-Q
    - Check the pH
    - Set the pH to the desired value by adding HCl or NaOH with a transfer pipette;
- After 3 hours:
- Read the oxygen measurement
- Remove the oxygen sensor and the spargers
- Pour the iron(II) or manganese(II) solution into all the serum bottles. Allow a headspace of around 1 cm.
- Close the serum bottles with the hand crimper.
- Close the nitrogen gas valve;
- Open the glovebox;
- Purge all the serum bottles with nitrogen to remove remaining oxygen in the headspace and liquid:
    - Attach a needle to the air tubing used to purge remaining oxygen out of glassware earlier;
    - Allow a gentle flow of nitrogen through the needle
    - Insert the needle through the rubber stopper of the serum bottle. The needle should be in the liquid.
    - Insert a second needle through the rubber stopper. This needle is used to vent exes of nitrogen.
    - Purge each the serum bottle 1 minute.
    - Remove first the outflow needle and there after the inflow needle
- Measure the weight of the 18 closed serum bottles
- Transfer the serum bottles to the incubator, on the stirrers
- Adjust the speed of the stirrers to 100 rpm.
- Stir the serum bottles until the required adsorption time has passed.

Glovebox experiments day 2

- Place in the glovebox:
  - hand crimper and hand decapper
  - calibrated oxygen measurement
  - 18 syringes
  - 24 0.45 um filters
  - remove the plungers, keep the plungers inside the glovebox
  - attach the 0.45 um filters to the syringes, 6 filters are spare.
- When the required adsorption time has passed, transfer the serum bottles to the glovebox;
- Close the glovebox
- Open the nitrogen gas valve and set the flow to 1200 L/h. Keep the gauge pressure below 30 mbar.
- After 1 hour:
  - Reduce the nitrogen gas flow to 400 L/h;
- After 3 hours:
  - Read the oxygen measurement
  - Repeat the procedure below for each serum bottle:
    - Purge a syringe with nitrogen
    - Purge a sample bottle with nitrogen
    - Open a serum bottle with a decapper and pour around 40 mL in the tube of the syringe
    - Place the plunger
    - Expel the liquid into the sample bottle
  - Collect non filtered samples of the blanks
- Open the glovebox
- Analyze the samples on iron and manganese
- Measure the mass of the seals and stoppers

Elaboration results

Calculate the adsorbed amount of iron or manganese:

$$q = \frac{mass\ adsorbed\ solute}{mass\ adsorbent} = \frac{\frac{(m3-m2-m4)}{\rho w} * (\mathrm{Cb}-\mathrm{Ce})}{dm * (m2-m1)}$$

Where:

q = mass adsorbed iron or manganese per mass adsorbent (g/g)
m1 = mass serum bottle + stir bar (g)
m2 = mass serum bottle + stir bar + adsorbent (g)
m3 = mass serum bottle + stir bar + adsorbent + synthetic water + seal + stopper (g)
m4 = average mass seal + stopper (g)
Ce = equilibrium concentration iron or manganese (g/L)
Cb = average iron or manganese concentration in filtered blank (g/L)
dm = dry matter percentage adsorbent (%)
ρw = density water (g/L)

Plot q versus Ce, and loq(q) versus log(Ce). Determine the k and n value of the Freundlich isotherm equation.

Annex 2: Particle size measurements

Virgin sand: grain size 0.8-1.25 mm

Result: Vitens Histogram Report, filtermateriaal

Sample Details

Sample ID : V1312149822
Sample File : DROOG
Sample Path : C:\SIZERS\DATA\
Sample Notes:

Run Number : 15
Record Number : 4020

Measured: Fri 13 Dec 2013 13:10
Analysed : Fri 13 Dec 2013 13:10
Result Source: Analysed

System Details

Range Lens: 1000 mm
Presentation: 3RHA
Analysis Model: Polydisperse
Modifications: None

Beam Length: 10.00 mm
[Particle R.I. = (1.4500, 0.1000); Dispersant R.I. = 1.0000]

Sampler: MS64

Obscuration: 5.5 %

Residual: 0.701 %

Result Statistics

Uc = 1.40
Mean Diameters:

Deh = 1207.28
D10 = 931.86 µm
D50 = 1236.93 µm
D60 = 1308.26 µm
D90 = 1826.19 µm

Size (um)	Volume Under %	Size (um)	Volume Under %	Size (um)	Volume Under %	Size (um)	Volume Under %
125.0	0.18	350.0	0.41	700.0	1.96	2500.0	96.25
150.0	0.23	400.0	0.45	800.0	4.16	3000.0	98.47
160.0	0.25	420.0	0.48	1000.0	16.04	3150.0	98.99
200.0	0.32	425.0	0.49	1250.0	51.92	4000.0	100.00
250.0	0.36	500.0	0.66	1500.0	78.81	5000.0	100.00
300.0	0.38	600.0	1.12	1680.0	86.49		
315.0	0.39	630.0	1.33	2000.0	92.63		

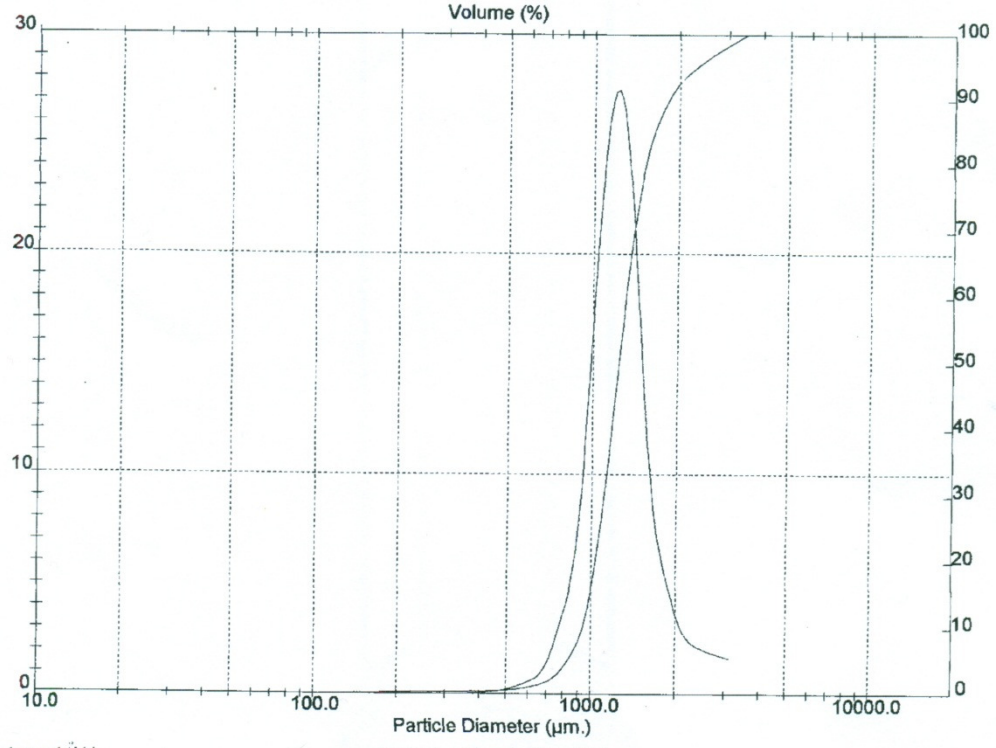

ılvern Instruments Ltd.
ılvern, UK
l:=+[44] (0)1684-892456 Fax:+[44] (0)1684-892789

Mastersizer S long bed Ver. 2.19
Serial Number: 33265-95

p. 11
13 Dec 13 13:10

Holten pre-filter 1, sample depth 0-50 cm

Result: Vitens Histogram Report, filtermateriaal

Sample Details

Sample ID : V1312149823
Sample File : DROOG
Sample Path : C:\SIZERS\DATA\
Sample Notes:

Run Number : 4
Record Number : 4009

Measured: Fri 13 Dec 2013 12:49
Analysed : Fri 13 Dec 2013 12:49
Result Source: Analysed

System Details

Range Lens: 1000 mm
Presentation: 3RHA
Analysis Model: Polydisperse
Modifications: None

Beam Length: 10.00 mm
[Particle R.I. = (1.4500, 0.1000); Dispersant R.I. = 1.0000]

Sampler: MS64

Obscuration: 12.8 %
Residual: 12.247 %

Result Statistics

Uc = 1.65
Mean Diameters:

Deh = 1769.30
D10 = 1228.20 µm
D50 = 1897.66 µm
D60 = 2026.28 µm
D90 = 2515.82 µm

Size (um)	Volume Under %	Size (um)	Volume Under %	Size (um)	Volume Under %	Size (um)	Volume Under %
125.0	0.00	350.0	0.00	700.0	0.40	2500.0	89.34
150.0	0.00	400.0	0.00	800.0	1.03	3000.0	100.00
160.0	0.00	420.0	0.00	1000.0	3.80	3150.0	100.00
200.0	0.00	425.0	0.00	1250.0	10.78	4000.0	100.00
250.0	0.00	500.0	0.01	1500.0	22.06	5000.0	100.00
300.0	0.00	600.0	0.10	1680.0	33.42		
315.0	0.00	630.0	0.16	2000.0	57.99		

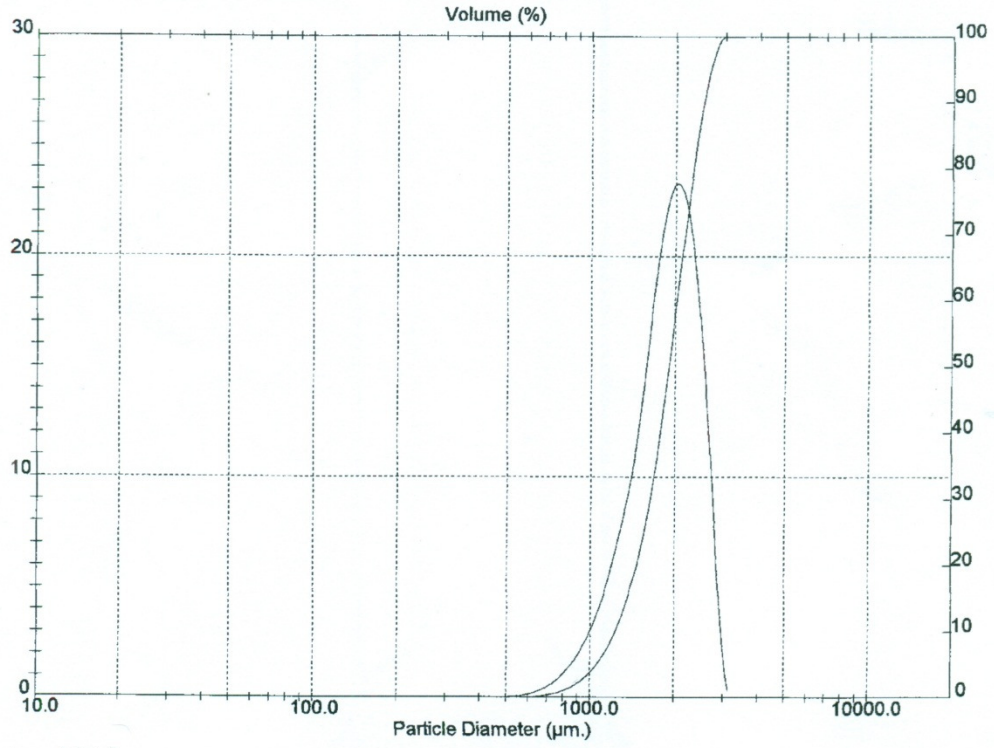

Spannenburg, pre-filter 11, sample depth 0-50 cm

Result: Vitens Histogram Report, filtermateriaal

Sample Details

Sample ID : V1312149827
Sample File : DROOG
Sample Path : C:\SIZERS\DATA\
Sample Notes:

Run Number : 18
Record Number : 4023

Measured: Fri 13 Dec 2013 13:23
Analysed : Fri 13 Dec 2013 13:23
Result Source: Analysed

System Details

Range Lens: 1000 mm
Presentation: 3RHA
Analysis Model: Polydisperse
Modifications: None

Beam Length: 10.00 mm
[Particle R.I. = (1.4500, 0.1000); Dispersant R.I. = 1.0000]

Sampler: MS64

Obscuration: 23.6 %
Residual: 3.528 %

Result Statistics

Uc = 2.26
Mean Diameters:

Deh = 1118.24
D10 = 651.60 µm
D90 = 2265.54 µm

D50 = 1308.56 µm

D60 = 1472.20 µm

Size (um)	Volume Under %	Size (um)	Volume Under %	Size (um)	Volume Under %	Size (um)	Volume Under %
125.0	0.52	350.0	2.11	700.0	12.23	2500.0	94.08
150.0	0.78	400.0	2.67	800.0	17.52	3000.0	98.81
180.0	0.87	420.0	2.97	1000.0	29.91	3150.0	99.39
200.0	1.21	425.0	3.06	1250.0	46.29	4000.0	100.00
250.0	1.50	500.0	4.66	1500.0	61.62	5000.0	100.00
300.0	1.75	600.0	7.88	1680.0	71.10		
315.0	1.84	630.0	9.08	2000.0	83.33		

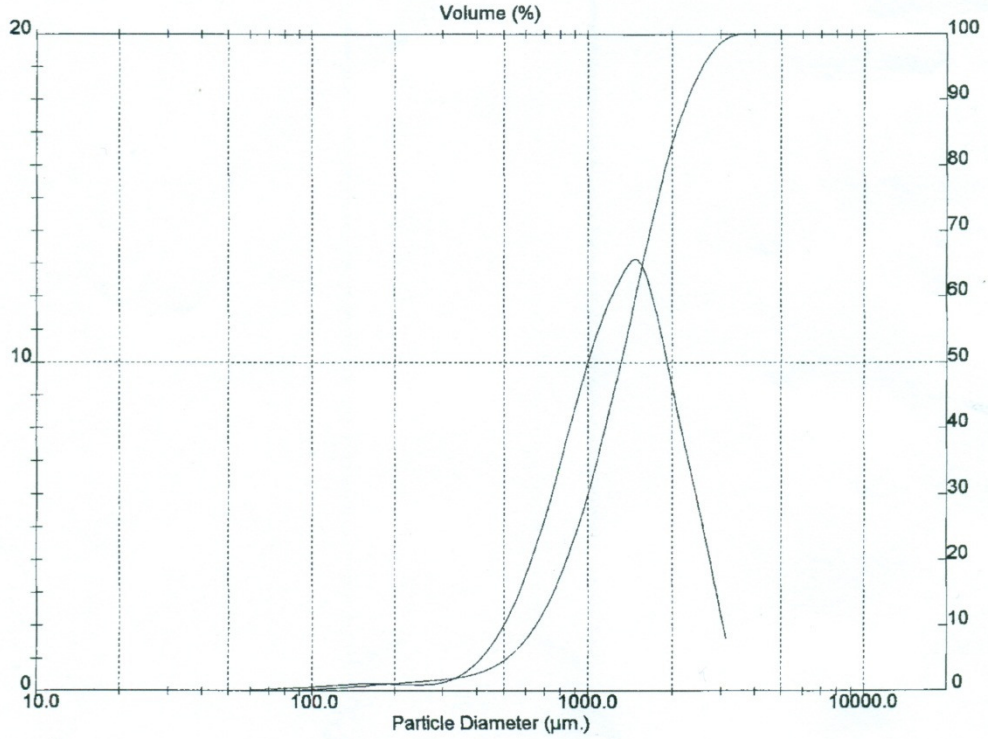

Malvern Instruments Ltd.
Malvern, UK
Tel:=+[44] (0)1684-892456 Fax:+[44] (0)1684-892789

Mastersizer S long bed Ver. 2.19
Serial Number: 33265-95

Annex 3: Unprocessed data adsorption on Spannenburg filtermedium

Table 1: Results iron adsorption on Spannenburg filter medium, derived Freundlich isotherm constants

pH	T	log k	K	n	R2
6.5	10	-2.46	3.47E-03	0.33	0.77
7	4	-1.24	5.75E-02	0.81	0.81
7	10	-0.71	1.95E-01	0.93	0.56
7	20	-1.46	3.47E-02	0.6	0.73
7.5	10	-1.72	1.91E-02	0.52	0.61

Table 2: Results manganese adsorption on Spannenburg filter medium, derived Freundlich isotherm constants

pH	T	log k	K	n	R2
6.5	10	-1.6	2.51E-02	0.68	0.41
7	4	0.9	7.94E+00	1.62	0.74
7	10	-1.44	3.63E-02	0.76	0.88
7	20	-1.02	9.55E-02	0.87	0.65
7.5	10	-0.69	2.04E-01	1.03	0.86

Annex 4: Iron adsorption isotherms, Holten filter medium

Annex 4 contains iron adsorption isotherms derived from glovebox experiments with filter medium acquired from production site Holten. The left figure depicts the adsorption isotherm with 95% confidence bounds. The right figure depicts the studentized residuals as described in chapter 3.
Fox (2008) recommends to call attention to studentized residuals (Ei*) that are $|Ei^*| \geq 2$.

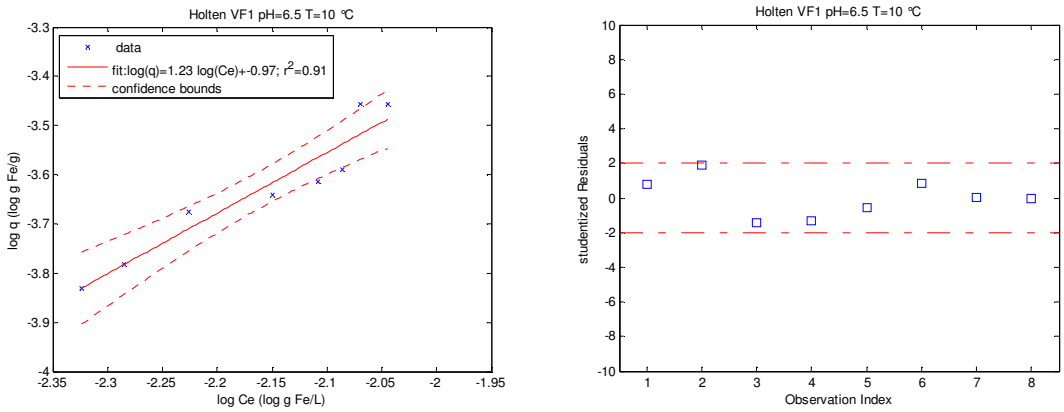

Figure 1: Iron adsorption isotherms, pH=6.5 and T=10 °C, no observations discarded

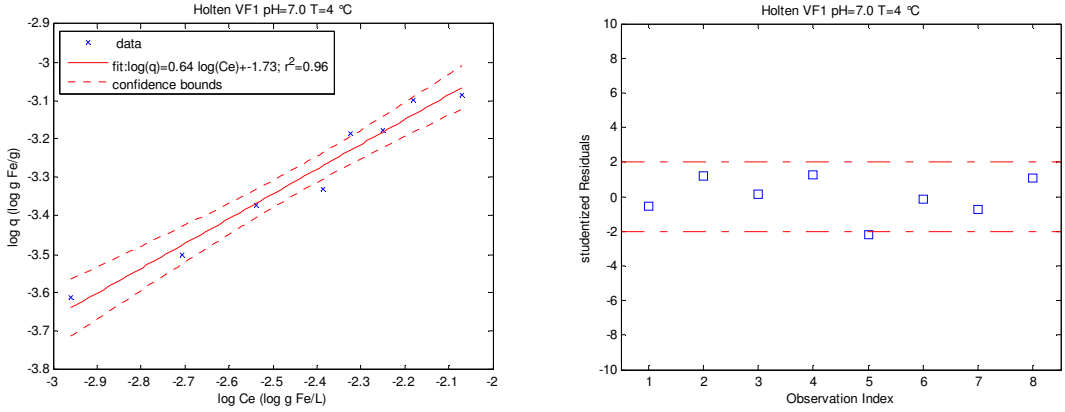

Figure 2: Iron adsorption isotherms, pH=7.0 and T=4 °C, no observations discarded

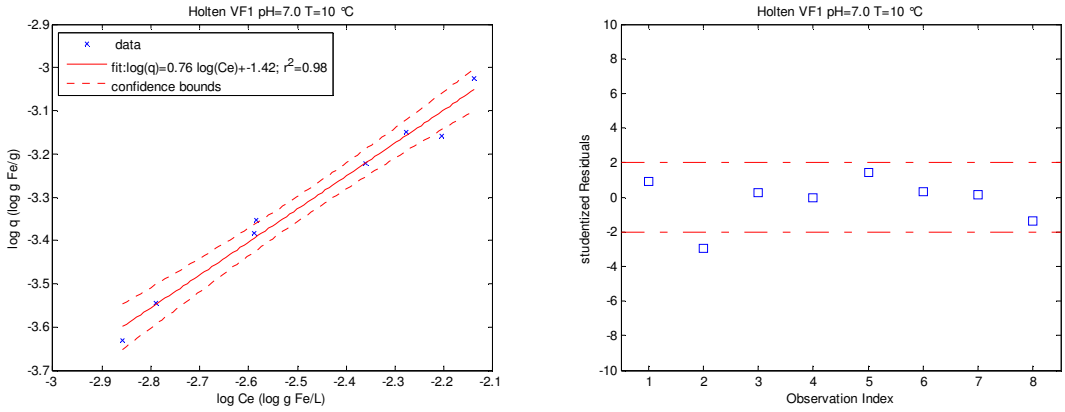

Figure 3: Iron adsorption isotherms, pH=7.0 and T=10 °C, no observations discarded

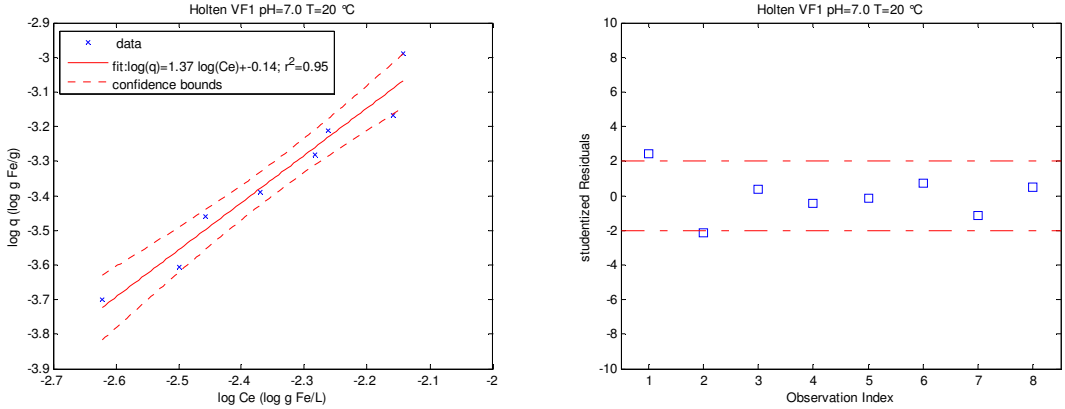

Figure 4: Iron adsorption isotherms, pH=7.0 and T=20 °C, no observations discarded

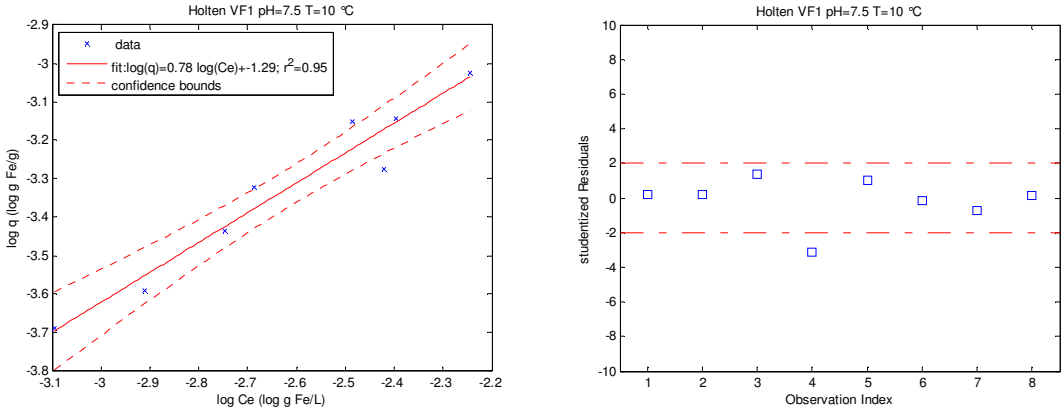

Figure 5: Iron adsorption isotherms, pH=7.5 and T=10 °C, no observations discarded

Annex 5: Iron adsorption isotherms, Spannenburg filter medium

Annex 5 contains iron adsorption isotherms derived from glovebox experiments with filter medium acquired from production site Spannenburg. The upper left figure depicts the adsorption isotherm with 95% confidence bounds. The upper right graph depicts the studentized residuals as described in chapter 3. Fox (2008) recommends to call attention to studentized residuals (Ei*) that are |Ei*|≥2.

Freundlich isotherms derived from the experiments with the filter medium collected in Spannenburg showed a poor correlation. Therefore, a dataset which satisfies |Ei*|≥2 is discarded. It was necessary to discard one outlier to obtain a better correlation in all cases. The outcome is depicted in the lower left and right figures.

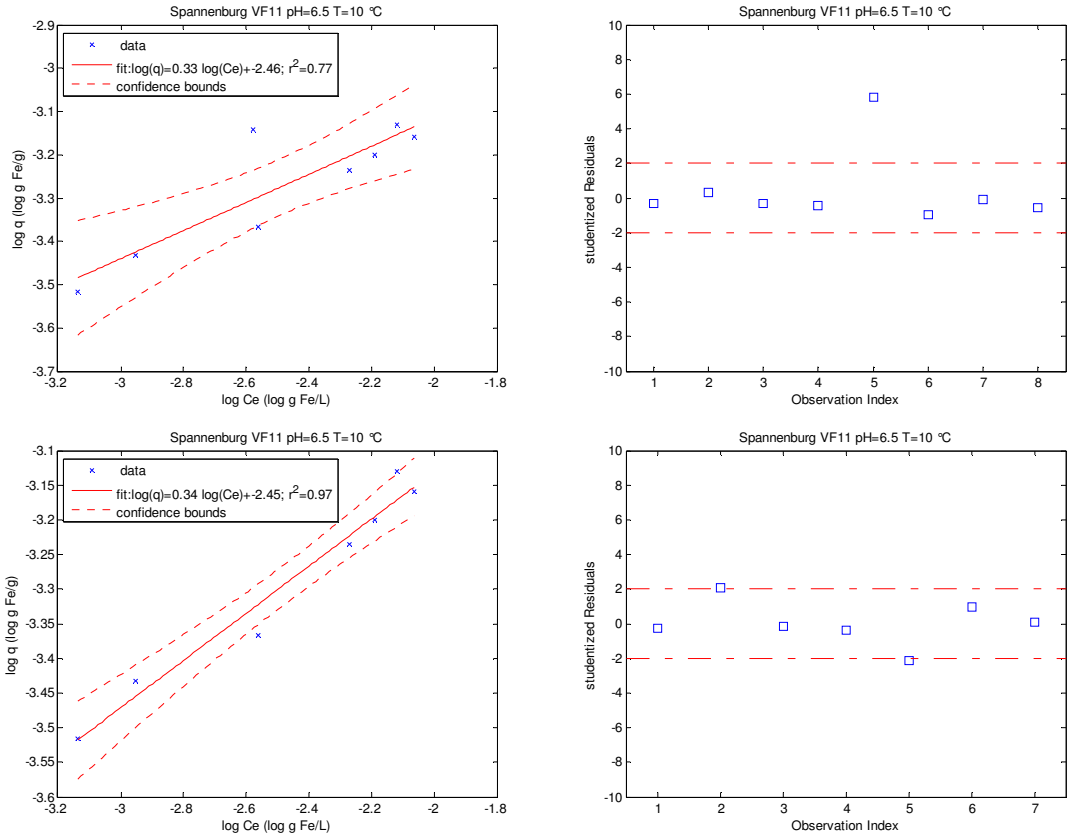

Figure 1 Iron adsorption isotherms, pH=6.5 and T=10 °C, lowest graphs observation 5 discarded

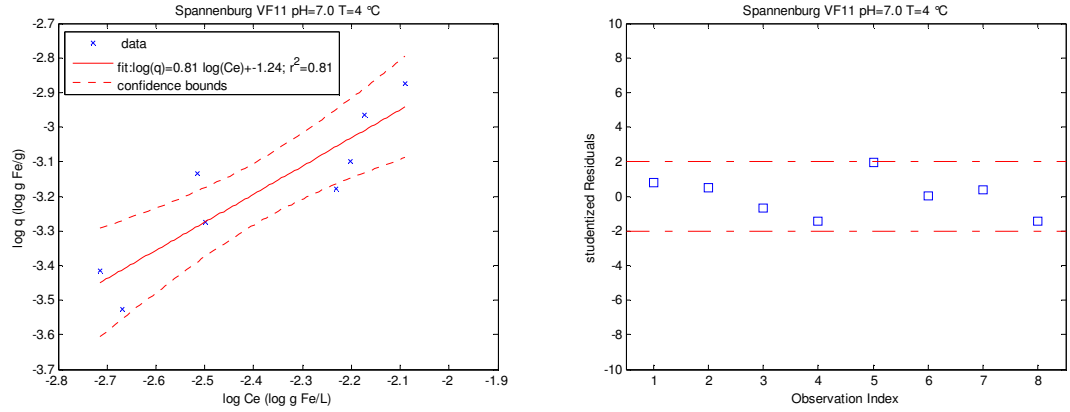

Figure 2: Iron adsorption isotherms, pH=7.0 and T=4 °C, no observations discarded

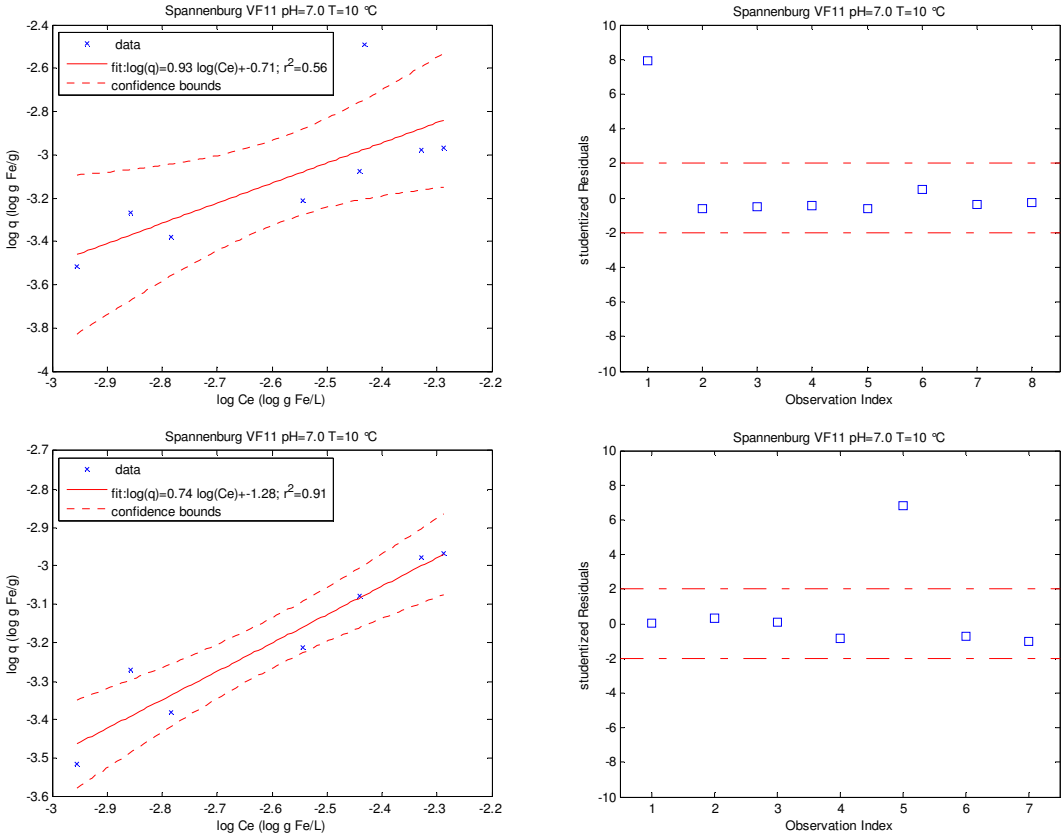

Figure 3: Iron adsorption isotherms, pH=7.0 and T=10 °C, lowest graphs observation 1 discarded

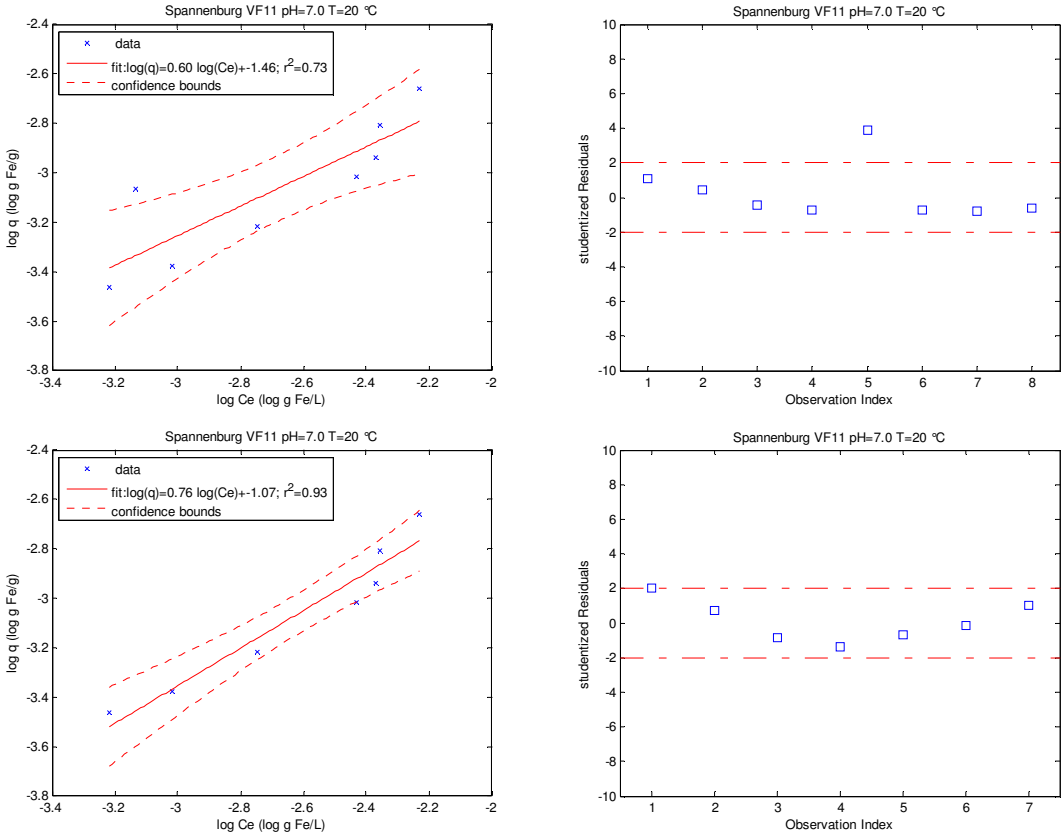

Figure 4: Iron adsorption isotherms, pH=7.0 and T=20 °C, lowest graphs observation 5 discarded

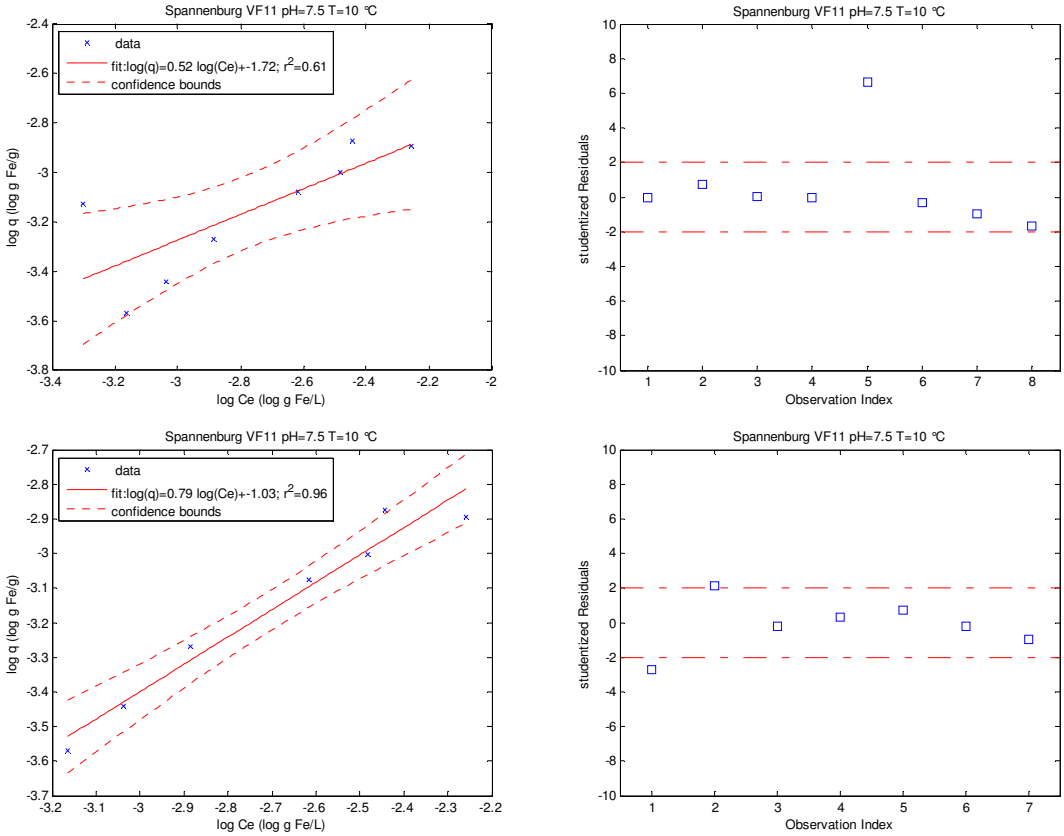

Figure 5: Iron adsorption isotherms, pH=7.5 and T=10 °C, lowest graphs observation 5 discarded

Annex 6: Manganese adsorption isotherms, Holten filter medium

Annex 6 contains manganese adsorption isotherms derived from glovebox experiments with filter medium acquired from production site Holten. The left figure depicts the adsorption isotherm with 95% confidence bounds. The right figure depicts the studentized residuals as described in chapter 3.
Fox (2008) recommends to call attention to studentized residuals (Ei*) that are $|Ei^*| \geq 2$.

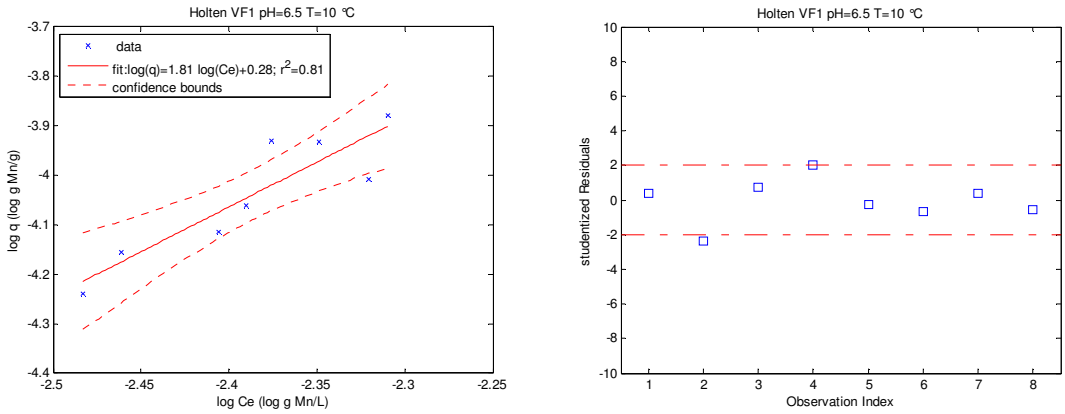

Figure 1 Iron adsorption isotherms, pH=6.5 and T=10 °C, no observation discarded

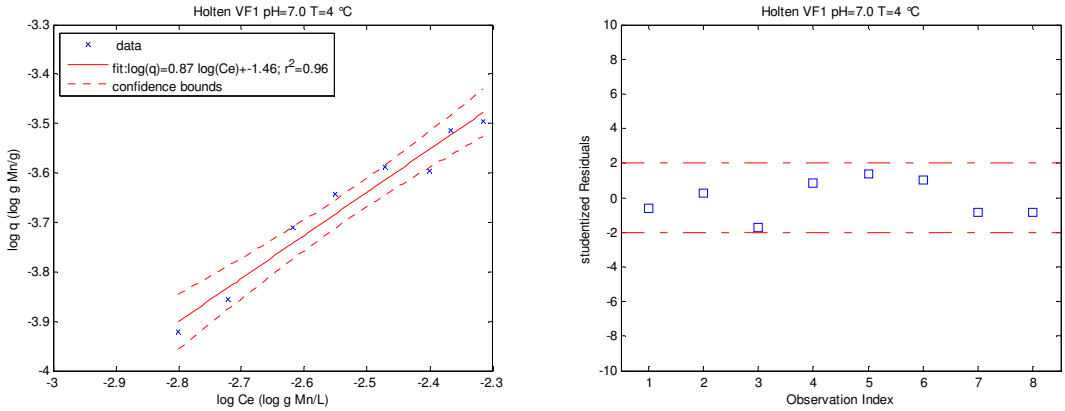

Figure 2: Iron adsorption isotherms, pH=7.0 and T=4 °C, no observation discarded

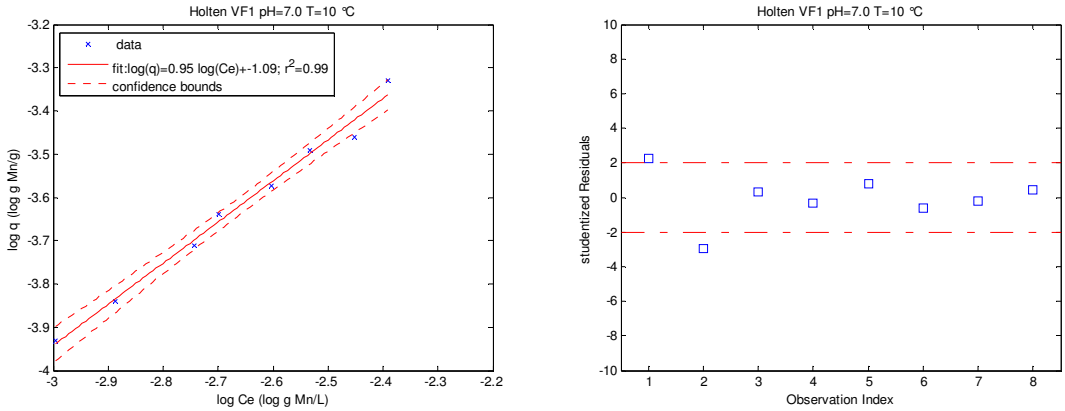

Figure 3: Iron adsorption isotherms, pH=7.0 and T=10 °C, no observation discarded

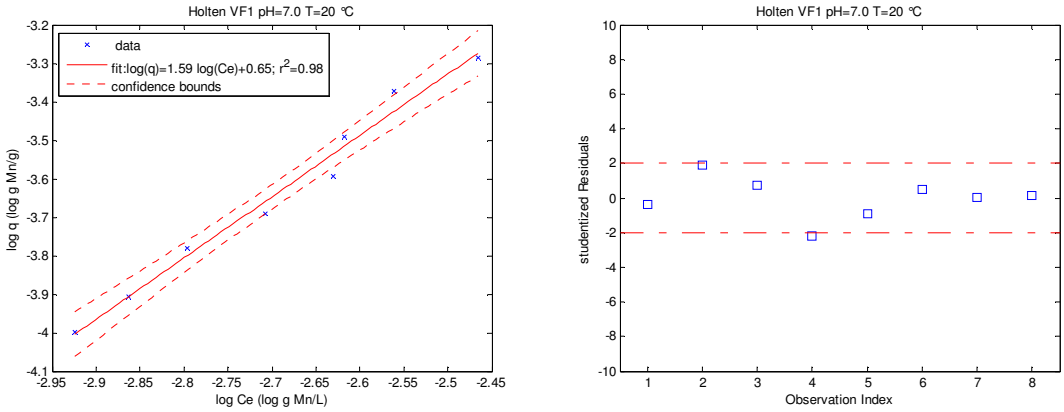

Figure 4: Iron adsorption isotherms, pH=7.0 and T=20 °C, no observation discarded

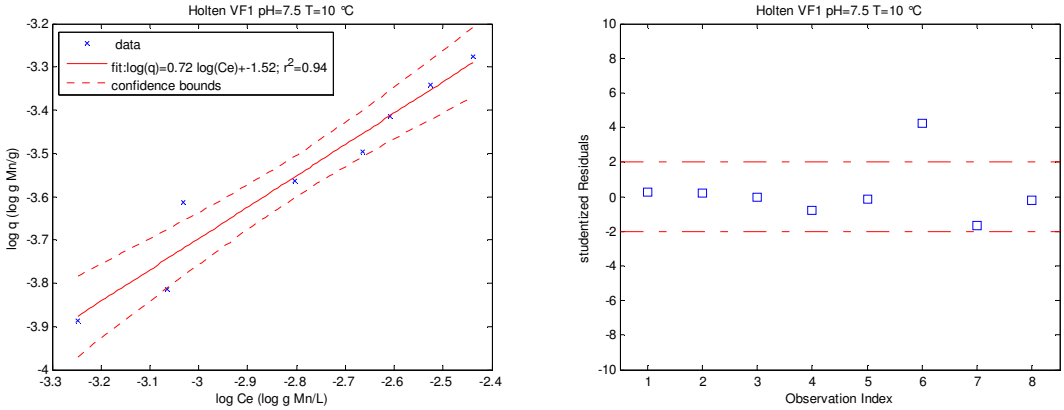

Figure 5: Iron adsorption isotherms, pH=7.5 and T=10 °C, no observation discarded

Annex 7: Manganese adsorption isotherms, Spannenburg filter medium

Annex 7 contains manganese adsorption isotherms derived from glovebox experiments with filter medium acquired from production site Spannenburg. The upper left figure depicts the adsorption isotherm with 95% confidence bounds. The upper right graph depicts the studentized residuals as described in chapter 3. Fox (2008) recommends to call attention to studentized residuals (Ei*) that are $|Ei^*| \geq 2$.

Freundlich isotherms derived from the experiments with the filter medium collected in Spannenburg showed a poor correlation. Therefore, a dataset which satisfies $|Ei^*| \geq 2$ is discarded. It was necessary to discard one outlier to obtain a better correlation in all cases. The outcome is depicted in the lower left and right figures.

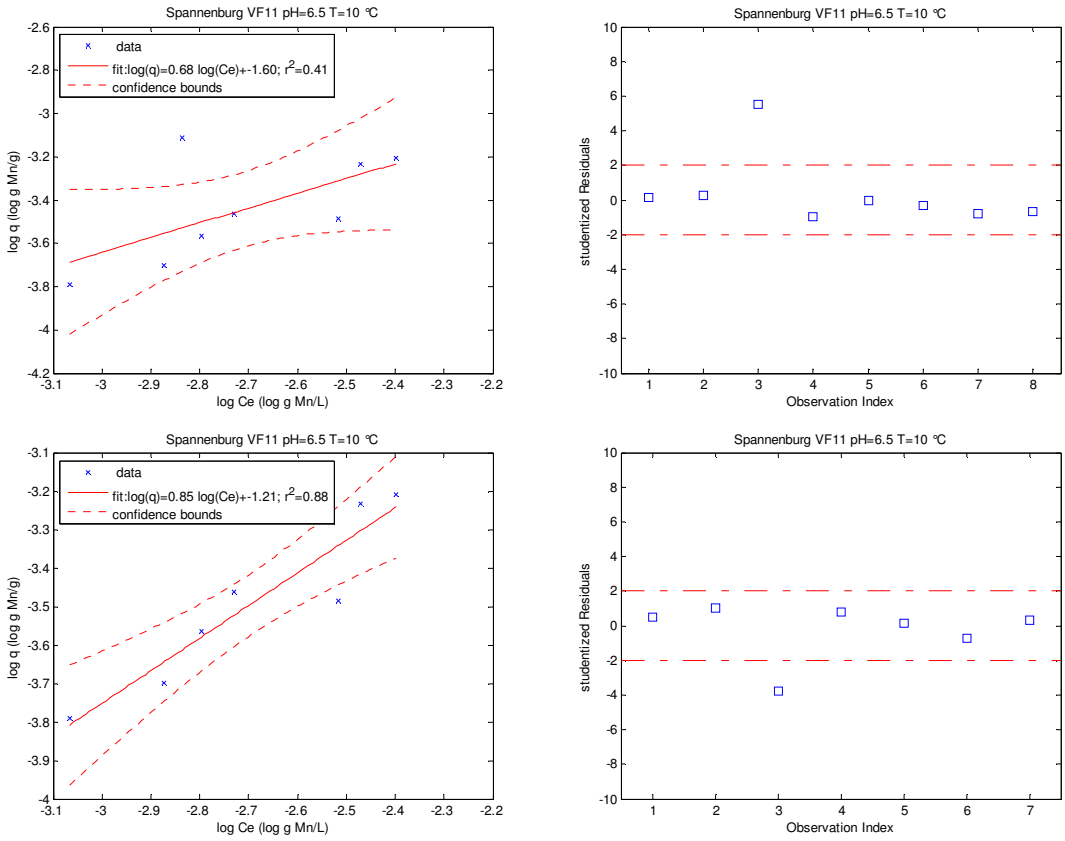

Figure 1 Iron adsorption isotherms, pH=6.5 and T=10 °C, lowest graphs observation 3 discarded

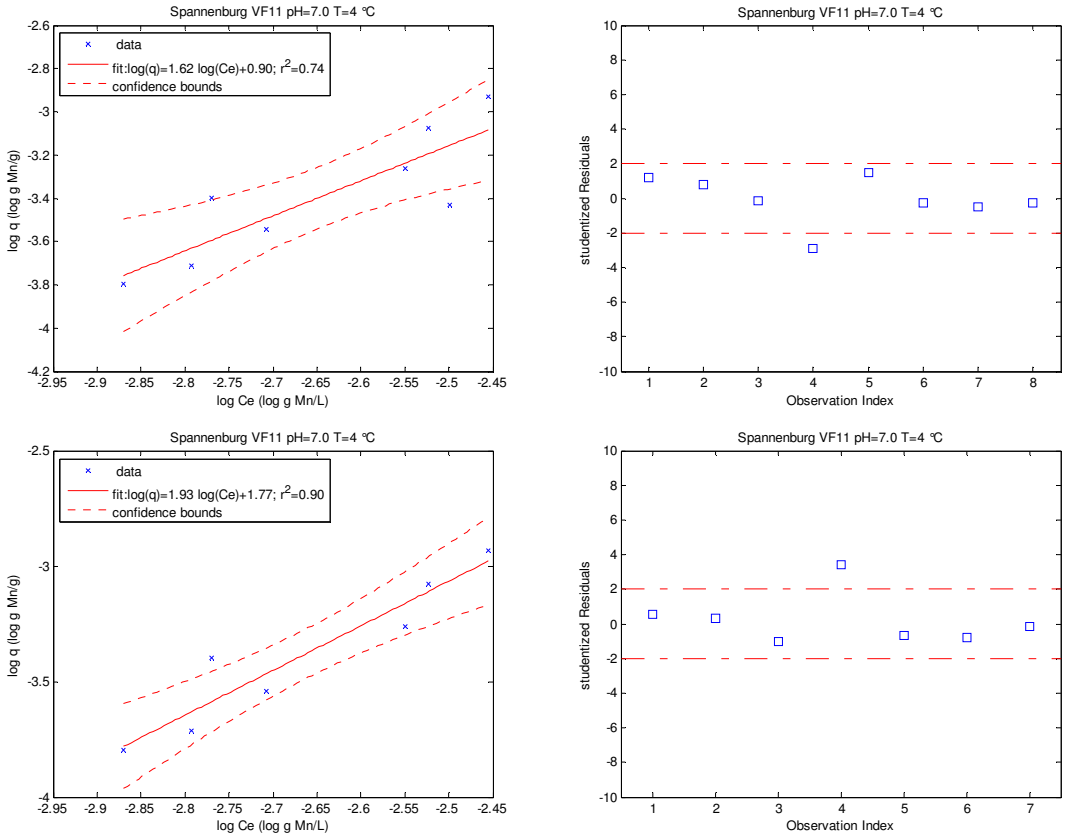

Figure 2: Iron adsorption isotherms, pH=7.0 and T=4 °C, lowest graphs observation 4 discarded

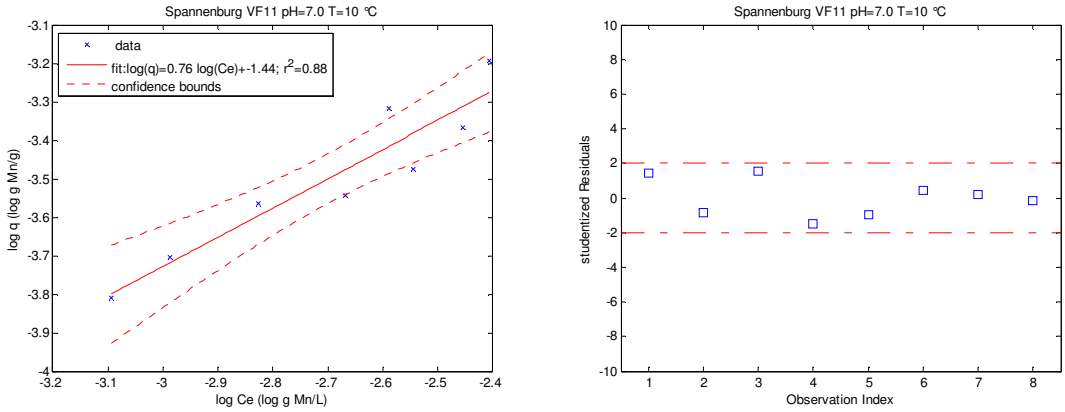

Figure 3: Iron adsorption isotherms, pH=7.0 and T=10 °C, no observations discarded

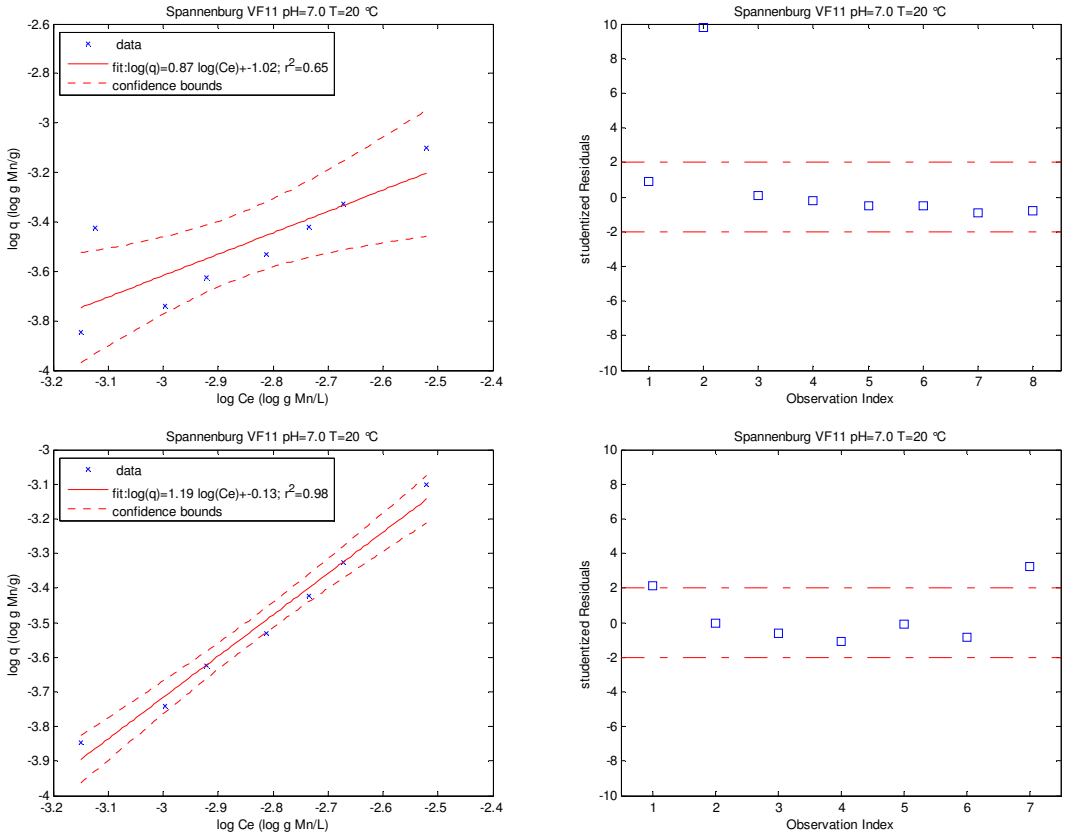

Figure 4: Iron adsorption isotherms, pH=7.0 and T=20 °C, lowest graphs observation 2 discarded

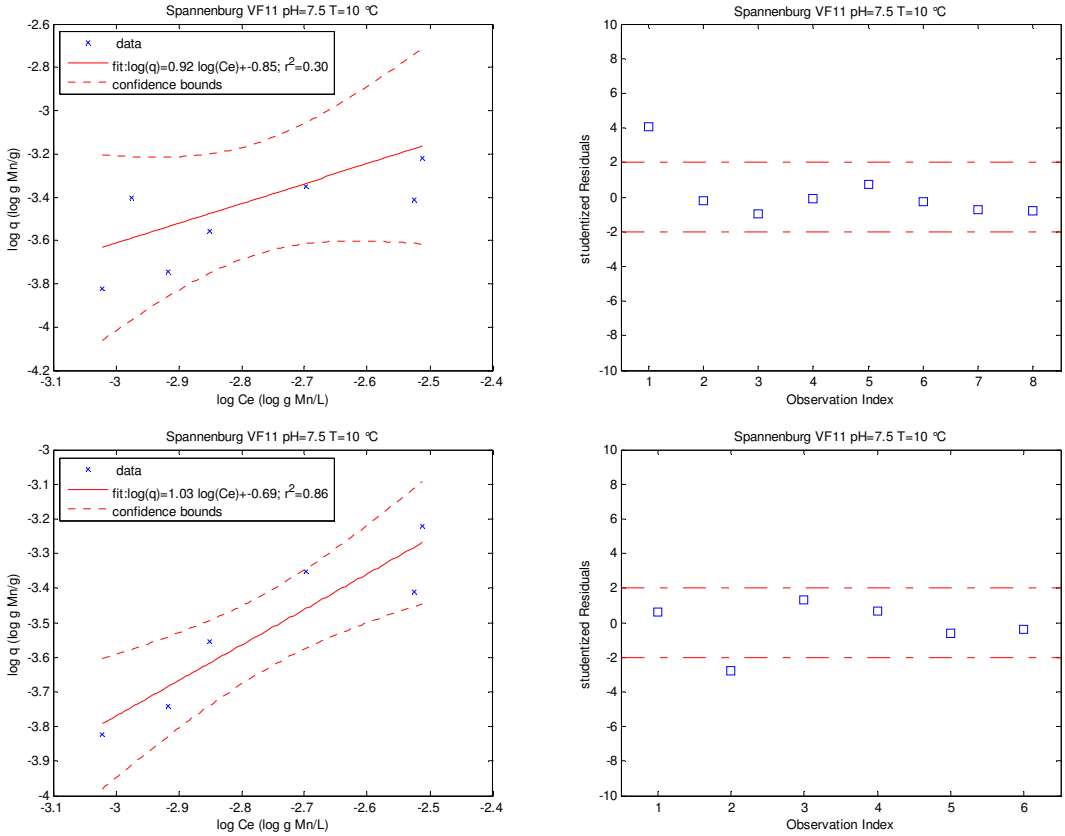

Figure 5: Iron adsorption isotherms, pH=7.5 and T=10 °C, lowest graphs observation 1 and 5 discarded

Annex 8: Freundlich isotherm constants

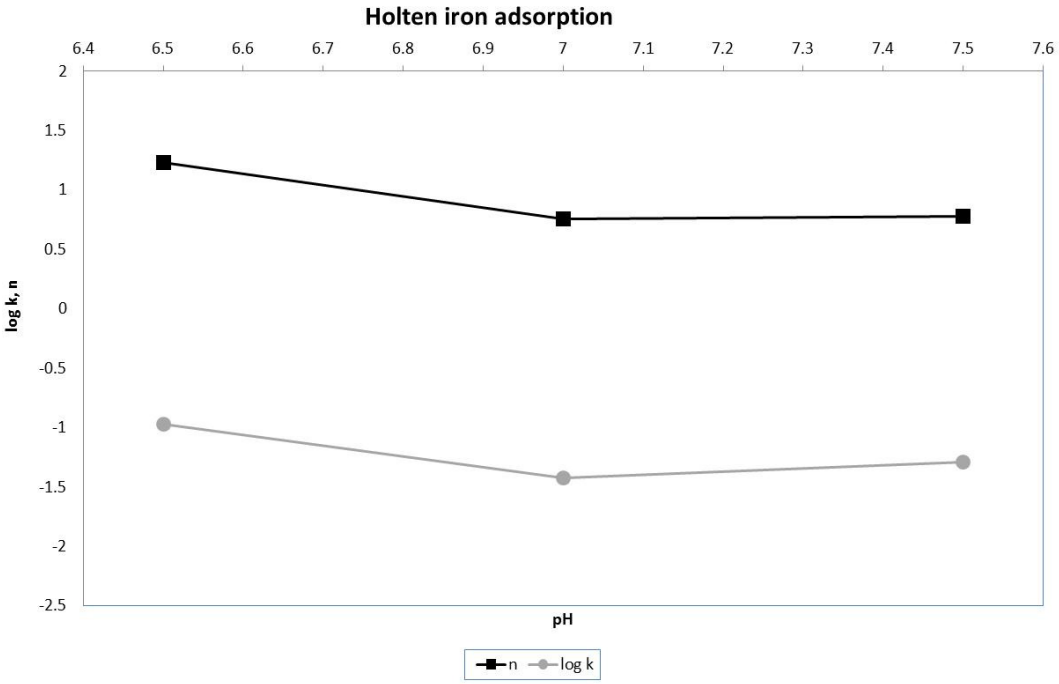

Figure 39: Iron adsorption isotherm Holten filter medium, influence of the pH

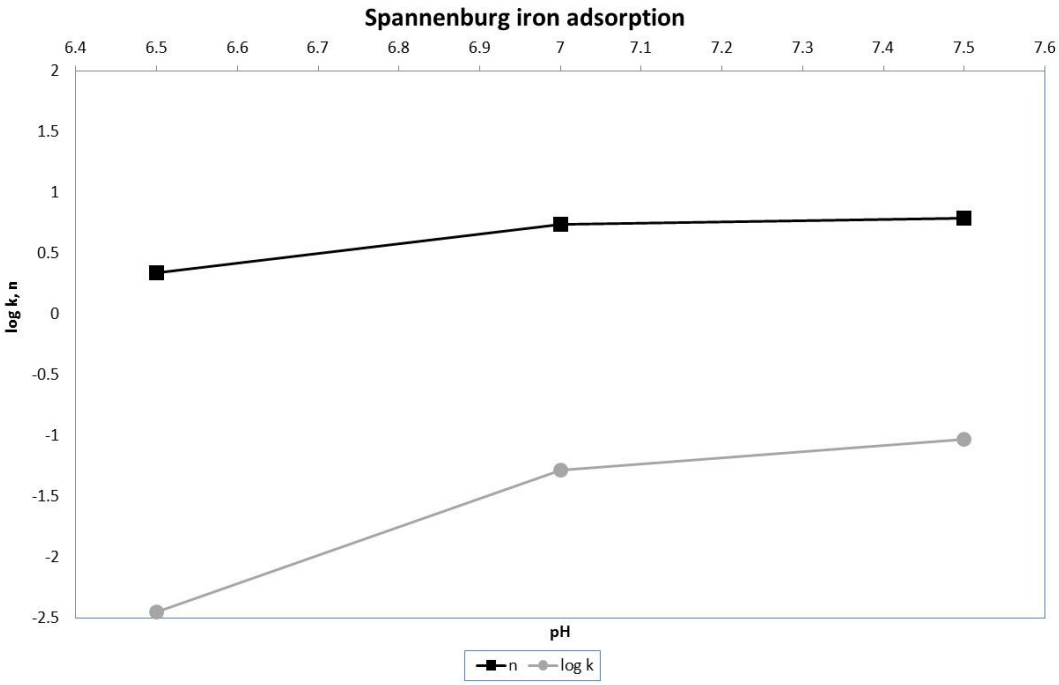

Figure 40: Iron adsorption isotherm Spannenburg filter medium, influence of the pH

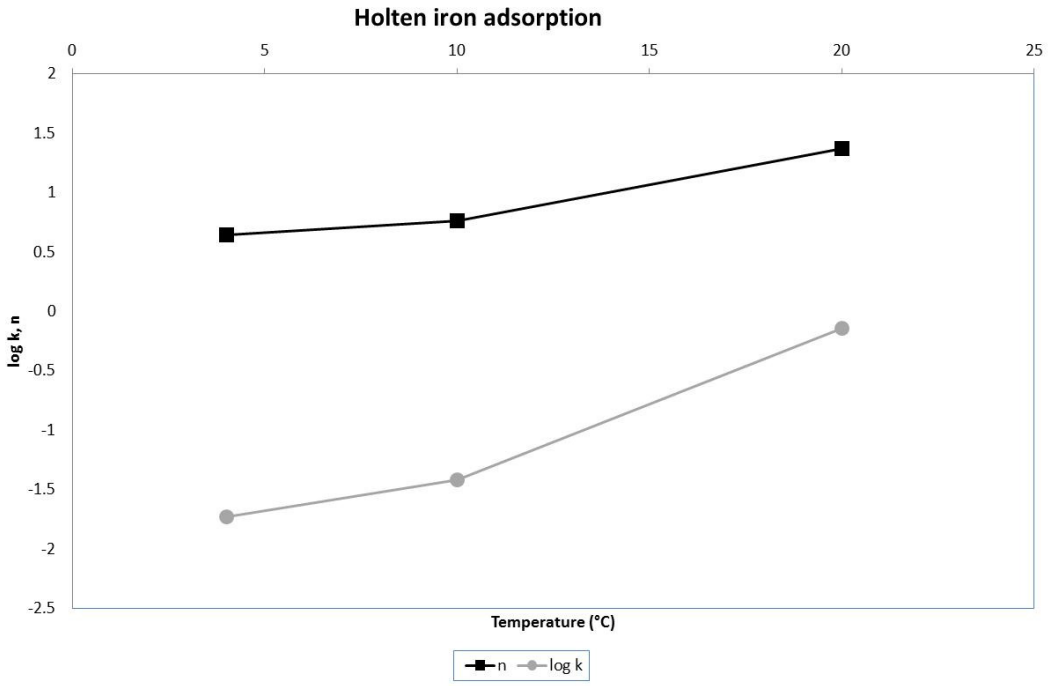

Figure 41: Iron adsorption isotherm Holten filter medium, influence of the temperature

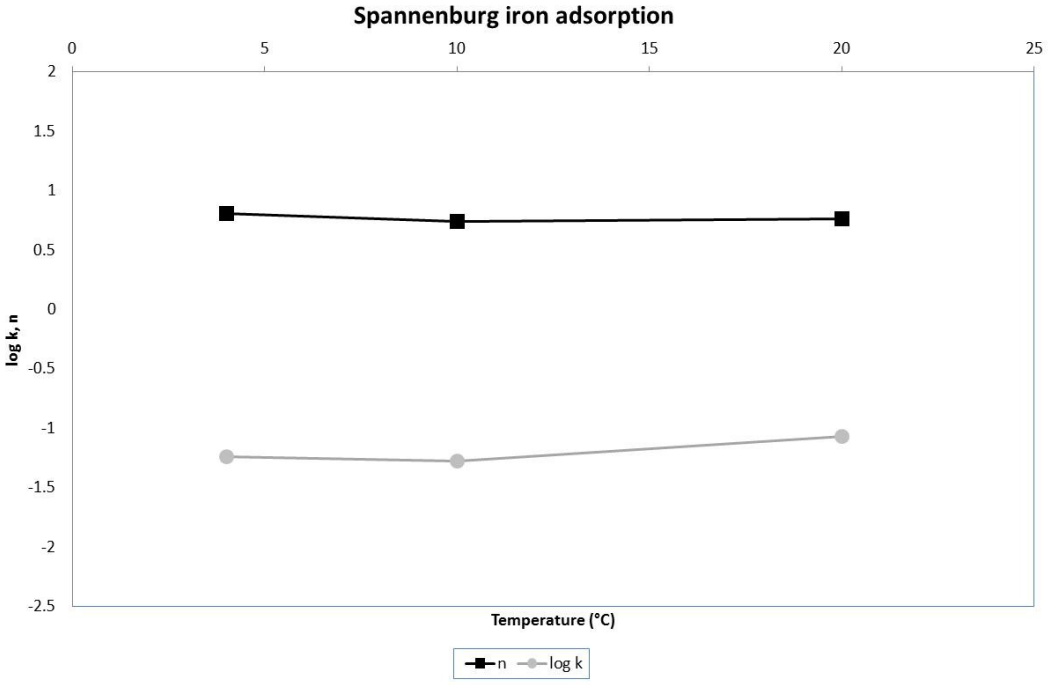

Figure 42: Iron adsorption isotherm Spannenburg filter medium, influence of the temperature

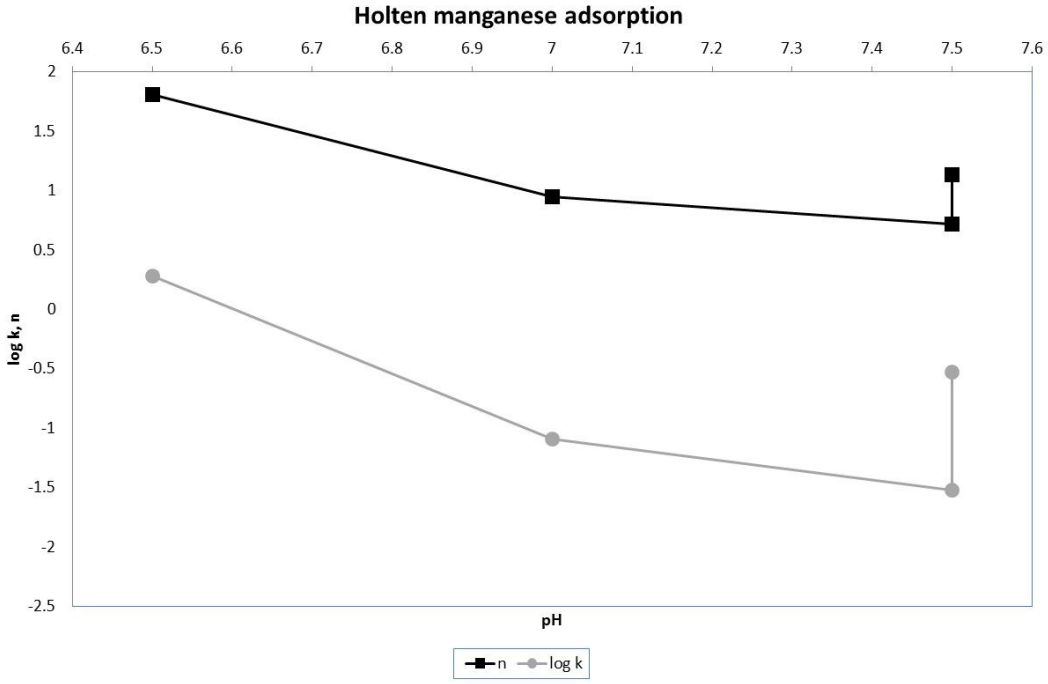

Figure 43: Manganese adsorption isotherm Holten filter medium, influence of the pH

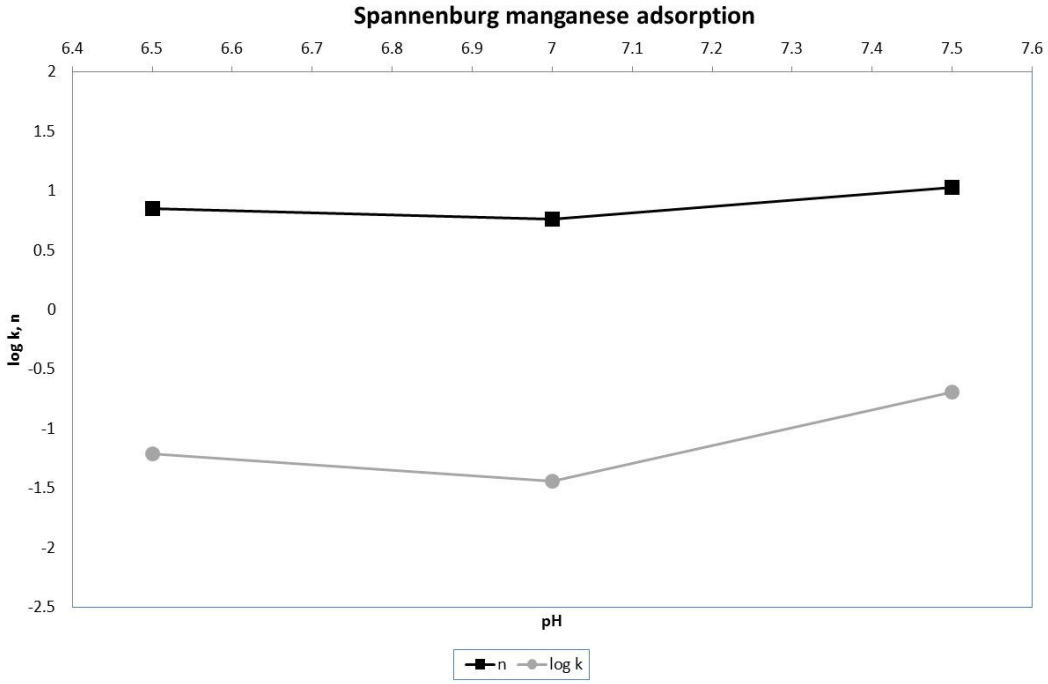

Figure 44: Manganese adsorption isotherm Spannenburg filter medium, influence of the pH

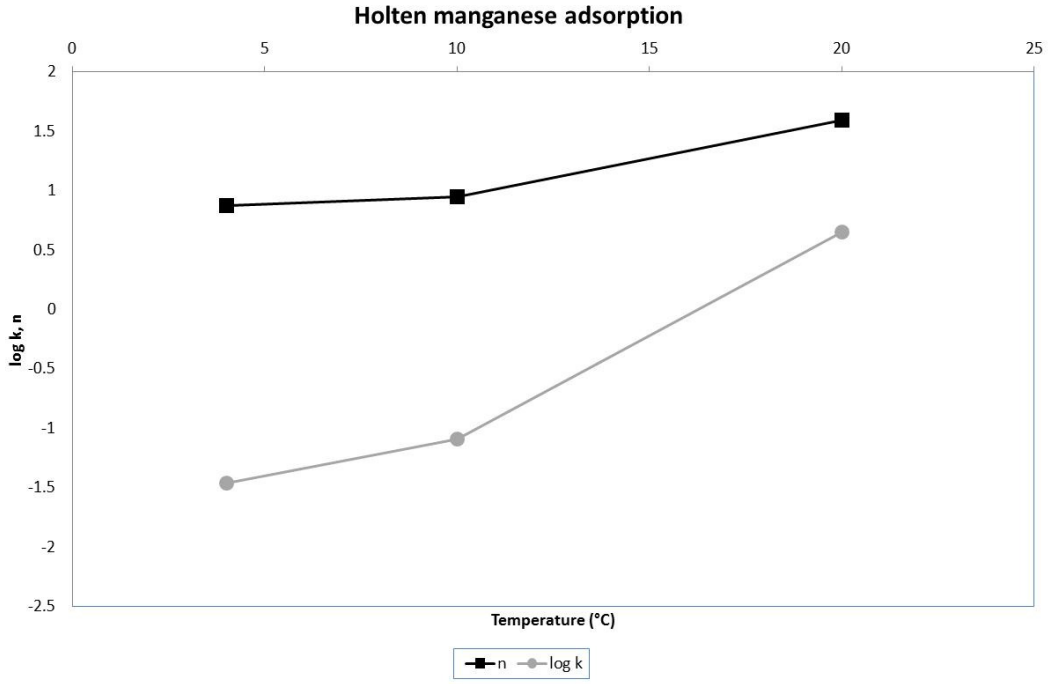

Figure 45: Manganese adsorption isotherm Holten filter medium, influence of the temperature

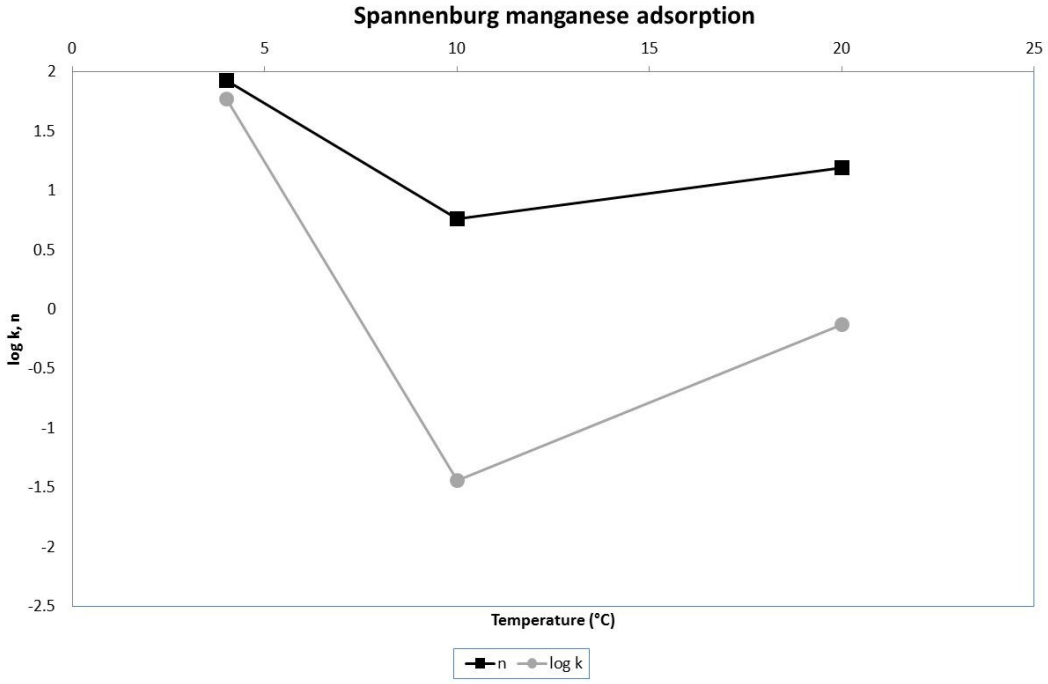

Figure 46: Manganese adsorption isotherm Spannenburg filter medium, influence of the temperature

Annex 9: Matlab script calculation Hat matrix

```
path(path,'C:\Users\schoonenbergf\Documents\afstuderen\glovebox\uit
werking')
filename = 'uitwerking_proef_2_en_3_januari_2014_R2.xlsx';
sheet = 'Meetdata';
xlRangeA = 'e22:e29';
subsetA = xlsread(filename, sheet, xlRangeA);
xlRangeB = 'n22:n29';
subsetB = xlsread(filename, sheet, xlRangeB);
xlRangeC = 'p22:p29';
subsetC = xlsread(filename, sheet, xlRangeC);
xlRangeD = 'o22:o29';
subsetD = xlsread(filename, sheet, xlRangeD);
xlRangeE = 'e1:f1';
subsetE = xlsread(filename, sheet, xlRangeE);
Ce=(subsetA)/1000;%equilibrium concentration in g/L
Q=subsetB;%load in g/g
logCe=subsetC; %log equilibrium concentration in log g/L
logQ=subsetD; %log load in log g/g
formatSpec= 'Spannenburg VF11 pH=%0.1f T=%0.0f %cC';
temp=subsetE(1,2);
ph=subsetE(1,1);
celcius=char(176);
conditie= sprintf(formatSpec,ph,temp,celcius);
m=length(Ce);
mdl=fitlm(logCe,logQ);
a=anova(mdl);
whichstats={'hatmat','leverage','studres','beta','rsquare'};
stats=regstats(logQ,logCe,'linear',whichstats);
beta=stats.beta;
rsquare=stats.rsquare;
hatmat=stats.hatmat;
leverage=stats.leverage;
studres=stats.studres;
d=diag(hatmat);
streepjes='==========================================================
==========================================================
==';
tekstinput='Ýnput data'
tekst0='lineair regression model';
tekst1='resultaat anova:';
tekst2='hat matrix';
tekst3='diagonaal hat matrix';
tekst4='studentized residuals';
tekst5='leverage';
tekst8='power curve fit';
tekst9='tweede graad polynoom';
disp(streepjes);
disp(conditie);
disp(streepjes);
logCe
logQ
Ce
Q
disp(streepjes);
disp(tekst0);
disp(mdl);
```

```
disp(tekst1);
disp(a);
disp(tekst2);
disp(hatmat);
disp(tekst3);
disp(d);
disp(tekst4);
disp(studres);
disp(tekst5);
disp(leverage);
figure(1)
%beta
%rsquare
plot(mdl);
title(conditie);
xlabel('log Ce (log g Mn/L)');
ylabel('log q (log g Mn/g)');
formatSpec1 = 'fit:log(q)=%0.2f log(Ce)+%0.2f; r^2=%0.2f';
A1 = beta(2,1);
B1 = beta(1,1);
R1 = rsquare;
str1 = sprintf(formatSpec1,A1,B1,R1);
legend(' data',str1,'confidence bounds','Location','northwest')
figure (2)%functie y=ax^b
[f2,goodness2] = fit(Ce,Q,'power1');
plot(f2,Ce,Q,'predfunc');
power2coeff=coeffvalues(f2);
formatSpec2 = 'fit:q=%0.5f Ce^{%0.5f} ; r^2=%0.2f'; %
A2=power2coeff(1,1);
B2=power2coeff(1,2);
r2=goodness2.rsquare;
str2 = sprintf(formatSpec2,A2,B2,r2);
title(conditie);
legend(' data',str2,'Location','northwest')
xlabel('Ce (g Mn/L)');
ylabel('q (g Mn/g)');
figure (3)%Y = p1*x^2+p2*x+p3
[f3,goodness3] = fit(Ce,Q,'poly2');
plot(f3,Ce,Q,'predfunc');
power3coeff=coeffvalues(f3);
formatSpec3 = 'fit:q=%0.5f Ce^2 +{%0.5f}Ce+%0.5f ; r^2=%0.2f'; %
A3=power3coeff(1,1);
B3=power3coeff(1,2);
C3=power3coeff(1,3);
r3=goodness3.rsquare;
str3 = sprintf(formatSpec3,A3,B3,C3,r3);
title(conditie);
legend(' data',str3,'Location','northwest')
xlabel('Ce (g Mn/L)');
ylabel('q (g Mn/g)');
figure (4)%Hat Values
plot(d,'sb');
xmax=m+0.5;
xlim([0.4 xmax]);
ylim([0 1]);
title(conditie);
xlabel('Observation Index');
ylabel('Hat Values');
```

```
hold on;
xhat=(10);
testhat1=[0 xmax];
testhat2=[0.5 0.5];%should have been corrected for number of
observations, easy
plot(testhat1,testhat2,'-.r');
hold off;
figure (5)%studentized residuals
plot(studres,'sb');
xlim([0.5 xmax]);
ylim([-10 10]);
title(conditie);
xlabel('Observation Index');
ylabel('studentized Residuals');
hold on;
xhat=(10);
teststud1=[0 xmax];
teststud2=[2 2];
teststud3=[-2 -2];
plot(teststud1,teststud2,'-.r');
plot(teststud1,teststud3,'-.r');
hold off;
disp(streepjes);
disp(tekst8);
f2
goodness2
disp(streepjes);
disp(tekst9);
f3
goodness3
```